AN ABSTRACT OF THE THESIS OF

Tamao Kasahara for the degree of <u>Master of Science</u> in <u>Forest Science</u> presented on <u>August 17, 2000</u>. Title: <u>Geomorphic Controls on Hyporheic Exchange Flow in Mountain Streams</u>

Abstract approved: _____

Steven M. Wondzell

_____

Frederick J. Swanson

Simulations of stream-subsurface water exchange (hyporheic exchange) using a three-dimensional steady state groundwater flow model and a particle tracking model in unconstrained and constrained reaches of small (2nd-order) and intermediate (5th-order) mountain streams were conducted to estimate the effects of geomorphic features on the extent, volume and residence time of hyporheic exchange flow. Study sites were located in the Lookout Creek drainage in the western Cascades of Oregon. Stream water and water table elevations and saturated hydraulic conductivity were collected from four field sites.

Steps were the dominant geomorphic features creating vertical complexity in 2nd-order streams and dominating hyporheic exchange flow. The removal of steps from the simulation models of 2nd-order stream reduced the total volume of hyporheic exchange by 54 %. Furthermore, hyporheic exchange flows resulting from steps had relatively short residence times.

Horizontal complexity, resulting from secondary channels and channel splits, had strong effects on hyporheic exchange, as did vertically extensive features, such as

riffles, in 5th-order streams. Removal of secondary channels, channel splits and riffles from the simulation models reduced hyporheic exchange flow by 25 %, 30 % and 40 %, respectively. Secondary channels contributed to hyporheic exchange with relatively long residence time, where as channel splits and riffles contributed to hyporheic exchange with short residence time. Thus, multiple features strongly contributed to the creation of hyporheic exchange flow and drove various types of the exchange flows. Also, the simulation results and stream survey showed that the interactions between multiple features, for example secondary channels and riffles, enhanced hyporheic exchange. Because horizontally extensive features were important in driving hyporheic exchange flow in the studied unconstrained reaches, the width of the valley floor strongly controlled hyporheic exchange flow in 5th-order streams.

Geomorphic controls on hyporheic exchange flow differed between the two stream sizes sampled. Second-order streams had a single key geomorphic feature (i.e. steps) influencing the hyporheic exchange flow, whereas multiple geomorphic features (i.e. riffles, secondary channels and channel splits) were important in 5th-order streams. As a result, residence time distribution of hyporheic exchange flow was narrow in 2nd-order stream and wide in 5th-order stream.

Geomorphic Controls on Hyporheic Exchange Flow
in Mountain Streams

by

Tamao Kasahara

A THESIS

Submitted to

Oregon State University

In partial fulfillment of
the requirements for the
degree of

Master of Science

Presented August 17, 2000
Commencement June 2001

Master of Science thesis of Tamao Kasahara presented on August 17, 2000

APPROVED:

_____

Co-Major Professor, representing Forest Science

_____

Co-Major Professor, representing Forest Science

_____

Head of Department of Forest Science

_____

Dean of Graduate School

I understand that my thesis will become part of the permanent collection of Oregon State University libraries. My signature below authorizes release of my thesis to any reader upon request.

_____

Tamao Kasahara, Author

ACKNOWLEDGEMENT

When I first started here as a student, I could not picture myself defending my work and writing up a thesis in English. I remember the days that I was asking myself, like "why did you choose to come this scary country and study?". However, after the three years of struggling, I now became capable to face up to the defense day. It is pretty amazing that how people, even I, can adjust themselves to the difficult situations. Of course as you imagine, I could not accomplish this thesis without numerous helps, suggestions and smiles from variety of people. Here, I would like to take time to express my appreciations to the people.

Dr. Steve Wondzell, who is my major advisor, invested a lot of his time and gave me great directions and suggestions to my work all the way through. Apparently, I could not even come close to the ending without him. Dr. Fred Swanson, who is my co-major advisor, helped me having large pictures and gave me great suggestions, especially in geological parts. Also, if I did not meet him at Tomakomai in 1997, I might not have opportunity to study at Oregon State University. Dr. Roy Haggerty, who is a committee member, was a critical supporter for the hydrological approaches of my works. Kermit Cromack gave me inputs from the biogeochemical point of view, which I am planning to precede next. Sherri Johnson was kind enough to let me use her water temperature data and was a great supporter for fieldwork and future determination. Dr. Adriana Huyer was kind to be the Grad. Rep. of my committee. I deeply thank you to all.

Nathan Klinkhammer, Kristin May, and Nicole Walter spent majority of summer at H.J. Andrews to help the stream survey for this research project. I greatly thank to

their works and time. I appreciate Takeru and Taku Kasahara helped fieldwork during their precious time spending in US.

It was exciting and fulfilling experience for me to be involved with LTER. Networks among people and intensive ongoing research projects within the H.J. Andrews stimulated me in many ways. I especially thank to the site manager, who made the life in H.J. Andrews comfortable and hydrological technician, Creag Creel, who kindly lend me his equipments.

I thank professor Futoshi Nakamura at Hokkaido University for helping me to have the opportunity to study here and give me suggestions and connections through the process of this thesis. Congratulations for your promotion.

I greatly thank to Steven Wondzell and Dominique Bachelet for making it easy to start the new life here in Corvallis and at OSU. They were kind enough to let me stay in their house while I was looking for place to live the first time and invited me to many activities during last three years. I enjoyed many things inside and outside of school life because of them. Thank you very much. I promised myself to do same things to younger generation people.

Punlop Kuntiyong has been my best friend. Without him, I could not have as much fun and good time as I had here. I was not a good person sometimes, especially when I was stressful under the research, but he was patient enough to allow me to be so. I would like to say thank you very much to him.

Lastly, I specially thank family, Yoshitaka, Taka and Takashi Kasahara, and my grand parents, Shigeyuki and Keiko Sasaki. They were always wonderful psychological supporters.

TABLE OF CONTENTS

LIST OF FIGURES

LIST OF TABLES

Geomorphic Controls on Hyporheic Exchange Flow in Two Sizes of Mountain Streams

1.   **INTRODUCTION**

1.1   Definition of Hyporheic Exchange Flow

Stream ecosystems interact with surrounding terrestrial and atmospheric systems. Hyporheic exchange is a subsurface interaction that occurs between stream and terrestrial ecosystems and can have strong effects on stream water chemistry and stream ecosystems (Ward 1989, Stanford and Ward 1993, Triska et al. 1993, Jones and Holmes 1996, Townsend 1996). Stream water locally enters subsurface areas due to hydraulic gradients, and the water returns to the wetted-channel over relatively short distances. This movement of stream water is called hyporheic exchange, and the hyporheic zone is defined as a saturated subsurface area containing hyporheic exchange flow. The primary interests in the hyporheic zone concern biological and geochemical processes. Therefore, multiple criteria, such as tracer concentration (Triska et al. 1989), background conservative ions (Hill and Lymburner 1998) or subsurface residence time (Wroblicky et al. 1994), have been used to arbitrarily delineate the biologically and geochemically important hyporheic zone. The hyporheic zone has been delineated as the area, for example, containing at least 10 % of stream-originated water (Triska et al. 1989) or containing hyporheic exchange flow that has residence time less than 10 days (Wroblicky et al. 1994). However, I focused on hydrological processes and defined the hyporheic

zone as the entire area where hyporheic exchange flow is present. The hyporheic zone

extends in vertical and lateral directions from wetted-channels, at scales ranging from a

few centimeters to tens of meters depending on the channel sizes, morphology and

hydraulic conductivity (White 1993, Morrice et al. 1997). The hyporheic zone extended

10 m vertically and more than 2 km laterally in one extreme example (Stanford and Ward,

1988).
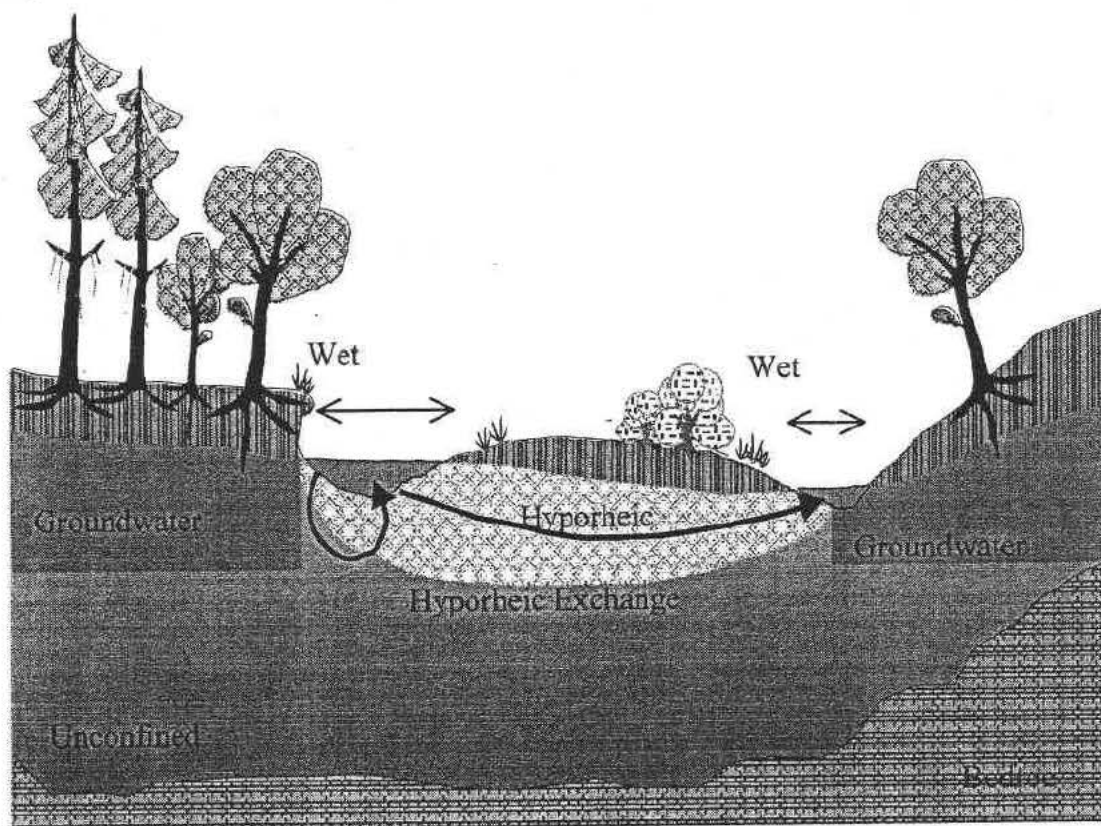
Figure 1.1 Definition of hyporheic exchange flow and hyporheic

1.2   Roles of Hyporheic Exchange Flow in Stream Ecosystem

Hyporheic exchange flow has been intensely studied in the last few decades

because of its biological, chemical and hydrological effects on stream ecosystems

(Stanford and Ward 1993, Findlay 1995). The significance of the hyporheic zone

originally focused on its function as habitat for aquatic invertebrates (Stanford and Ward 1988, Williams 1993). Many aquatic invertebrates require relatively high concentrations of dissolved oxygen to sustain their aerobic metabolisms (Triska et al. 1993b). Presence of stream water in the subsurface may increase the concentrations of dissolved oxygen, creating aerobic conditions in the hyporheic zone, especially at sites of downwelling. Additionally, the hyporheic zone functions as refugia for benthic organisms during floods (Stanford and Ward 1988), which may speed the recovery of benthic communities following disturbances.

Riparian areas, including the hyporheic zone, are hot spots for nutrient and carbon transformations (Hedin et al. 1996), and these transformations affect stream water chemistry and stream ecosystems. Many previous studies have focused on nitrogen dynamics in the hyporheic zone. High rates of nitrification are supported by aerobic condition and high rate in supply of organic matter (Jones et al. 1995). High rate of denitrification may also be found because of the high production of nitrate (Holmes et al. 1996). Nitrification tends to occur close to wetted channels, whereas denitrification may occur throughout the hyporheic zone (Triska et al. 1993a, Jones et al. 1995, Holmes et al. 1996). Mountain streams are often nutrient limited, and the transformed nutrients, such as nitrate, returned from the hyporheic zone to the stream are important sources of limiting nutrients for the aquatic biota (Triska et al. 1989, Holmes et al. 1994, Jones et al. 1995, Wondzell and Swanson 1996 b). In contrast, lowland streams have high rate of denitrification because they are often nutrient rich (Pinay et al. 1994). Fine sediment and low channel complexity in channel morphology may slow the rates of hyporheic exchange and create relatively anaerobic hyporheic zone in low land streams (Valett et al.

1998), and large amount of dissolved inorganic nitrogen is denitrified at the stream-sediment interface before it enters the wetted-channels (Hill and Lymburner 1998, Hedin et al. 1996, Dahm et al. 1998). Hyporheic exchange may also create preferential spawning locations for samonid species (Geist and Dauble 1998). Also, in a hydrological sense, hyporheic exchange flow may help the reduction of peak discharge during storm events. Thus, hyporheic zones may have multiple important roles in stream ecosystems.

Although the biological and chemical processes are important in the hyporheic zone, rates of these processes are controlled by the flow of water through the hyporheic zone. Thus, hydrological processes are key to understanding the influence of the hyporheic zone on stream ecosystems. However, the hydraulic processes are relatively less well studied (Triska et al. 1993b, Stanley and Boulton, 1993, Bencala 1993). Development of understanding of hydrological processes and the integration of hydrological processes and biogeochemical processes are needed to understand better the role of hyporheic exchange in stream ecosystems.

1.3   Methods to Investigate the Hydrological Processes of Hyporheic Exchange Flow

The primary method used to investigate hydrological processes in the hyporheic zone are stream tracer experiments analyzed with OTIS, a one-dimensional solute transport model with inflow and storage components (Runkel and Broshears 1991, Triska et al. 1993a, Triska et al. 1993b, D'Angelo et al. 1993, Valett et al. 1996, Morrice et al. 1997). OTIS separates streams into two compartments, a wetted-channel and a transient

storage zone, and estimates cross-sectional area of both compartments as well as an exchange coefficient to describe flow between the two compartments.

OTIS has several limitations. First, this model estimates the average exchange rate and average resident time in a stream reach. However, the variation in exchange rate or hydraulic residence time is important because the hyporheic zone is not spatially homogeneous (Castro and Hornberger 1991, Harvey et al. 1996). Secondly, long, continuous-tracer injections are necessary to identify hyporheic exchange with long residence time. Most previous studies conducted relatively short injections (Triska et al. 1993a, D'Angelo et al. 1993, Morrice et al. 1997), and probably underestimate the volume of total hyporheic exchange flow. Third, it is difficult to compare sizes of hyporheic zone under different stream discharge because OTIS is sensitive to stream discharge. Hyporheic exchange flow is underestimated when stream discharge is high (Harvey et al. 1996). Fourth, OTIS estimates only the reach averaged cross sectional area of transient storage zone, and there is not sub-reach information. Finally, because the descriptions of mass transfer is phenomelogical, the cross-sectional area of the transient storage zone estimated by OTIS is not directly related to any specific physical features in real stream channels so that it is difficult to use for the quantification of the biogeochemical effects of hyporheic exchange flow in stream ecosystems.

Hydrometric method (Harvey et al. 1996) provides an alternative to OTIS. It is physically based method that uses closely spaced hydraulic head measurements taken from wells and estimates of saturated hydraulic conductivity to compute subsurface water flow. This method provides a quantitative estimate of hyporheic exchange flow. A modular three-dimensional finite-difference groundwater flow model, MODFLOW

(McDonald and Harbaugh 1988), is commonly used in applications of the hydrometric method. The model is based on the finite difference equation derived by combining conservation of mass and Darcy's Law. Several researchers have successfully used MODFLOW to simulate the shallow subsurface flows (Wroblicky et al. 1994, Maddock et al. 1995, Wondzell and Swanson 1996a)

The strengths of MODFLOW are the capabilities to 1) estimate relatively realistic volume and extent of hyporheic exchange flow, 2) examine the distributions of residence time of hyporheic exchange water by coupling the simulation results with MODPATH (Pollock 1991) and 3) adjust the spatial scale depending on research interests.

The volume, extent and residence time strongly control of biological processes in the hyporheic zone, and it will be exciting to combine them with measurements of biogeochemical processes. The flexibility in scaling by hydrometric methods is an advantage for investigating the effects of geomorphic features on hyporheic exchange flow.

1.4 Geomorphology and Hyporheic Exchange Flow

Hydraulic gradients and hydraulic conductivity are the controller of hyporheic exchange flow (Fetter 1994). Channel morphology (Harvey and Bencala 1993, D'Angelo et al. 1993, White 1993, Williams 1993, Wondzell and Swanson 1996a) and geology (Valett et al. 1996, Morrice et al. 1997) have controls on hyporheic exchange flow because geomorphic features affect hydraulic gradients and saturated hydraulic

conductivity. If groundwater flow models, like MODFLOW, can accurately characterize hyporheic exchange flow, examination of geomorphic features may allow expansion of studies on hyporheic exchange flow to the stream network scale. The ability to accurately estimate the extent, volume and residence time of hyporheic exchange flow at the stream-network scale would greatly improve our understanding of the importance of hyporheic zone in stream ecosystem processes.

Channel morphology controls hyporheic exchange because channel complexity changes local hydraulic head gradients. For example, positive hydraulic gradients from the wetted-channel to adjacent subsurface are often created at the heads of riffles and steps so that stream water flows into subsurface. The hyporheic water flows back to the wetted-channel at the heads of pools because the hydraulic gradient reverses (Harvey and Bencala 1993). The hyporheic exchange flow created by steps and riffles extends both laterally and vertically from the wetted channel, but the flow paths tend to be relatively short (White et al. 1987, Harvey and Bencala 1993, White 1993). Presence of secondary channels and channel sinuosity can drive exchange flow over longer flow paths creating laterally extensive hyporheic zones (Wondzell and Swanson 1996a, Triska et al. 1993). Unconstrained reaches have potential to have more hyporheic exchange than do constrained reaches (D'Angelo et al. 1993).

The objective of this study was to examine the effects of geomorphic features on hyporheic exchange flow in streams of two sizes. Specifically, I 1) estimated the extent, volume and residence time of hyporheic exchange flow at well-network sites located in unconstrained and constrained reaches of 2nd-order and 5th-order streams, 2) estimated the relative importance of different geomorphic features driving hyporheic exchange flow at

each well-network site, and 3) estimated the relative contribution of each geomorphic feature to hyporheic exchange at the reach scale. MODFLOW simulations were used to estimate the hyporheic exchange flow. Comparisons between 2nd-order and 5th-order streams were conducted to examine changes in influence of geomorphic features in different sized streams. I looked at features that previous studies had shown to be important in driving hyporheic exchange flow, including channel constraint, presence of secondary channels, change in gradients (Harvey and Bencala 1993, D'Angelo et al. 1993, White 1993, Wondzell and Swanson 1996a).

2.   METHODS

2.1 Study site descriptions

Lookout Creek and the streams draining study watershed 1 (WS01) and 3 (WS03) are located in the H.J. Andrews Experimental Forest (44°20′ N, 122°20′ W) in the western Cascade Range of Oregon (Figure 2.1). Average annual precipitation ranges between 2300 mm to 3550 mm depending on the elevation and falls mainly from November to March (Bierlmaier and McKee 1989). Summer in Oregon is dry, and winter is wet, and field work was conducted during the summer low-flow period.

Lookout Creek is a 5th-order stream and drains an area of 6400 ha. Elevations within the watershed range from 428 m to 1620 m. Typical summer discharge is about 720 l/s and average wetted channel width is 8.6 m. The stream flows through forests dominated by Douglas-fir (*Psudotsuga menziesii* -Mirb. -Franco), western hemlock (*Tsuga beterophylla* -Raf. - Sarg), and western redcedar (*Thuja plicata* Donn ex D. Don). Red alder (*Alnus rubra* Bong.) and willow (Salix spp.) grow along the stream. Underlying bedrock is composed of volcaniclastic rocks (Swanson and James 1975).

WS01 and WS03, 2nd-order streams, are tributaries of Lookout Creek and drain areas of 95.9 ha and 101.1 ha, respectively. WS01 was clear-cut and reforested in the mid 1960s, but no roads were built in the watershed. Upland areas are dominated by Douglas-fir, but Red alder is common in riparian areas. Typical summer discharge is about 3 l/s, and the average wetted-channel width is 1.8 m. WS03 was partially cut with three small clear cuts in 1963, and roads were built to access to the cutting units in 1959.

The forest is dominated by Douglas-fir and western hemlock. Typical summer discharge is about 4 l/s and average wetted channel width is 1.8 m. A large debris flow occurred in February 1996 and scoured the valley floor so that the floodplain is currently unvegetated. Underlying bedrock of these two small watersheds are basaltic lava flow and other volcanic rocks (Swanson and James 1975).

Four stream reaches were used in this study. Two study reaches were located in 5th-order, Lookout Creek. The unconstrained reach, Middle Lookout, is about 1500 m long, and the valley floor is about 90 m wide. The constrained reach of Lower Lookout, where the valley floor is strongly constrained by bedrock walls, is about 350 m long, and the valley floor width was about 16 m. Two study reaches were located in 2nd-order streams. The WS01 reach is about 200 m long and has an unconstrained valley floor. The WS03 reach is about 250 m long and has a constrained valley floor.
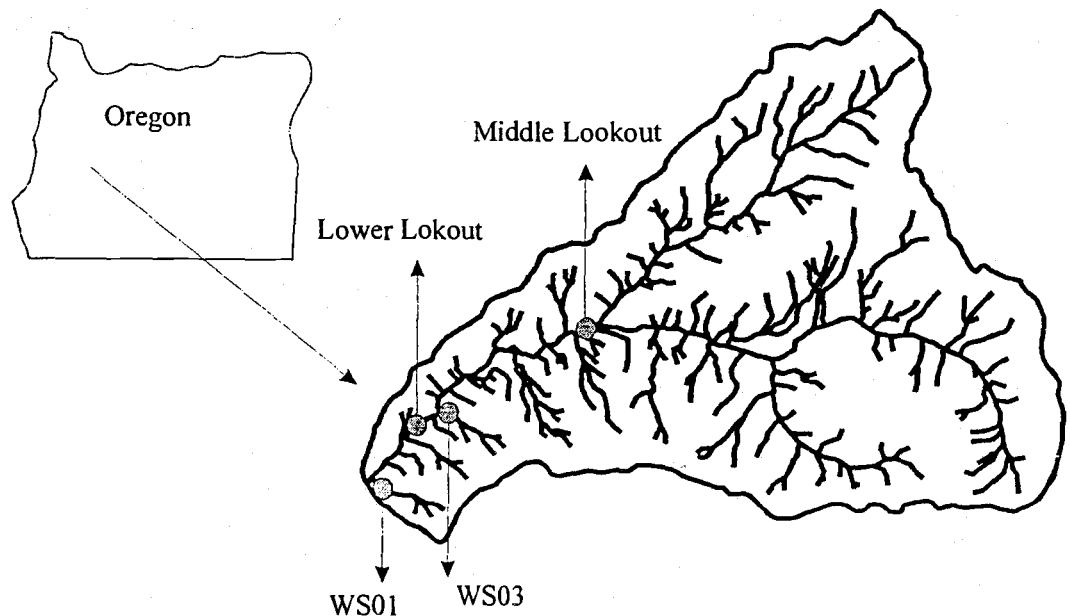
Figure 2.1 Study site locations in the Lookout Creel watershed, western Cascades, Oregon

2.2 Well Networks

PVC pipes, which have diameter of 3.2 cm and are about 1 ~ 2 m long (Figure 2.2), were installed into parts of the study reaches to measure water table elevations and saturated hydraulic conductivities. All wells are screened over the lower 50 cm, except for the wells located in the wetted channel, which have 5 cm long screens. The well networks in Middle Lookout and Lower Lookout were established during the summer of 1996 (see Wondzell and Swanson 1999). About 40 wells were installed in 170 m stretch of Middle Lookout reach (Fig. 2.3-a). Lower Lookout has six transects of wells on the left side of the wetted channel in a 60 m long stretch (Fig. 2.3-b). The well networks in WS01 and WS03 were installed in summer of 1997. WS01 has 6 well transects in a 40 m long stretch. Each transect has 6 to 7 wells from the south side slope through the wetted-channel and to the north side slope (Fig. 2.4-a). WS03 has 7 well transects in a 40 m stretch. Each transect contains 4 to 6 wells (Fig 2.4-b). The parts of the study reaches, where the wells were installed, are called well-network sites.

2.3 Mapping of study reaches

Stream surveys were conducted in the summers of 1998 and 1999. I surveyed the longitudinal profiles of surface-water and water table elevations, and measured the shapes of wetted-channels, boundaries of active channels and boundaries of floodplains of all four study-reaches. Field survey data were used to map the study reaches on grid paper.
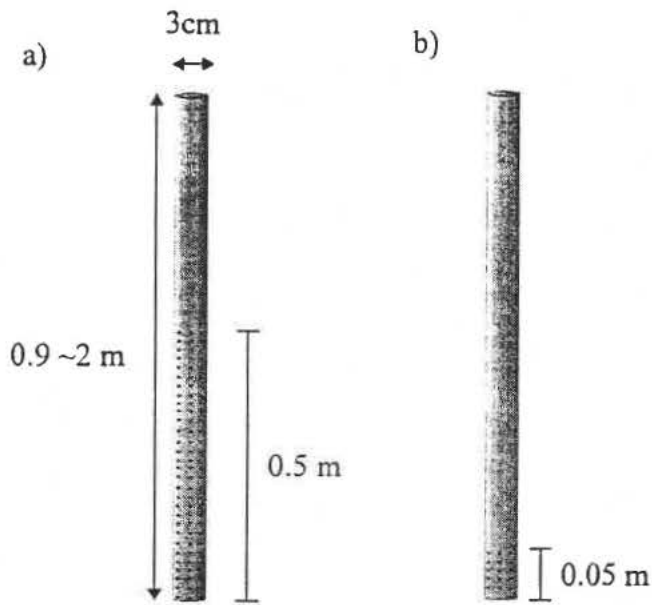
Figure 2.2 PVC pipes installed in the well-network site
a) well and **b)** piezometer

Wetted channels are channels where flowing surface water is present. Active channels are the area inundated annually by stream flow, and usually lack vegetation cover (Grant and Swanson 1995). I defined the active channel in Middle Lookout reach as the area scoured of vegetation by a flood in 1996. Floodplains are vegetated and extend to the base of valley walls (Figure 2.5-a). Secondary channels have less discharge than main channel and are connected with the main channel at either the upstream or downstream end. Channel splits are defined by islands in the main channel so that the split channels join at both upstream and downstream ends (Figure 2.5-b).

A tape was stretched down the center of the wetted channel to follow the axis of flow and measure the distance along that path. Stream water elevations were measured every 5 to 10 m in 5th-order streams depending on the channel complexity. For example, I measured elevation every 5 m along the main axis of flow where channels split or where
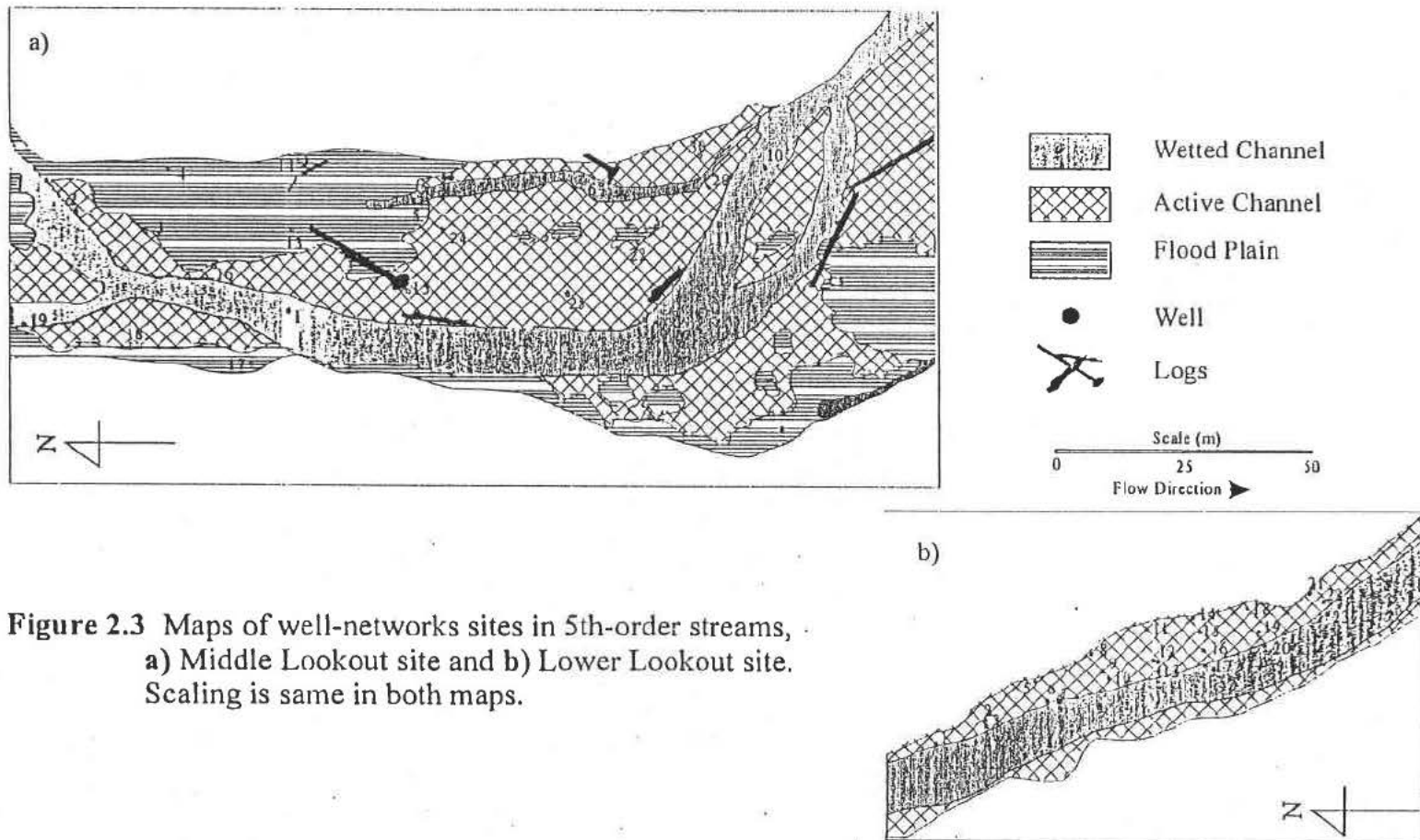
Figure 2.3 Maps of well-networks sites in 5th-order streams,
a) Middle Lookout site and b) Lower Lookout site.
Scaling is same in both maps.

Legend:
- Wetted Channel
- Active Channel
- Flood Plain
- Well
- Logs

Scale (m): 0 — 25 — 50

Flow Direction ▶
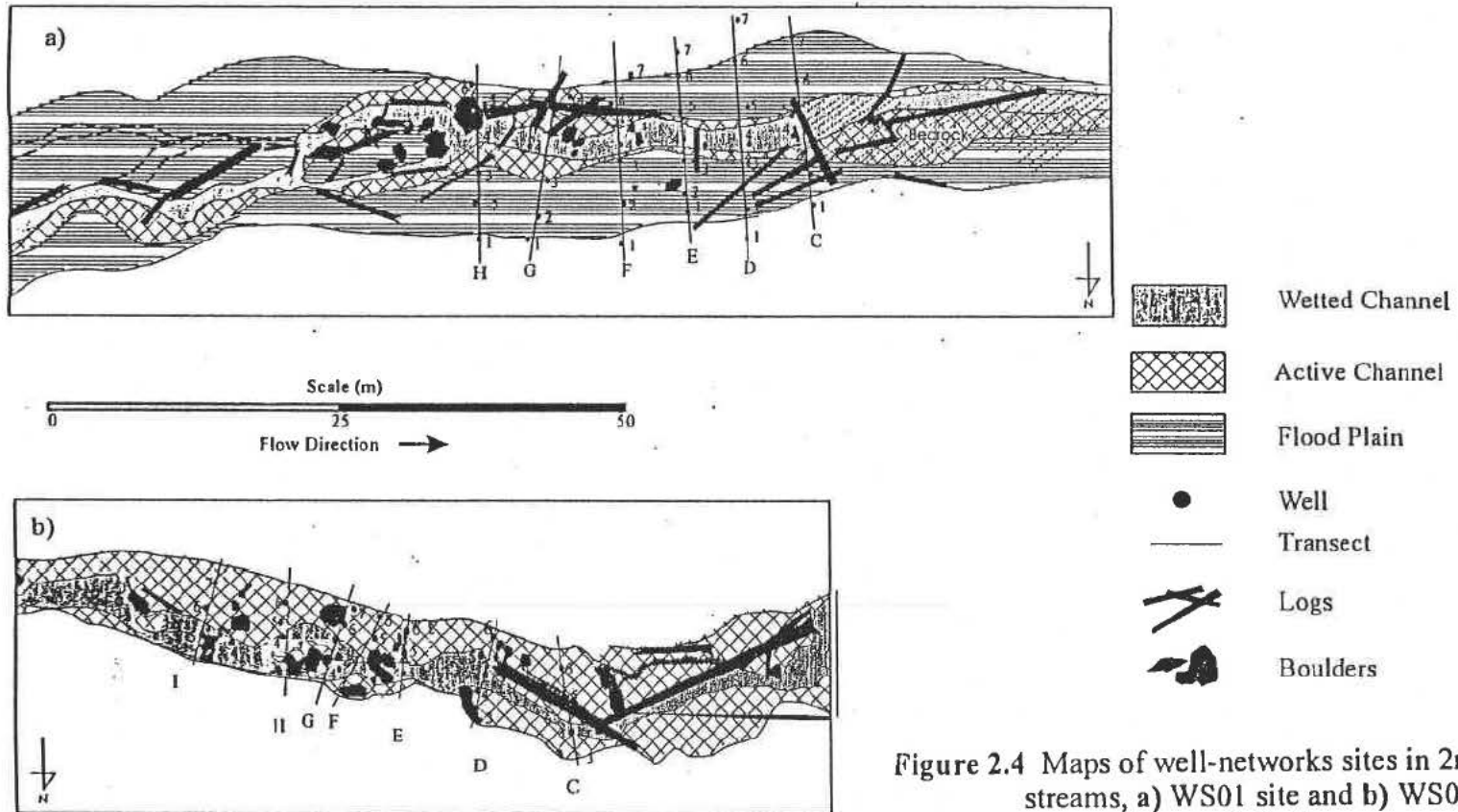
Figure 2.4 Maps of well-networks sites in 2nd-order streams, a) WS01 site and b) WS03 site. Scaling is same in both maps.

Legend:
- Wetted Channel
- Active Channel
- Flood Plain
- Well
- Transect
- Logs
- Boulders

Scale (m)
0   25   50

Flow Direction →

a)

Hill slope

Hill slope

Floodplain

Active Channel

Wetted Channel

b)

Channel split

Secondary channel

C)

Steps

Riffles
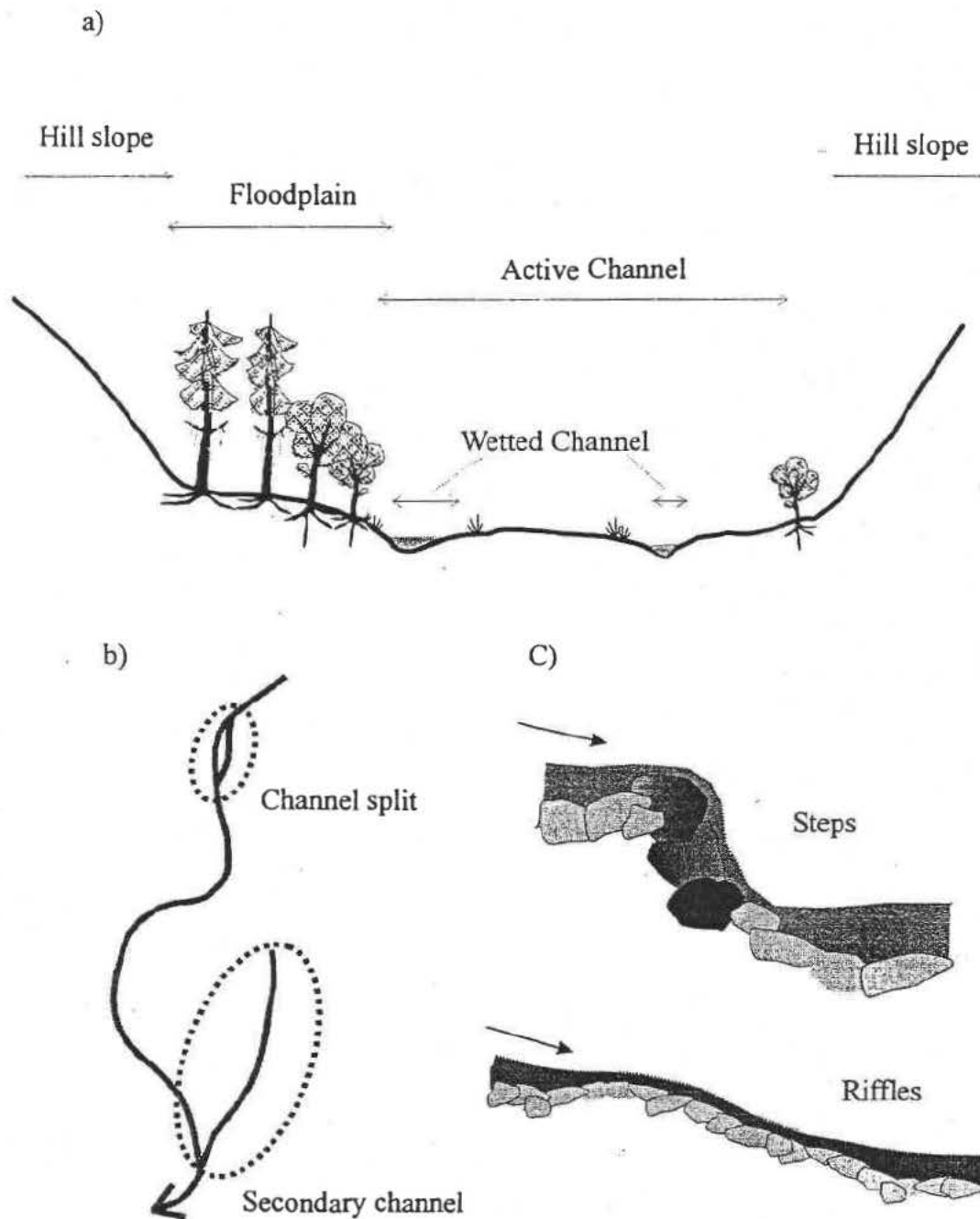
Figure 2.5 Definition of geomorphic features in
a) cross sectional view, **b)** horizontal view, and
c) longitudinal vertical-section view

channels had high gradients. Otherwise, I measured water elevation every 10 m.

Water elevations in secondary channels with surface water were surveyed using the same

procedure as above. Wetted channel width and active-channel width were measured at

every other survey point. A series of low-level aerial photographs taken from a tethered

blimp in August of 1997, aerial photographs, and a vegetation map (Kennedy,

unpublished senior thesis 1998) were available for the Middle Lookout reach. Therefore,

the channel shape and the extent of active channel were taken from these sources.

Survey points in the 2nd-order streams were located every 1 m where the steps

existed, where secondary channels were present or where steps were present. Otherwise,

measurements were taken every 2 to 4 m. The wetted-channel width and floodplain

width were measured with another tape, perpendicular to the axis of the main channel, at

every survey point. Angles between the stakes in wetted-channel were measured using

compass to capture the channel shape.

I did not survey or map the portion of the study reaches within the well-network

sites in WS01 and WS03, and existing maps of well network sites (from Wondzell,

unpublished data) were combined with the rest of the maps of study reaches I created.

2.4   Frequency distribution of geomorphic features

The maps of the study reaches were used to quantify the characteristics of

geomorphic features present at each study reach. Study reaches were divided into several

representative survey lengths (RSL), and the frequency of geomorphic features was

recorded in each RSL (Figure 2.6). Geomorphic features, such as channel sinuosity, were
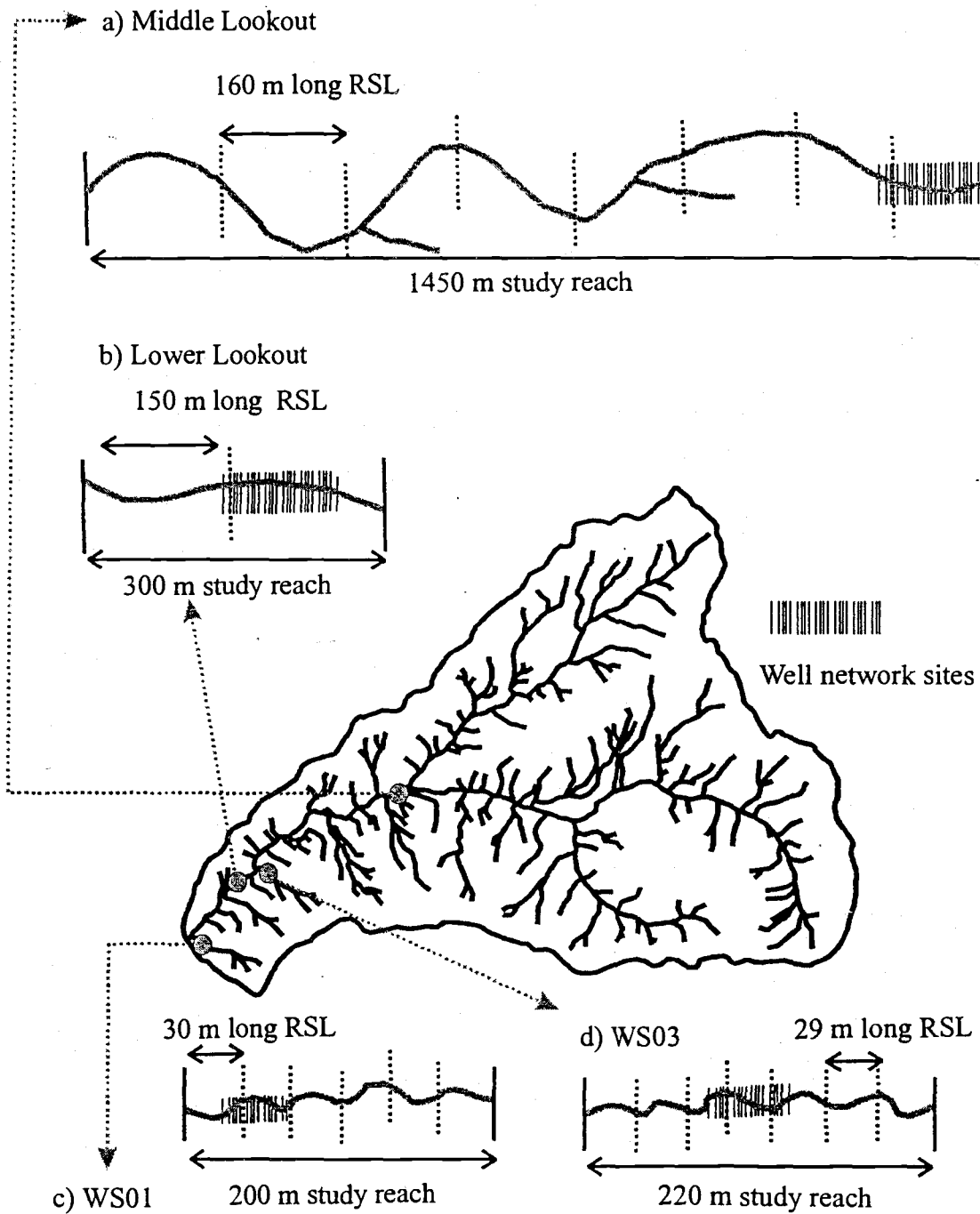
Figure 2.6 Division of study reaches into RSLs in **a)** Middle Lookout reach, **b)** Lower Lookout reach, **c)** WS01 reach, and **d)** WS03 reach
* The shapes of wetted-channels are idealized for illustration, and do not represent the actual reaches surveyed.

not used to delineate RSL because of scaling differences between 2nd-order and 5th-order streams. Instead, I used fixed lengths to systematically divide the study reaches into RSLs. The lengths of RSL were about 20 times the wetted-channel width during summer base-flow. This arbitrarily delineation ensured consistency among study reaches. The RSL length in the Middle Lookout was 160 m, and the reach had 8 RSLs. Lower Lookout had two 162 m long RSLs. WS01 had six 29-m long RSLs, and WS03 had five 30-m long RSLs. I combined Middle Lookout and Lower Lookout, and WS01 and WS03 to represent the characteristics of 5th-order and 2nd-order streams, respectively. Therefore, there were total 10 RSLs for 5th-order streams and total 13 RSLs for 2nd-order streams. The division of study reaches into RSLs cut both channel units and reach-scale features, such as secondary channels and channel splits. The resulting errors are small for channel units because there are multiple units per RSL. However, secondary channels and channel splits were less common, and of larger size, so that their analysis within a single RSL was problematic. Therefore, I analyzed secondary channel and channel splits independently of RSL delineation.

The frequency and size of five features, 1) channel gradients, 2) steps and riffles, 3) channel sinuosity, 4) wetted-channel width, 5) active-channel or floodplain width, were measured for each RSL. Slope of streambed (longitudinal gradient) was calculated by dividing the change in streambed elevation in the RSL by RSL length. Steps and riffles were defined as the locations where gradient exceeded 1.5 times the average channel gradient of the study reach. The number and gradient of each step were recorded. Contribution of steps to streambed gradient was also calculated by dividing change in elevation created by steps by the total change in elevation within the RSL. Channel sinuosity was calculated by

dividing wetted-channel length by the RSL length. Finally, measurements of wetted-channel width, active-channel width and floodplain width were averaged for each RSL.

As mentioned above, secondary channels and channel splits were measured independently of RSL. Two components, length and cross-valley gradient, were measured for these features. I measured the length of secondary channels only where surface water was present. The lengths of channel splits were reported as the length of island between the two channels. Cross-valley gradients between secondary and main channels and between two split channels were calculated from measurements of distance between channels and difference in hydraulic heads. The width to length ratio of each bar was also measured independently from RSL.

2.5   Saturated Hydraulic Conductivity (K)

Saturated hydraulic conductivity was estimated using two approaches, slug tests and continuous well injections. Slug tests give many point measures and are indicative of spatial heterogeneity in saturated hydraulic conductivity. However, results of slug tests apply to a small area around each well and also may contain order of magnitude errors (Hyder and Butler 1995). Conversely, continuous tracer injections may give better estimates of conductivity, but estimates are spatial averages of the area between the injection and observation wells. Consequently, this method is not sensitive to spatial heterogeneity.

2.5.1 Slug test

I used falling-head slug tests and analyzed the results with the Bouwer and Rice technique (Bouwer and Rice 1976), which is appropriate for unconfined aquifer with partially penetrating wells (Hyder et al. 1994, Hyder and Butler 1995). This technique measures the recovery of head after an instantaneous increase or decrease in water table elevation in the well. Saturated hydraulic conductivity is calculated as:

$$K = \frac{r_c^2 \ln(R/r_c)}{2(l-d)t_L}$$

where K is saturated hydraulic conductivity, d is the distance from the water table to the well screen, l is distance from water table to bottom of the well, R is the radius of influence, t_L is time length, and r_c is the radius of well.

This method is widely used because it requires relatively simple equipment and a short-duration test. The assumptions of this slug test are, such that 1) the specific storage is negligible, 2) change in water table is small enough to treat water table as a constant head, 3) unsaturated flow above the water table is negligible, 4) the installation of wells did not change the conductivity of the surrounding sediment, and 5) the material is isotropic (Hyder and Butler 1995).

Falling-head slug tests were conducted by pouring water into the well as quickly as possible to increase the water table elevation. The recovery of the water table was monitored by recording the change in water table at one-second intervals, and the test ended when the head dropped to the beginning elevation. This test was repeated three times for each well using different initial changes in head. The conductivity values reported for each well are the average of these three tests.

2.5.2 Well injection tests

I conducted continuous well injection tests at Middle Lookout, Lower Lookout and WS01 well-network sites to get additional information of the saturated hydraulic conductivity. The advantages of well injection are increased reliability and the applicability to larger areas than are slug tests. I only conducted one tracer-injection test at each site because the duration of continuous well injection tests is long.

NaCl was used as a tracer and was injected into a well at a constant rate. Electric conductivity (EC) was measured as a surrogate for Cl⁻ concentration. EC was measured in all wells before starting the injection test to check the background values and was measured periodically during the tests to monitor the arrival of the tracer. The tracer injection test continued until at least one well reached plateau tracer concentration (EC). Median travel time was estimated as the time when tracer concentration reached half the plateau concentration. Saturated hydraulic conductivity was calculated by multiplying median travel time with hydraulic gradient and porosity, following the equation;

$$q = n \cdot \frac{dl}{T} , \quad K = q \cdot \frac{dl}{dh}$$

where q is the Darcy's velocity, T is median travel time, n is the porosity, dl is the distance between two points and dh is the change in water table between the two points. This simple method is strictly valid only in a homogeneous medium within simple boundary condition so that it yields only a very rough estimate of K in the heterogeneous medium of the study sites.

2.6   MODFLOW simulations

2.6.1 Model descriptions

A modular three-dimensional finite-difference groundwater flow model – MODFLOW (McDonald and Harbaugh 1988) – was used to simulate the subsurface flow in the study sites.   The MODFLOW is based on Darcy's law and conservation of mass,

Darcy's law for three dimensions in isotropic medium is;

$$q_x = -K_x\frac{\partial h}{\partial x} \qquad q_y = -K_y\frac{\partial h}{\partial y} \qquad q_z = -K_z\frac{\partial h}{\partial z}$$

where q_x, q_y and q_z are Darcy's velocity for each direction; K_x, K_y and K_z are saturated hydraulic conductivities for each direction; ∂h represents changes in head between two points; ∂x, ∂y and ∂z represent the distance between those points in x, y and z direction.

Law of Mass Conservation for steady state condition is;

$$\frac{dq_x}{dx} + \frac{dq_y}{dy} + \frac{dq_z}{dz} = \frac{d}{dx}\left(-K_x\frac{dh}{dx}\right) + \frac{d}{dy}\left(-K_y\frac{dh}{dy}\right) + \frac{d}{dz}\left(-K_z\frac{dh}{dz}\right) = 0$$

MODFLOW was developed by US Geological Survey and is widely used to solve a variety of groundwater problems (McDonald and Harbaugh 1988).   Data required for the groundwater model are physical data, such as boundary of the system and thickness of sediment, and hydrogeologic data, such as water table, surface water elevation and saturated hydraulic conductivity (Anderson and Woessner 1992).

I used MODFLOW in the groundwater modeling system – GMS.   GMS was developed by the Engineering Computer Graphics Laboratory at Brigham Young

University and was designed as a comprehensive graphic modeling environment. The GMS includes a Map module, a 2-D scatter point module, and a 3-D grid module. The map module is used to construct conceptual models and to develop the presentations of simulation results. The 2-D scatter point module interpolates 2-D spatial data to the entire model domain using a variety of geostatistical tools. The 3-D grid module has a complete interface to MODFLOW (GMS v2.1 Reference Manual). The strength of GMS is the creation of conceptual models (Map module) and the automatic conversion of the conceptual model to MODFLOW models. Also, GMS provides graphical interface to present results of simulation and to help calibrate the model to observed data.

2.6.2 Well-network site models

Models were built for each well-network site to simulate water interaction between the stream and underlying unconfined aquifer under summer base-flow conditions. Subsurface flows were simulated as steady state conditions. I assumed the amount of water flowing into the system was equal to the amount of water flowing out from the system (steady state). I also assumed the aquifer was heterogeneous and isotropic.

Boundary conditions were defined based on field observations and survey data. Three types of boundaries, specified-head boundaries, general-head boundaries and no-flow boundaries, were used in the models. Specified-head boundary cells have constant head values throughout simulations. General-head boundary cells are described by a specified head and a conductance. If the calculated water table elevation at the boundary was above the specified head, water flows out of the aquifer. If the water table was

below the specified head, water flows into the aquifer. No-flow boundary cells do not allow water to flow across the boundary, and water near this boundary flows parallel to the boundary. Upstream and downstream limits of model domain were located across the width of the valley-floor, some distance above and below the well networks, and were treated as specified-head boundaries. The water tables and surface-water elevation observed on these boundaries determined the hydraulic head values for specified head cells. Left and right side limits of the model domain were located on the edges of active channels in 5th-order streams and on the edge of floodplains in 2nd-order streams. These sides were treated as a combination of no-flow boundaries, general head boundaries and specified-head boundaries. General head boundaries were used where the water tables could be measured from wells, otherwise I used no-flow boundaries. Specified-head boundaries were only used where general-head boundary did not work well, probably because of strong groundwater inflows. The bottom of the model domain was treated as impermeable.

Thickness of the aquifers was unknown. However, bedrock material was exposed in stream channels in several places, and I assumed the aquifers were not thick. I set the saturated thickness of the aquifer as 4.2 m in 5th-order streams and 2.15 m in 2nd-order streams, uniformly throughout the model domain. Average wetted-channel depths in well-network sites were about 0.3 m in the 5th-order stream and about 0.13 m in the 2nd-order stream. I set the wetted-channel depth as 0.3 m in 5th-order stream and 0.15 m in 2nd-order stream, uniformly through out the model domain.

Surface water elevation profiles were input to the model as an initial condition. I used specified-head cells to represent wetted-channel in the model (Figure 2.7).

Upstream

5th-order stream

0.5 m 0.5 m
0.3 m
1.0 m
1.0 m
1.0 m
1.0 m

2nd-order stream

0.3 m 0.3 m
0.15 m
0.5 m
0.5 m
0.5 m
0.5 m

Downstream

Variable head cells

Specified-head cells

General-head or Specified-head cells
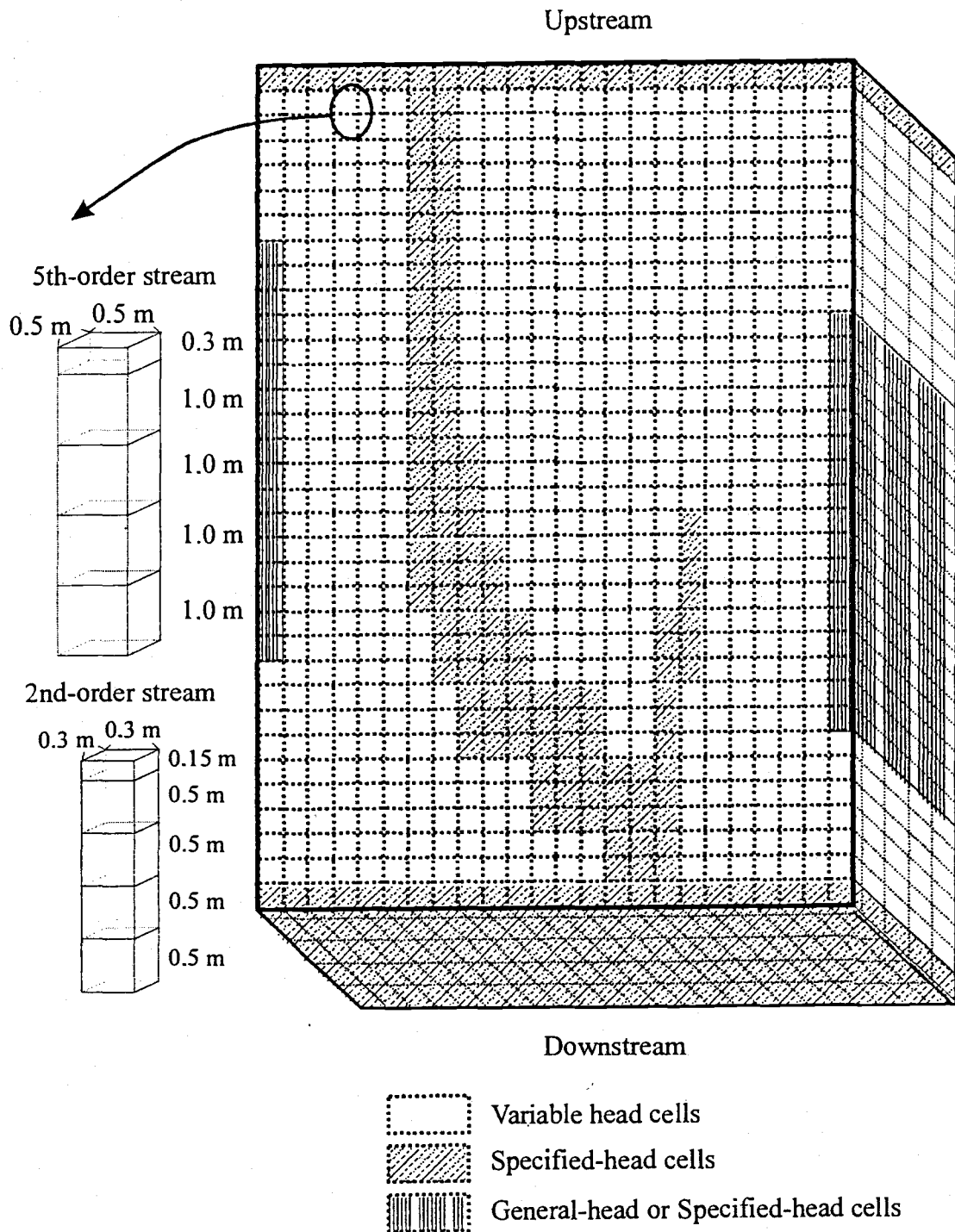
Figure2.7 Idealized figure of 3D view of conceptual model.
Cells in the model domain are for display only
and not shown to actual scale.

Alternatively wetted-channels would have been simulated using the stream package or the river package. The stream package can simulate changes in stream discharge, however, the wetted-channel must be expressed as a single arc. Because my area of interest was small, and the relative size of wetted-channel was large, the stream would have to be represented as multiple arcs running down the wetted-channel. The stream package cannot route stream flow under these conditions and thus could not be used for my simulations. The river package uses conductance to represent a thin, low-conductivity layer between aquifer and the wetted-channel. The conductance, C, is calculated as:

$$C = \frac{K * A}{L}$$

where K is saturated hydraulic conductivity, A is the area through which water flows, and L is the thickness of streambed layer. Distinctive layers with low hydraulic conductivities were not observed in the study reach. Therefore, L is close to 0, and the conductance must be infinitely large. Infinite conductance maximizes water exchanges between river cells and the underlying cells. Consequently, cells below the stream will have the same head value as the river cells, and the bottom of underlying cell will function as the actual streambed in the model. This is identical to treating the stream as a specified-head cell. Therefore, I used specified-head cells to simulate the wetted-channels.

Each model consisted of five layers in a three-dimensional grid. Grid cells in 5th-order stream model were 0.5 m*0.5 m and 0.3 m deep in first layer because this layer contains the stream, and 0.5 m*0.5 m and 1.0 m deep in from the second to fifth layers.

The grid cells in the 2nd-order stream models were 0.3 m*0.3 m and 0.15 m deep in first layer, and 0.3 m*0.3 m and 0.5 m deep in from the second to fifth layer (Figure 2.7).

Parameters, such as saturated hydraulic conductivity and leakance were assigned to each cell in the model domain. Hydraulic conductivity was measured at each well, and was interpolated to the entire model domain. Leakance, LEAK, between the layers was calculated from saturated hydraulic conductivity values as:

$$LEAK = \frac{1}{\frac{\Delta Z_i}{2K_i} + \frac{\Delta Z_{i-1}}{2K_{i-1}}}$$

where ΔZ is the one half distance between mid-points of each cell in the vertical dimension; and K is saturated hydraulic conductivity.

I used the same interpretation tools, as for hydraulic conductivity, to interpolate those values to the entire domain.

The preconditioned conjugate-gradient 2 solver (PCG2, Hill 1990) was used for all simulations. Preconditioned conjugate-gradient is an iterative method, which can be used to solve matrix equations, and PCG2 is a numerical code used with MODFLOW.

The volume of hyporheic exchange flow was calculated as the amount of water flowing out of the wetted-channel and into aquifer, assuming all water, which flows out of the wetted-channel, would flow back into the wetted-channel at some point downstream, and thus represents hyporheic exchange flow.

2.6.3 Model Calibrations

Models were calibrated after the initial run to fit predicted hydraulic head distribution to the observed water table elevation in wells. I calibrated the models by

changing the distribution of saturated hydraulic conductivity and side-boundary conditions. Mean absolute errors of predicted head values were used as criteria to choose final models.

I tried Universal Kriging, Section average and Thiessen Polygon methods to interpolate the saturated hydraulic conductivity to the model domain. Kriging is a generalized linear regression and estimates variables in the sense of minimizing the mean square error. Universal kriging removes two requirements from simple kriging; the need to have a known mean and to assume a constant head (Anderson and Woessner 1992, Olea 1999). The section average method divides the model domain into several sections using the trend of hydraulic conductivity. For example, if the conductivity values at toe slopes of hill were lower than in near-stream area, I would divide the floodplain into, hill side and streamside. Then, I would average the values within each section to get a representative value for the section. The Thiessen Polygon method estimates conductivity at each cell assuming that the cell has the same conductivity as the closest well. I also changed the boundary conditions during the calibration processes. Parts of general-head boundaries, where I detected strong lateral inflow, were switched to specified-head boundaries.

The final models used Thiessen polygon method because the Thiessen polygon methods had slightly smaller errors in simulation results than models using other interpretation methods in three out of four well networks. The results of model calibration are shown in Figure 2.8 and 2.9.

Models created for well-network sites were used as templates for the further analysis. I used the simulation model of WS01 to represent of 2nd-order streams and

a)

Simulation #	
1	K -- Universal Kriging
	Side-boundary -- Combination of general-head and no-flow boundaries
2	K -- Section Average
	Side-boundary -- Combination of general-head and no-flow boundaries
3	K -- Thiessen Polygon
	Side-boundary -- Combination of general-head and no-flow boundaries
4	K -- Thiessen Polygon, the value at well D5 was change to 0.006 m/min
	the value at well C5 was changed to 0.001 m/min
	the value at C6 was changed to 0.00218 m/min
	Side-boundary -- Combination of general-head and no-flow boundaries

b)

Simulation #	
1	K -- Universal Kriging
	Side-boundary -- Combination of general-head and no-flow boundaries
2	K -- Universal Kriging
	Side-boundary -- Combination of general-head, specified-head and no-flow boundaries
3	K -- Section Average
	Side-boundary -- Combination of general-head, specified-head and no-flow boundaries
4	K -- Thiessen Polygon
	Side-boundary -- Combination of general-head, specified-head and no-flow boundaries
5	K -- Thiessen Polygon, the value at well I6 was decreased to 0.009 m/min
	the value at well G4 was decreased to 0.0009 m/min
	the value at well G5 was decreased to 0.078 m/min
	the value at well I4 was increased to 0.046 m/min
	the value at well I6 was increased to 0.057 m/min
	Side-boundary -- Combination of general-head, specified-head and no-flow boundaries

Figure 2.8 Change in simulation errors through the calibration processes at **a)** WS01; **b)**WS03.

a)

Simulation #	
1	K – Universal Kriging Side Boundary -- Combination of general- head and no-flow boundaries
2	K-- Universal Kriging Side-boundary -- Combination of specified-head and no-flow boundaries
3	K – Section Average Side-boundary -- Combination of specified-head and no-flow boundaries
4	K – Thiessen Polygon Side-boundary -- Combination of specified-head and no-flow boundaries
5	K- Thiessen Polygon, the value at well 5 was increased to 0.420 m/min the value at well 6 was decreased to 0.445 m/min the value at, well 11 was decreased to 0.120 m/min the value at well 29 was decreased to .0230 m/min Side-boundary -- Combination of specified-head and no-flow boundaries
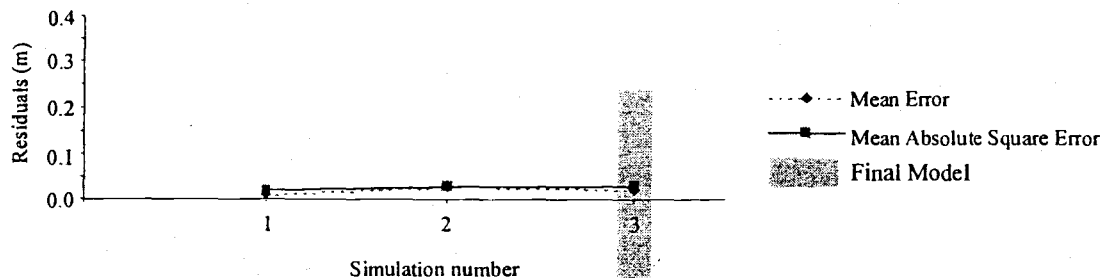
b)

Simulation #	
1	K – Universal Kriging Side-boundary -- Combination of general-head and no-flow boundaries
2	K -- Section Average Side-boundary -- Combination of general-head and no-flow boundaries
3	K -- Thiessen Polygon Side-boundary -- Combination of general-head and no-flow boundaries

Figure 2.9 Change in simulation errors through the calibration
processes at **a)** Middle Lookout site; **b)**Lower Lookout site.

Middle Lookout for 5th-order streams. I will call the model created for WS01 as the WS01 model, and the model for Middle Lookout as the Middle Lookout model.

2.6.4 Analysis to estimate effects of geomorphic features on hyporheic exchange

Calibrated models of 2nd and 5th order streams, WS01 and Middle Lookout models, were used to analyze the relative contribution of each geomorphic feature to hyporheic exchange. I removed one geomorphic feature at a time from the models and then reran the model to simulate subsurface flow without that particular feature. For each model run, I recorded the volume of hyporheic exchange flow, assuming that reduction in the volume of hyporheic exchange flow after the removal of features indicates the contribution of the particular feature. Both WS01 and Middle Lookout models contained secondary channels, channel splits, steps or riffles and sinuosity, so these features were removed from models. When secondary channels were removed, the main wetted channel was left unchanged. The channel with least discharge was removed from channel splits. I also straightened the main channel to remove the sinuosity, and steps and riffles were removed to smooth the longitudinal profile of the stream water elevation. However, well-network sites were not necessarily representative of geomorphic features found within the study reach. Therefore, I built simplified models of idealized streams to further analyze the range of geomorphic features present in the study reaches. I will call these models as simplified-stream models.

Simplified stream model were sized to represent the average RSL surveyed in 2nd- and 5th-order reaches, although the floodplain width and active channel width represent the unconstrained reach only. The model domains were 50 m long and 14.75 m wide for

the 2nd-order stream, and 160 m long and 46 m wide for the 5th-order stream. The grid cell sizes were the same as the models built for well-network sites: 0.3 m x 0.3 m x 0.15 for 1st layer and 0.3 m x 0.3 m x 0.5 m for the second through fifth layers and for 2nd-order stream; 0.5 m x 0.5 m x 0.3 m for 1st layer and 0.5 m x 0.5 m x 1.0 m for the second through fifth layers.

Geomorphic features were added to these simplified stream models. The size and frequency of occurrence of each feature was constructed to represent the average, maximum and minimum sizes of each feature measured in the stream survey. The range of effects caused by secondary channels and channel splits was examined by changing the length and the cross-valley gradient between the two wetted-channels. I changed the length of secondary channel while keeping average cross-valley gradient constant, and in the same way, I changed the cross-valley gradient while keeping average length constant. The effects of channel steps on hyporheic exchange flow result from both size and number, and I created maximum, average and minimum sizes of steps. The number of steps was determined by dividing the change in elevation within the model domains accounted for steps by the step size. The observed numbers of steps were used as cut-off values. The longitudinal length of each step was 1 m in 2nd-order stream and 5 m in 5th-order streams because those were the measurement intervals used to survey steps and riffles, respectively. Sinuosity was created in the simplified streams by bending the wetted-channels. Channel gradient itself does not drive exchange flow. However, channel gradient may interact with other features. Thus, I analyzed the interaction of channel gradient with steps and sinuosity. I changed the channel gradient in the simplified stream models, representing average sized steps and average sinuosity.

2.6.5 Estimation of residence time

A particle tracking post-processing package, MODPATH (Pollock 1994), was used to estimate the residence time of hyporheic exchange flows. The MODPATH model tracks particles using the flux and flow direction simulated by MODFLOW, and can estimate the time that each particle takes to travel from starting point to an end point. I used wetted-channels as starting points and tracked particles until these particles returned to the wetted-channels. I estimated residence time using the calibrated models of well-network sites. Nine particles per stream cell (specified head cells) were introduced in the WS01, WS03 and Lower Lookout models, and 3 particles per stream cell (specified head cells) were introduced in the Middle Lookout models. MODPATH requires porosity for each cell in the model domain. Porosity was not measured at any of the sites. Aquifer sediment at all sites was a mixture of boulders, gravel and sand, for which porosity ranges from 0.25 to 0.35 (Fetter 1994). I used an average value of 0.3 in all model simulations. I also simulated residence time of hyporheic exchange flow in the models, from which one of features was removed, for the WS01model or the Middle Lookout model, to analyze the effects of geomorphic features on residence time of hyporheic exchange flow.

Histograms of residence times were used to investigate the frequency distributions. Because the total numbers of particles were different among the models, I normalized the frequency distributions of residence time to a percentage of the total number of particles. Also, I estimated volume of hyporheic exchange flow with specific residence time by multiplying percentage of particles in each residence time class by the volume of hyporheic exchange flow in a 100 m stream length. To compare between

streams, I calculated the difference between distributions by subtracting one distribution

from another.

3.   **RESULTS**

3.1.   Geomorphic Characteristics of 2nd-order and 5th-order Streams

3.1.1 2nd-order streams

The valley floor of WS01 was twice as wide as the floor of WS03, although wetted-channel widths were the same. Because WS01 had a wider valley floor, I expected greater sinuosity in WS01 than in WS03. However, sinuosity was 1.1 m/m in both reaches (Table 3.1). The average longitudinal gradients were 0.13 m/m in both reaches, although the range among RSLs was greater in WS03 (0.09 to 0.16 m/m). Although high channel gradients suppress the development of meandering channels, boulders and logs obstruct water flow and deflect the wetted channels. Because the channel bends resulting from these obstructions are small, differences in valley constraint did not affect the sinuosity. Both sites averaged 3 to 4 steps per RSL. The contribution of steps to the change in elevation was significant, accounting for more than 50 % of the elevation changes in each reach (Table 3.1). Interactions between the stream and riparian forests introduce many logs and boulders into the stream channel. These large materials formed steep steps in the wetted-channels (Figure 3.1-a). Large wood was the key step-forming material in WS01, whereas boulders were the key materials in WS03. Large steps (>0.15 m/m) were created where large logs blocked the stream, and sediment accumulated behind the logs. Medium sized steps were created by jams of logs or of boulders. Small steps were created by collections of a few small boulders.

		Average Channel width (m)	Average valley width (m)	Average Channel gradient (m/m)	Sinuosity (m/m)	Number of Drops	Contribution of drops to the change in elevation (%)
WS01 (unconstrained)	RSL 1	1.47	14.51	0.141	1.183	5	67.1
	RSL 2	1.84	14.14	0.119	1.100	3	48.2
	RSL 3	1.30	12.43	0.106	1.033	3	53.0
	RSL 4	1.42	18.33	0.115	1.150	2	44.0
	RSL 5	2.43	15.61	0.151	1.350	6	50.6
	RSL 6	2.20	13.46	0.133	1.000	3	43.1
	Sub. Ave.	1.78	14.75	0.128	1.136	3.7	51.0
WS03 (constrained)	RSL 7	1.81	5.63	0.125	1.156	1	38.2
	RSL 8	1.37	5.24	0.138	1.020	4	56.9
	RSL 9	1.58	7.54	0.090	1.088	2	38.0
	RSL 10	1.86	7.47	0.139	1.190	5	60.1
	RSL 11	2.15	8.30	0.098	1.088	5	79.0
	RSL 12	2.35	9.70	0.135	1.293	3	55.6
	RSL 13	1.76	11.20	0.155	1.054	1	49.2
	Sub. Ave.	1.84	7.87	0.126	1.127	3.0	53.9
	Total Ave.	1.81	11.04	0.13	1.13	3.31	52.54
	Max.	2.43	18.33	0.155	1.350	6	79.0
	Mini.	1.30	5.24	0.090	1.020	1	38.0

Table 3.1 Channel characteristics measured in each RSL in the study reaches of the unconstrained (WS01) and constrained (WS03), 2nd-order streams

a)
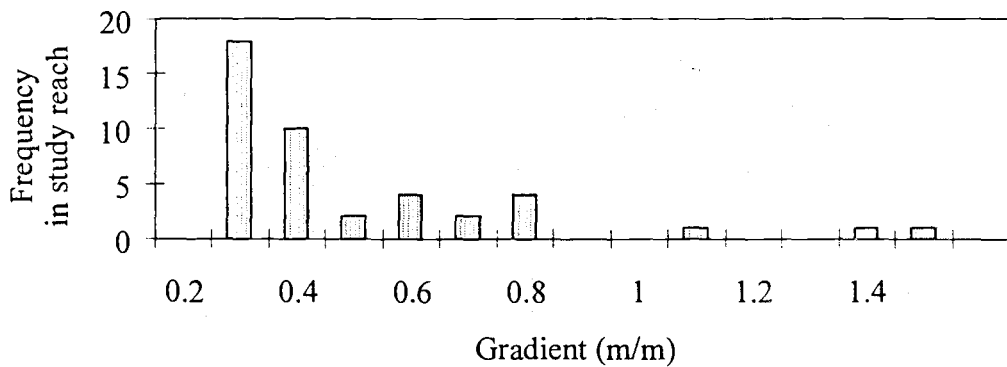
b)
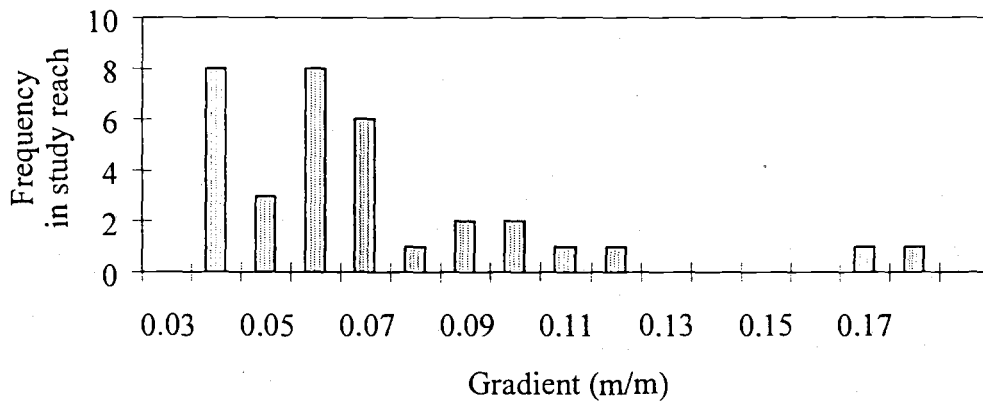
Figure 3.1 Frequency distribution of gradients of **a)** steps in 2nd-order streams,
b) riffles in 5th-order streams (All RSLs are combined)

Secondary channels and channel splits in 2nd-order streams were not easily

distinguishable, so I combined these two features, calling them all secondary channels.

The study reach of WS01 had three secondary channels, where as WS03 had seven

secondary channels. Most of those secondary channels were short, and water flowed

from main channel into the secondary channels in seven out of ten cases (Table 3.3-a).

The cross sections of water table observed in well networks showed there was little

lateral groundwater inflow at either site, although WS03 had slightly stronger

groundwater inflow than WS01.

a)

b)
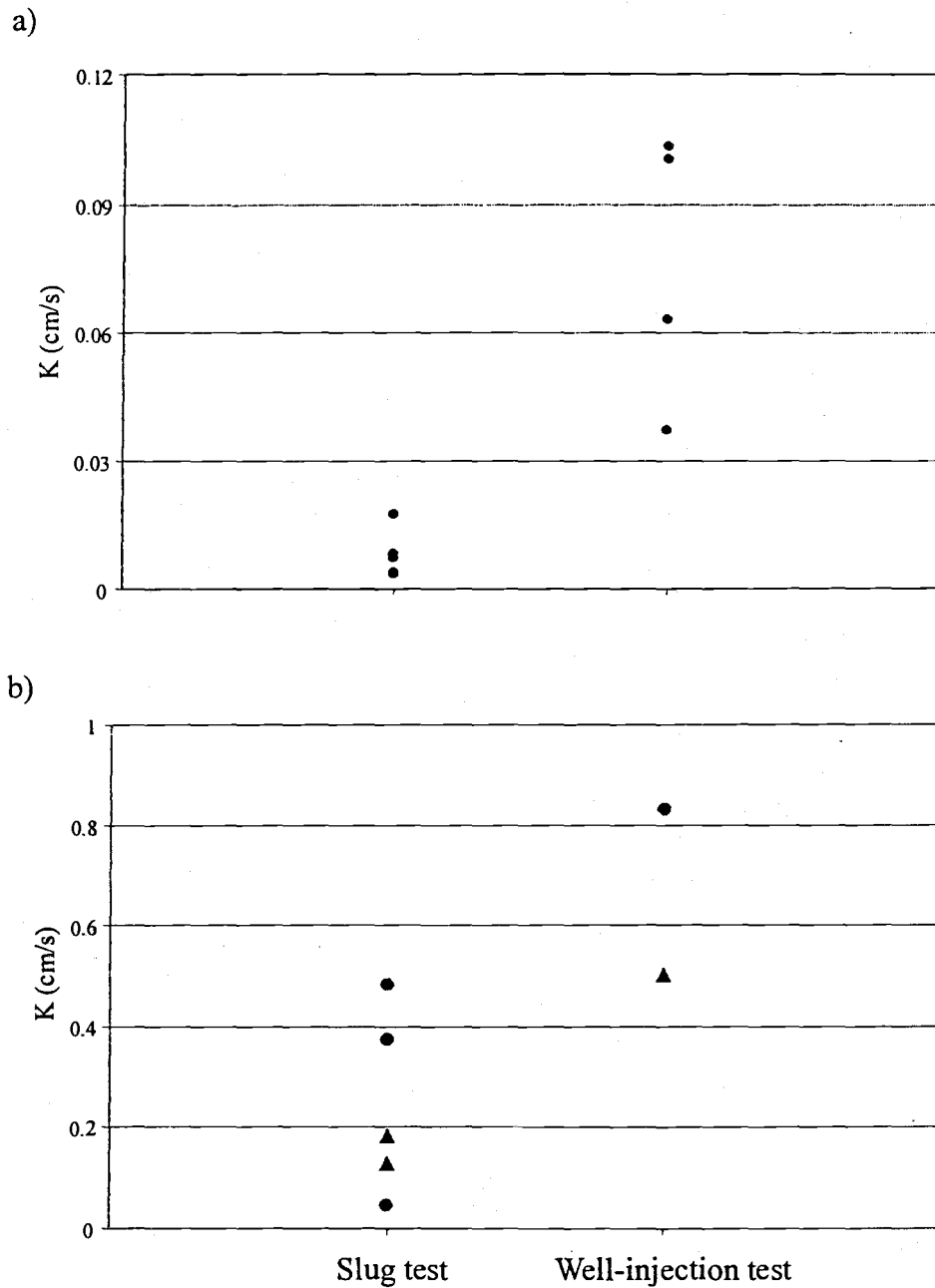
Figure 3.2 Comparison of saturated hydraulic conductivity estimated from tracer injections and from slug tests from wells where both techniques were used. **a)** WS01, and **b)** 5th-order stream, where ▲ is the Middle Lookout site, and • is the Lower Lookout site

Although I expected more complexity in WS01 because the study reach is less constrained, there was no substantial difference between the study reaches. Vertical features tended to dominate channel morphology, and there were few horizontally extensive features in either reach. Thus, valley-floor constraint did not appear to affect the types, size or frequency of geomorphic feature in either of these high gradient mountain streams. Also, the valley width was more than three times of the active channel width in WS03, and the valley floor might be wide relative to the stream size, even though the WS03 reach was more constrained than the WS01 reach.

Saturated hydraulic conductivities estimated from slug tests and a well injection test showed large differences. The geometric mean of saturated hydraulic conductivity obtained by continuous tracer injection in WS01 was 0.075 cm/s, which about 10 times higher than the conductivity obtained by slug tests (Figure 3.2-a). Only one tracer injection was conducted, and the results applied only to a small area of the WS01 well network. In contrast, the wells used for slug tests were widely spread across the well-network site. Therefore, I used only the conductivity obtained from slug tests for model simulations. The geometric averages of saturated hydraulic conductivity estimated by slug tests were 0.007 cm/s in both WS01 and WS03 sites. The conductivities range from 0.15 cm/s to 0.00001 cm/s (Figure 3.3).

3.1.2 5th-order streams

There were differences in number of RSLs surveyed in the constrained and unconstrained 5th-order stream reaches. I surveyed only two RSLs in the Lower Lookout reach, whereas I surveyed eight RSLs in Middle Lookout reach. Therefore, the
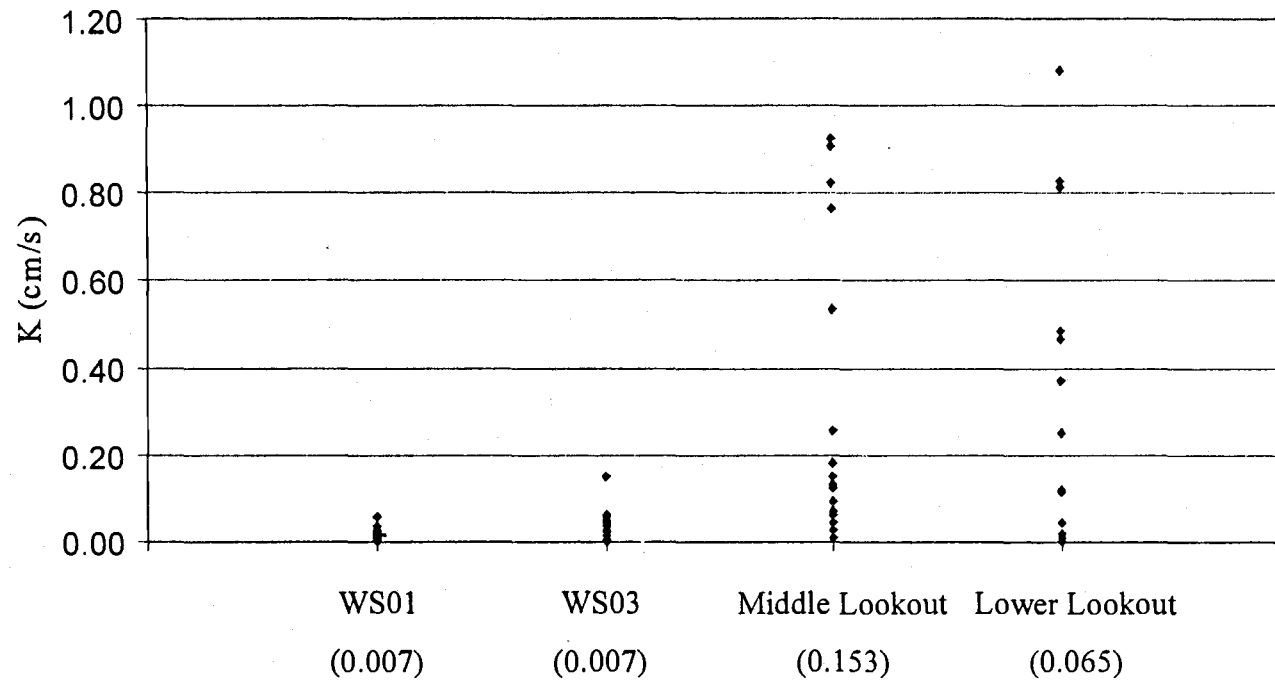
Figure 3.3 Saturate hydraulic conductivities (K) measured from all wells in each well-network site
* number in the ( ) is the geometric means

geomorphic features of the constrained reach may be poorly characterized in comparison with the unconstrained 5th-order study reach. However, the channel in Lower Lookout was very simple. I assumed that I captured the characteristics of geomorphic features with only two RSLs.

Average active-channel widths in Middle Lookout reach were more than twice as wide as in Lower Lookout, where as average wetted-channel widths were the same (Table 3.2). Bedrock walls in Lower Lookout constrained the channel, and limited sinuosity to only 1.09 m/m. Middle Lookout, where the wetted-channel often shifted location across the active channel, had average sinuosity of 1.3 m/m. Channel gradients were slightly higher in Middle Lookout reach than Lower Lookout reach, and gradients of 5th-order Lookout Creek were one tenth of the 2nd-order streams. On averaged 4 riffles per RSL were found in Middle Lookout and accounted for about 50 % of total elevation change within the study reach. In contrast, only 1.5 riffles per RSL were found in Lower Lookout reach and accounted for about 40 % of elevation change. The gradients of riffles were not diverse, ranging from 0.03 to 0.18 m/m (Figure 3.1-b).

Secondary channels seem to be common in the unconstrained reach of Lookout Creek. Six secondary channels were present in the 10 meander-bars surveyed in the Middle Lookout study reach (Table 3.3-b). Additionally, there were old channels, which do not have flowing surface water during summer base-flow period, at the bars lacking secondary channels. In all cases, secondary channels had lower surface water elevations than did the main channel so that hyporheic exchange flowed from the main channels toward the secondary channels. I separated channel splits from secondary channels because their locations were different, and because the channel splits had higher cross-

		Average Channel width (m)	Average valley width (m)	Average Channel gradient (m/m)	Sinuosity (m/m)	Number of Drops	Contribution of drops to the change in elevation (%)
Middle Lookout (unconstrained)	RSL 1	9.19	44.80	0.020	1.349	5	65.5
	RSL 2	8.47	48.84	0.023	1.158	4	68.0
	RSL 3	9.67	27.88	0.025	1.035	1	38.6
	RSL 4	9.26	44.04	0.022	1.075	3	36.0
	RSL 5	7.24	32.25	0.016	1.156	3	54.2
	RSL 6	10.01	27.53	0.019	1.168	2	28.8
	RSL 7	8.32	32.40	0.021	1.683	4	44.9
	RSL 8	6.26	52.00	0.024	1.492	10	66.3
	Sub. Ave.	8.55	38.72	0.021	1.264	4	50.3
Lower Lookout (Constrained)	RSL 9	8.36	16.17	0.013	1.013	1	38.7
	RSL 10	8.97	17.38	0.014	1.163	2	40.7
	Sub. Ave.	8.67	16.77	0.013	1.088	1.5	39.7
	Total Ave.	8.58	34.33	0.02	1.23	3.5	48.17
	Max.	10.01	52.00	0.025	1.683	10	68.0
	Mini.	6.26	16.17	0.013	1.0125	1	28.8

Table 3.2 Channel characteristics measured in each RSL in the study reaches of the unconstrained (Middle Lookout) and constrained (Lower Lookout), 5th-order streams

a) 2nd-order stream

| | Secondary Channel | |
	Length (m)	Average gradient (m/m)
#1	13.8	-0.082
#2	12.2	-0.090
#3	9.8	-
#4	2.8	0.055
#5	9.6	0.091
#6	8.4	0.191
#7	10.6	-0.123
#8	7.4	0.154
#9	9.0	0.074
#10	6.1	0.116
Ave.	8.97	0.097

b) 5th-order stream

| | Secondary Channel | | Channel Split | |
	Length (m)	Average gradient (m/m)	Length (m)	Average gradient (m/m)
#1	71.6	0.021	19.2	0.042
#2	100.8	0.007	28.0	0.038
#3	107.2	0.015	41.0	0.039
#4	48.8	0.019		
#5	88.6	0.005		
#6	54.0	0.017		
Ave.	78.5	0.014	29.4	0.040

Table 3.3 Secondary channels and channel splits surveyed in the study reaches of a) 2nd-order streams (WS01 and WS03) and b) 5th-order unconstrained, Middle Lookout (secondary channels and channel splits were not present in constrained, Lower Lookout)
*negative gradients indecates flow from secondary channel towatd main channel

valley gradients than did secondary channel (Table 3.3-b). The high gradients resulted from relatively short distances between the two channels because the absolute changes in head between split channels were similar to those measured between main channels and secondary channels.

The Middle Lookout reach had horizontally extensive features, such as secondary channels and channel splits, in addition to vertically extensive features. Because the channel gradients were relatively small, the location of the wetted-channel can easily shift where channels are not constrained. In contrast, riffles were the only sources of geomorphic complexity in the Lower Lookout study reach. Therefore, channel constraint strongly controlled the expression of geomorphic features in the two 5th-order streams reaches studied.

Saturated hydraulic conductivities estimated from slug test and well injection test showed large differences in both Middle and Lookout sites. The geometric mean of saturated hydraulic conductivity obtained by continuous tracer injection was 0.50 cm/s in Middle Lookout and 0.83 cm/s in Lower Lookout site. These values were about 3 to 4 times higher than the hydraulic conductivity estimated from slug tests (Figure 3.2-b). Only one tracer injection was conducted at each site, and the results apply only to a small area in each well network. In contrast, the wells used for slug tests were widely spread across each well-network site. Therefore, I used the conductivity estimated from slug tests in model simulations. The geometric means of saturated hydraulic conductivity were 0.15 cm/s in Middle Lookout and 0.07 cm/s in Lower Lookout (Figure 3.3).

3.2.   Hyporheic Exchange Flow in Well-Network Sites

3.2.1   Spatial Extent of the Hyporheic Zone

3.2.1.1   2nd-order streams

Distribution of hydraulic-head simulated in well-network sites of 2nd-order

streams (Figure 3.4-a, b) showed that steps were the primary features creating spatially

extensive hyporheic zones and those steps with higher head-gradients created more

extensive hyporheic zones. Further, steps were numerous, so that their contribution to

hyporheic exchange flow should be substantial (Figure 3.4-a, b). Although secondary

channels are known to drive hyporheic exchange, they appeared to have a relatively small

influence on the distribution of hydraulic head so that their contribution to the total

hyporheic exchanges flow should be small. Most hyporheic flow paths in 2nd-order

stream sites were short, although a few flow paths extended the full length of the well-

network sites. All flow paths were strongly directed down-valley, so that flow paths did

not extend far from the streams.

3.2.1.2   5th-order streams

Distribution of hydraulic heads simulated in groundwater flow model of well

network sites in 5th-order stream (Figure 3.4-c, d) showed that the secondary channels

and channel splits were the primary factors creating spatially extensive hyporheic zones.

Figure 3.4-a Equipotential lines (0.1 m interval) describing the spatial distribution of hydraulic head at WS01. Hydraulic heads are from MODFLOW simulations. Averaged difference in hydraulic head between simulation and observation was 0.09 m.
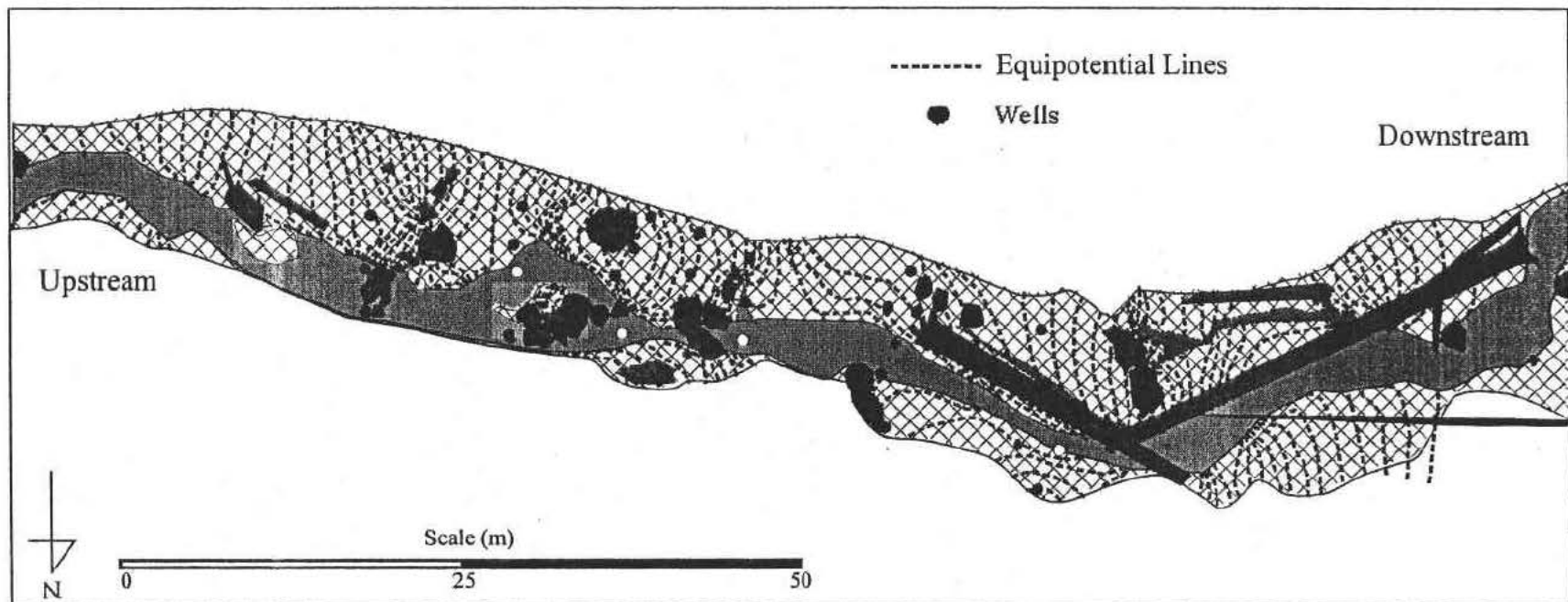
Figure 3.4-b Equipotential lines (0.1 m interval) describing the spatial distribution of hydraulic head at WS03. Hydraulic heads are from MODFLOW simulations. Averaged difference in hydraulic head between simulation and observation was 0.11 m.
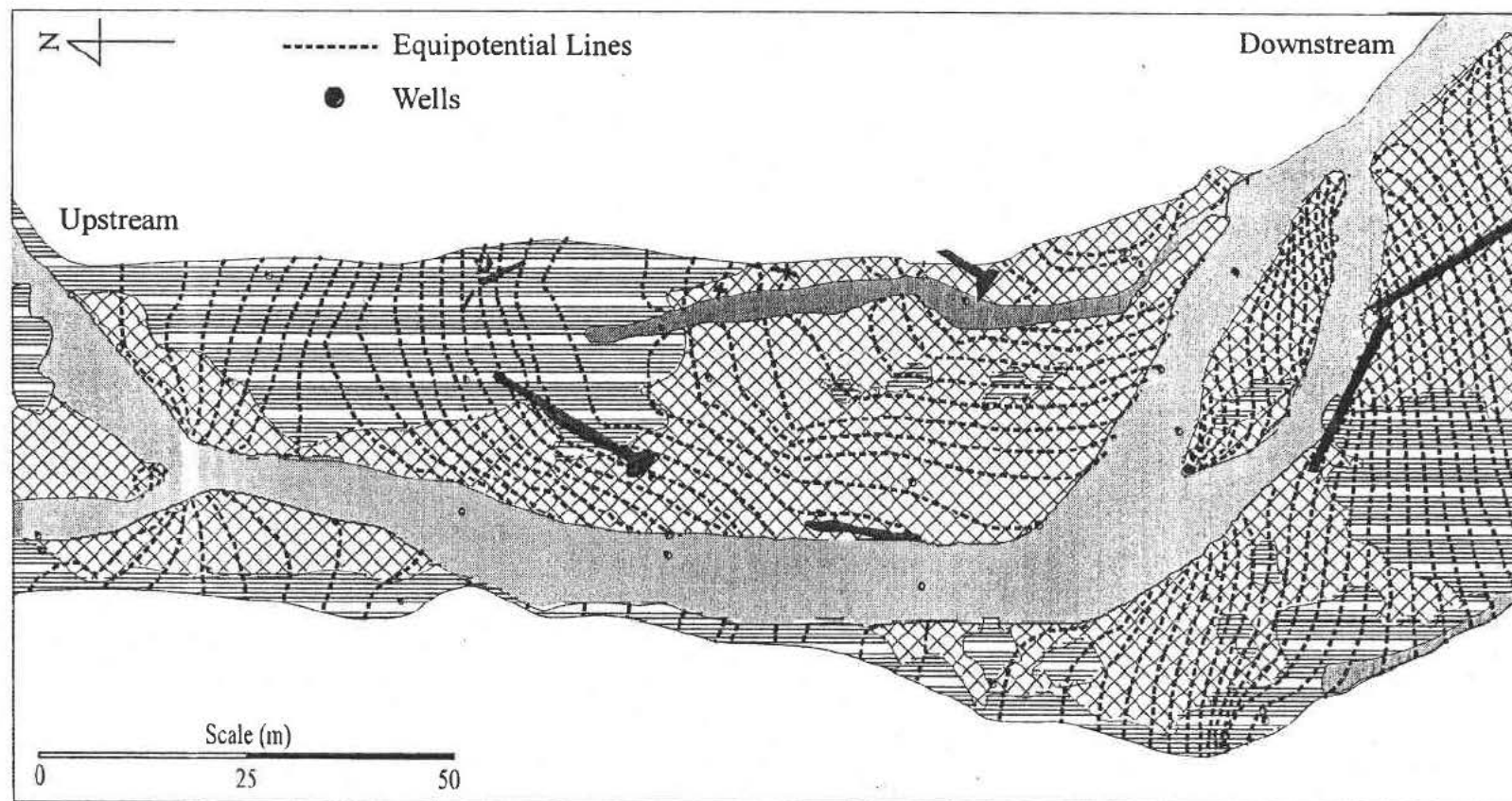
Figure 3.4-c Equipotential lines (0.1 m interval) describing the spatial distribution of hydraulic head at Middle Lookout.. Hydraulic heads are from MODFLOW simulations. Averaged difference in hydraulic head between simulation and observation was 0.16 m.
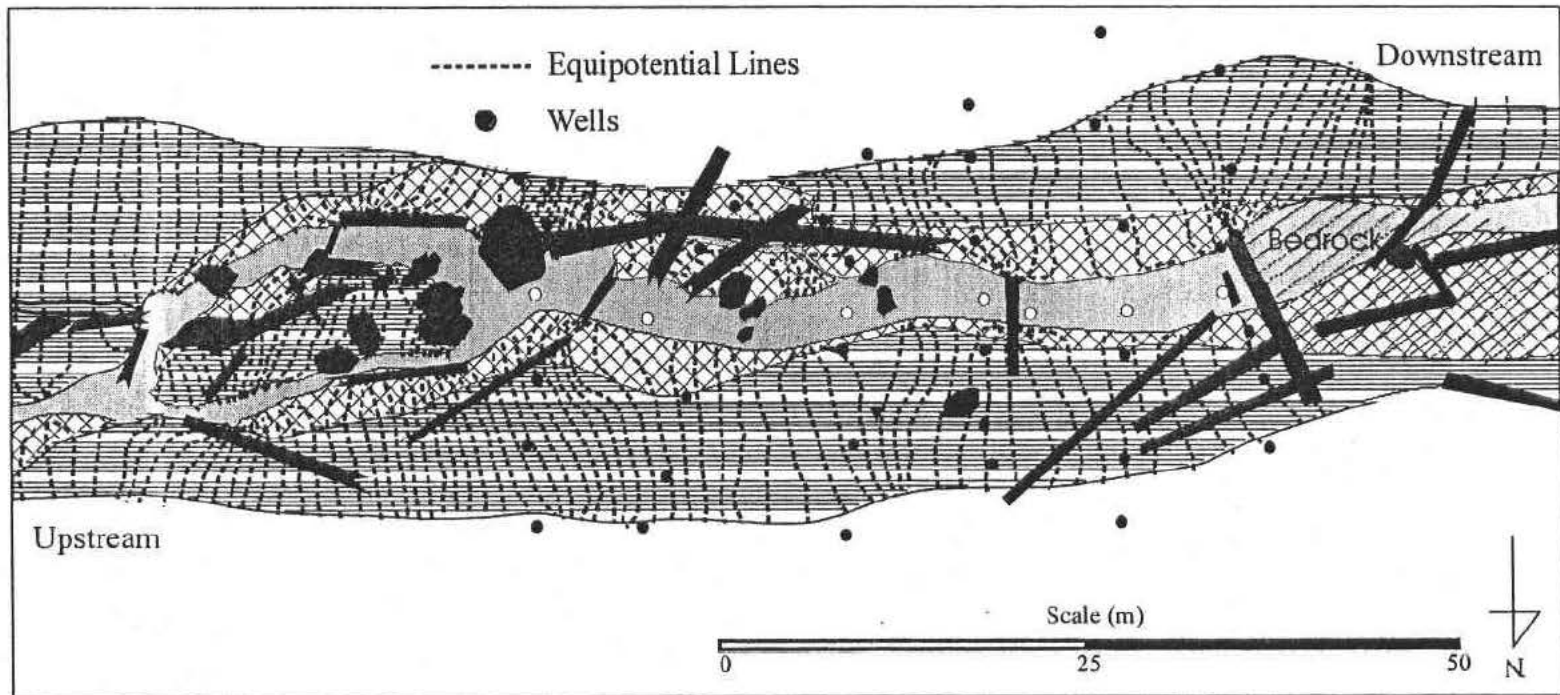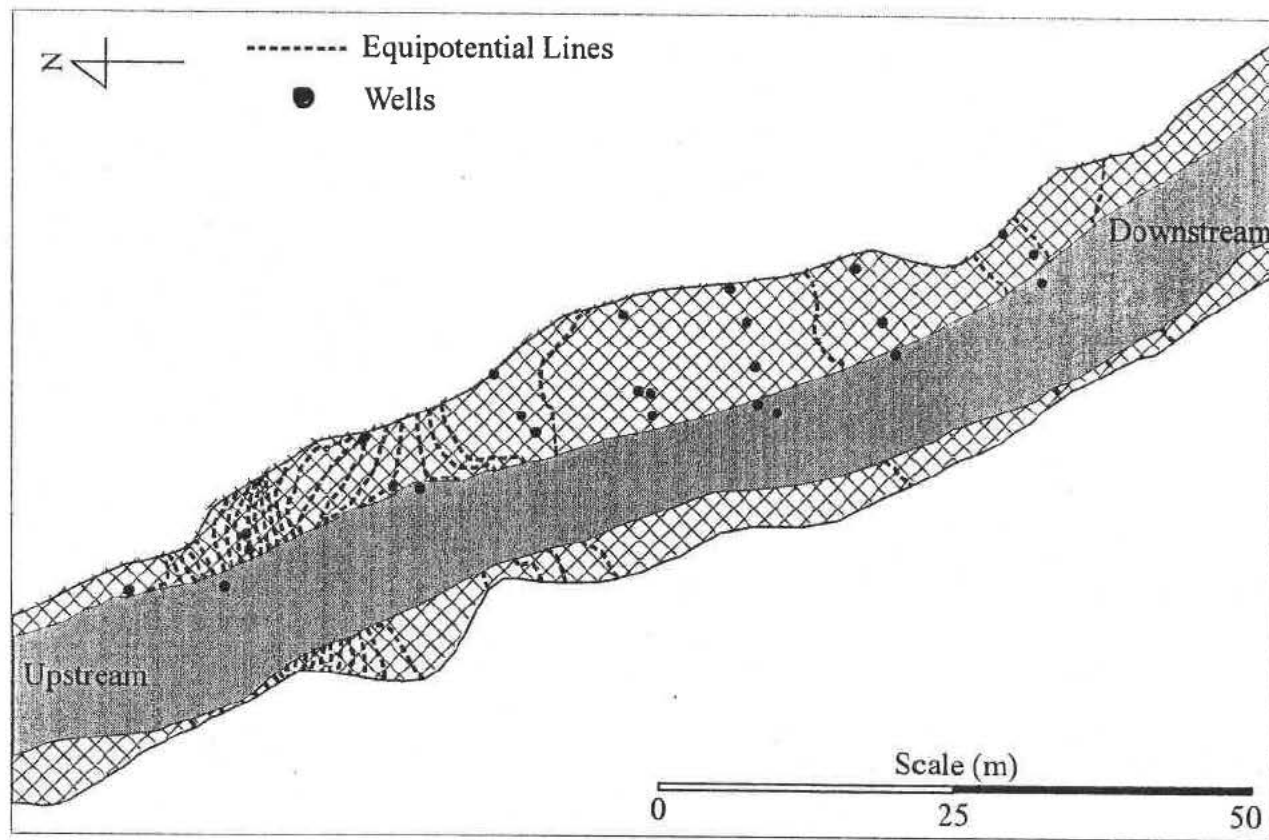
FIgure 3.4-d Equipotential lines (0.05 m interval) describing the spatial distribution of hydraulic head at Lower Lookout.. Hydraulic heads are from MODFLOW simulations. Averaged difference in hydraulic head between simulation and observation was 0.03 m.

Secondary channels, especially, drove laterally extensive hyporheic exchange flow, where hyporheic flow paths extended about 30 m from the main channel toward secondary channel. However, head gradients were shallow so that the exchange rates were relatively low. In contrast, teep cross-valley gradients were present between the split channels (Figure 3.4-c) and created hyporheic zones with short flow paths and high rates of exchange flow. Channel sinuosity was highly interactive with other features. For example, secondary channels were present in most meander bends. Thus, it was difficult to identify the effect of sinuosity alone.

Pool-riffle sequences were the primary geomorphic feature driving hyporheic exchange flow in the Lower Lookout study reach. However, the flow paths were short and only extended over limited areas (Figure 3.4-c), and so appeared to have little effect on overall hyporheic exchange flow. Secondary channel and channel splits were not present in Lower Lookout study reach. There were also stronger groundwater inflows at this site (Figure 3.4-d). Consequently, hyporheic exchange was limited in the 5th-order constrained site.

3.2.2 Volume of Hyporheic Exchange Flow

The hyporheic exchange flow budget estimated from calibrated MODFLOW simulations of the WS03 site was 6.67 l/s per 100m of stream channel which was twice as large as in WS01 (Figure 3.5-a). Hyporheic exchange in the Middle Lookout site was approximately 50 l/s per 100m of stream channel and about 20 times more than the Lower Lookout site (Figure 3.5-a). Thus, there were much larger differences in the
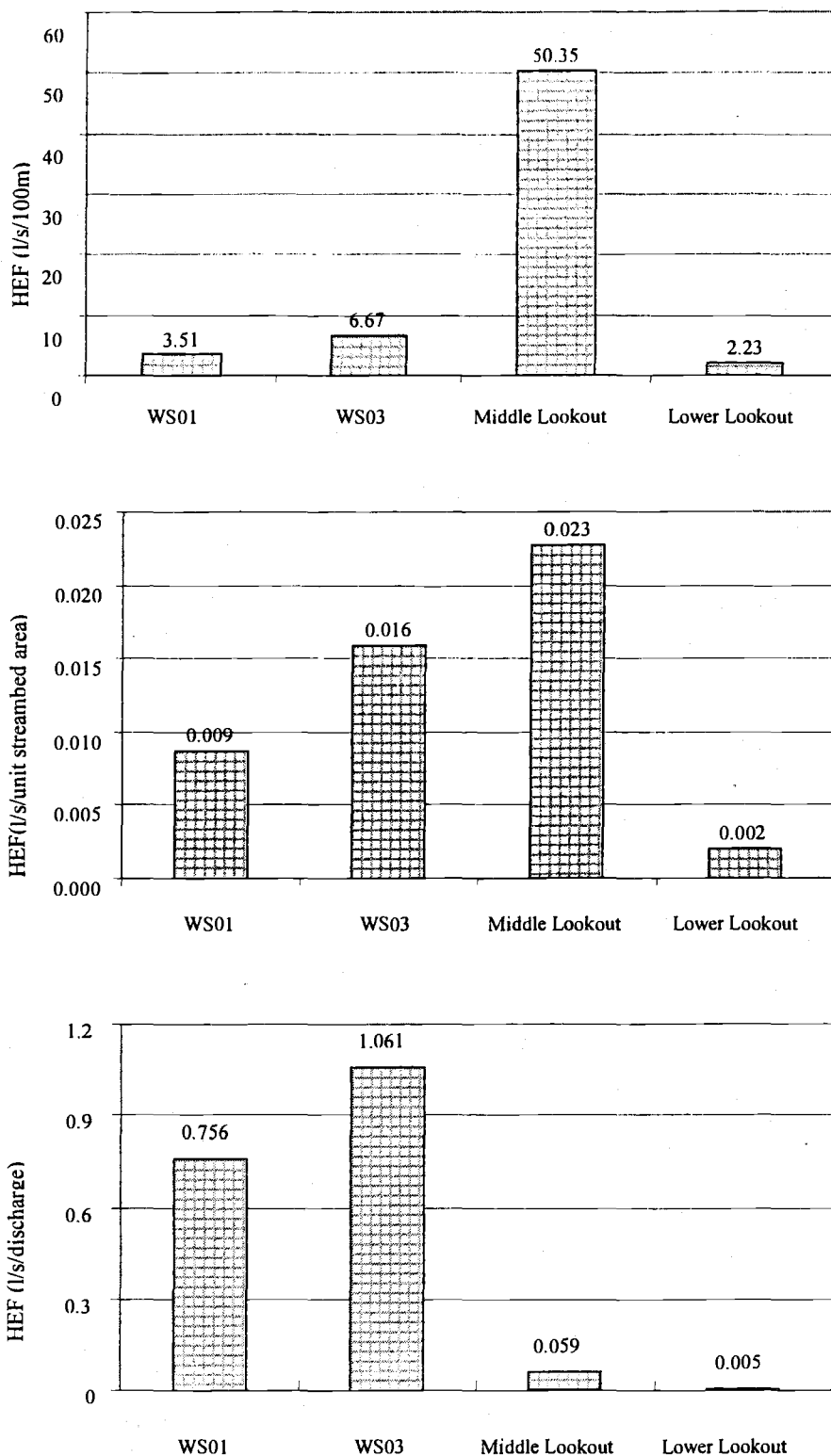
Figure 3.5 Hyporheic exchange flow (HEF) estimated from MODFLOW
simulations of the four well-network sites
a) HEF per 100 m of channel length, **b)** HEF per unit streambed
area, and **c)** relative volume of HEF to stream discharge

volume of hyporheic exchange between unconstrained and constrained sites in 5th-order stream sites than sites in 2nd-order streams.

There were also large differences between Middle Lookout and 2nd-order stream sites. For example, Middle Lookout site had about 8 times more hyporheic exchange than did the WS03 site when expressed per 100 m of stream channel (Fig 3.5-a). However, I expected that the area of wetted channel would, in part, determine the amount of hyporheic exchange flow, and would confound comparisons between streams of different orders. The larger contact areas increase opportunity of water exchange. Wider wetted-channels in 5th-order streams create more contact area between stream and sediment than do the narrow wetted-channels in 2nd-order streams. Normalizing hyporheic exchange flow to unit streambed area showed that 2nd-order streams were more similar to the 5th-order unconstrained site. The volume per unit streambed area in Middle Lookout was just 2.6 times of that in WS01 and 1.4 times of that in WS03. The volume per unit streambed area of hyporheic exchange in Lower Lookout was the smallest of the four sites and was about 10 times less than Middle Lookout site and 8 times less than WS03 (Figure 3.5-b). Although widths of wetted-channel in Middle Lookout and Lower Lookout sites were same, the hyporheic flow per unit area were considerably different, demonstrating the effects of channel constraint on the development of geomorphic features that control hyporheic exchange flow in the large streams. In contrast, 2nd-order streams had similar volume of hyporheic flow between unconstrained and constrained sites.

The effects of hyporheic exchange flow on stream ecosystems might be proportional to the ratio of hyporheic exchange to stream discharge. This relative volume

of hyporheic exchange to stream discharge has been compared among various streams in previous studies (D'Angelo et al. 1993, Morrice et al. 1997). The relative volume of hyporheic exchange was very large in 2nd-order streams. About 76 % of stream discharge flowed through the hyporheic zone in 100 m in WS01, and more than 100% of stream discharge flowed through the hyporheic zone in WS03. On the other hand, only 5 and 0.6 % of stream discharge were exchanged with the subsurface per 100 m of unconstrained and constrained 5th-order stream reaches, respectively (Figure 3.5-c). Clearly, the hyporheic exchange relative to stream discharge was small in the 5th-order stream.

3.2.3 Residence Time of Hyporheic Exchange Flow

Frequency distributions of estimated residence times of hyporheic exchange flow showed that high volume of hyporheic exchange had short residence times, and the residence time were exponentially distributed in Middle Lookout, WS01 and WS03 sites (Figure 3.6-a, b, c). Further, these sites had peaks in similar time ranges. The peaks of the frequency distribution were at 2 hours in Middle Lookout and WS03 sites and at 4 hours in WS01. Median residence time in Middle Lookout site was 27 h. Median residence times in WS01 and WS03 were 18 h.

Tails of the frequency distributions showed different trends. The Middle Lookout site and WS01 had short tails, and only 0.13 % and 0.9 % of hyporheic exchange had residence time over 800 hours (Figure 3.6-a, c). WS03 site had longer tails, and 5 % of hyporheic exchange had residence time longer than 800 h (Figure 3.6-b). The Lower Lookout site had a different distribution of estimated residence time
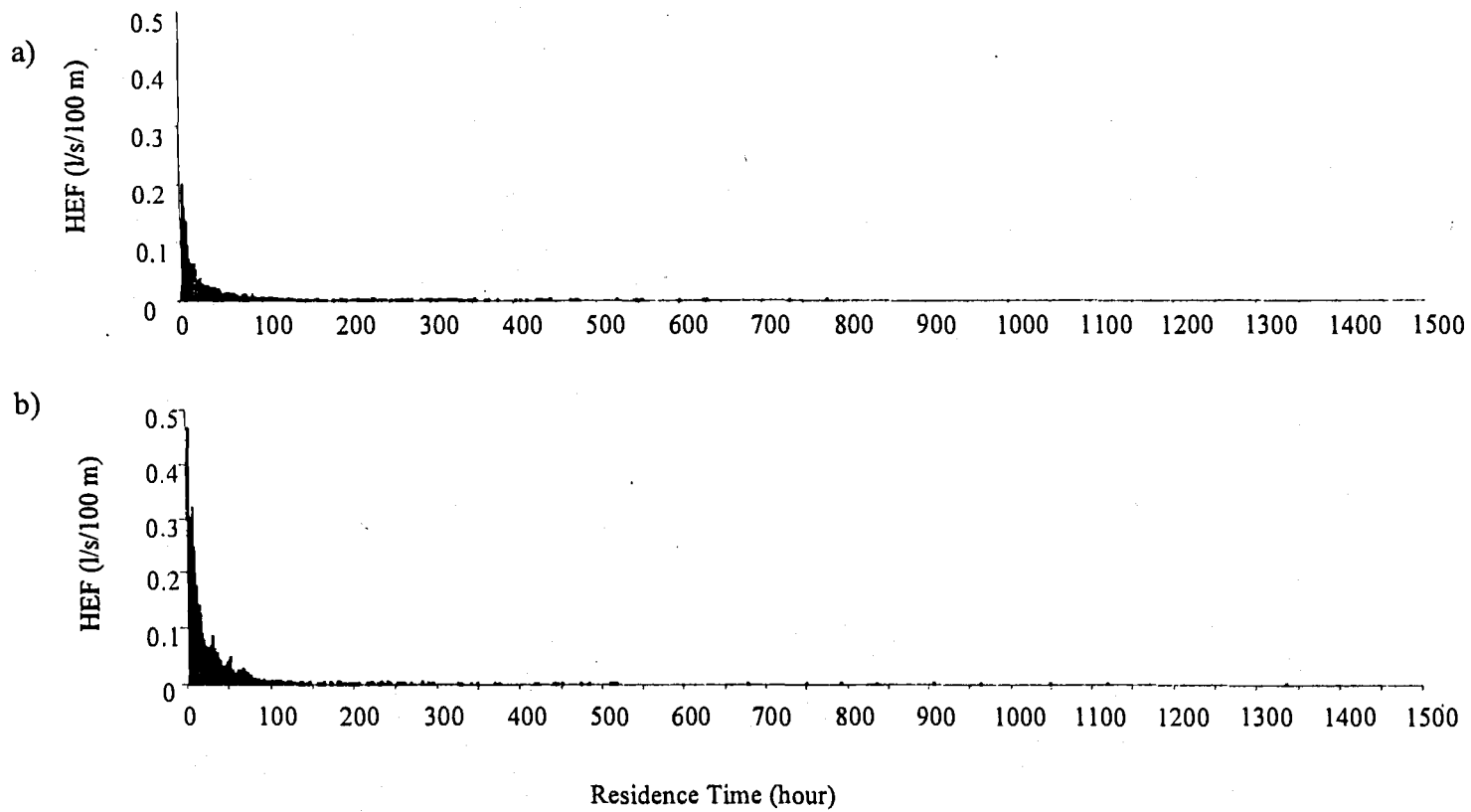
Figure 3.6-a Distribution of estimated residence time of hyporheic exchange flow
at **a)** WS01 and **b)** WS03

c)

d)

Residence Time (hour)
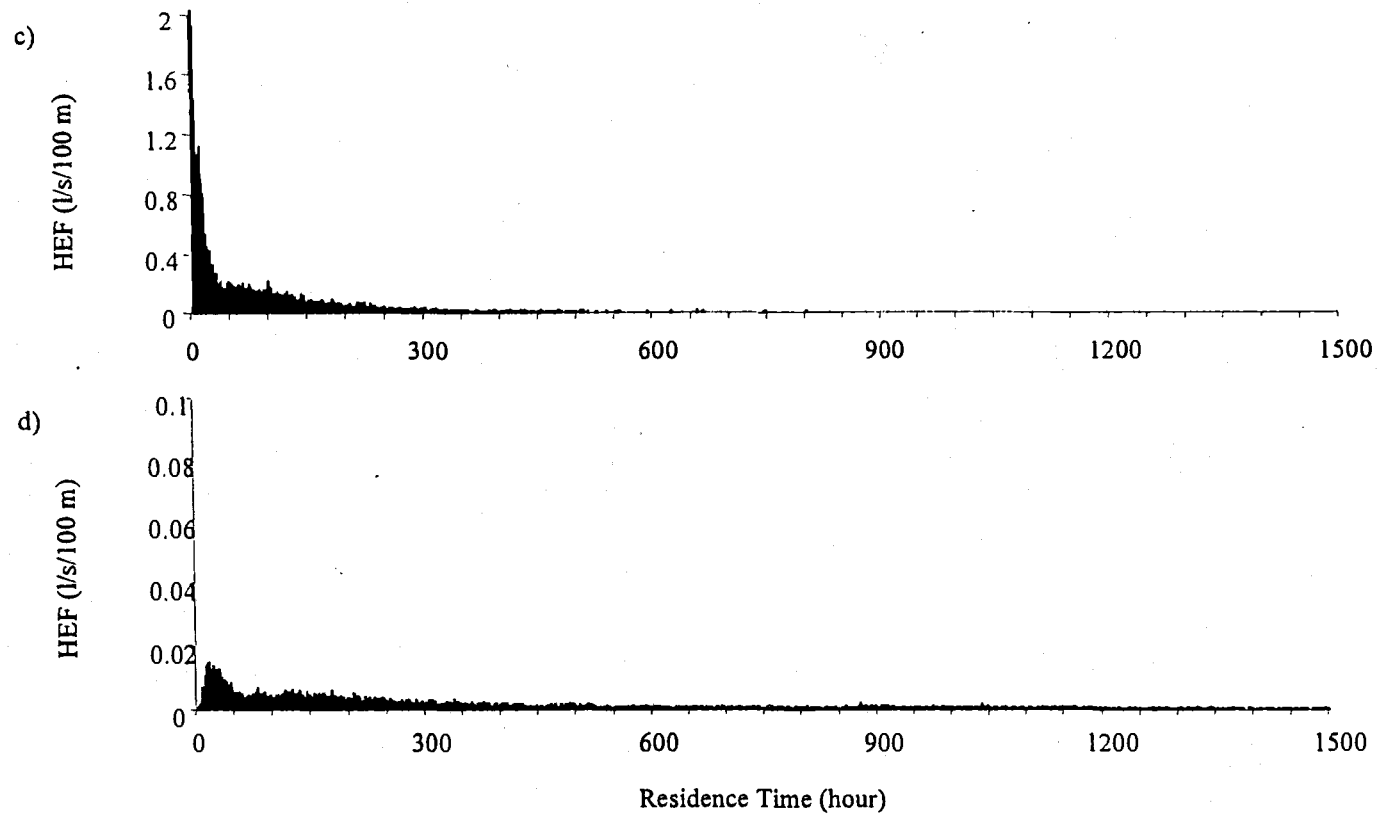
Figure 3.6-b Distribution of estimated residence time of hyporheic exchange flow
at **c)** Middle Lookout site and **d)** Lower Lookout site
*Scale of the hyporheic exchange flow are different between two sites

compared to other three sites (Figure 3.6-d). The peak of distribution was late, located between 13 to 22 hours. The peak was small and dull, and hyporheic exchange with 13 to 22 hours in residence time comprised only 5.8 % of total flow. Median residence time in Lower Lookout was 214 h. Only 11 % of hyporheic exchange had residence time less than 27 h. Also, the frequency distribution of residence times did not decrease exponentially, but decreased almost linearly, after the peak. About 22 % of hyporheic exchange had residence time longer than 800 hours.

WS03 had a higher proportion of hyporheic exchange in shorter residence time (less than 75 h) compared to WS01 (Figure 3.7-a). Because WS01 had slightly later peak than WS03, WS01 had a higher proportion in the residence time, between 3 to 7 hours. Middle Lookout site had a higher proportion of hyporheic exchange in shorter residence time (less than 120 h) compared to Lower Lookout site (Figure 3.7-b). Therefore, not only the volume but also the residence time of hyporheic exchange was very different between Middle Lookout and Lower Lookout sites.

The comparison of distributions of residence time between unconstrained 5th-order site (Middle Lookout) and unconstrained 2nd-order site (WS01) showed that the 2nd-order stream had higher proportion of hyporheic exchange in shorter residence time (Figure 3.8-a). Similarly, the constrained 2nd-order stream site (WS03) had a higher proportion of hyporheic exchange flow in short residence time flow paths than the constrained 5th-order stream site (Lower Lookout), although differences were larger in constrained sites (Figure 3.8-b).
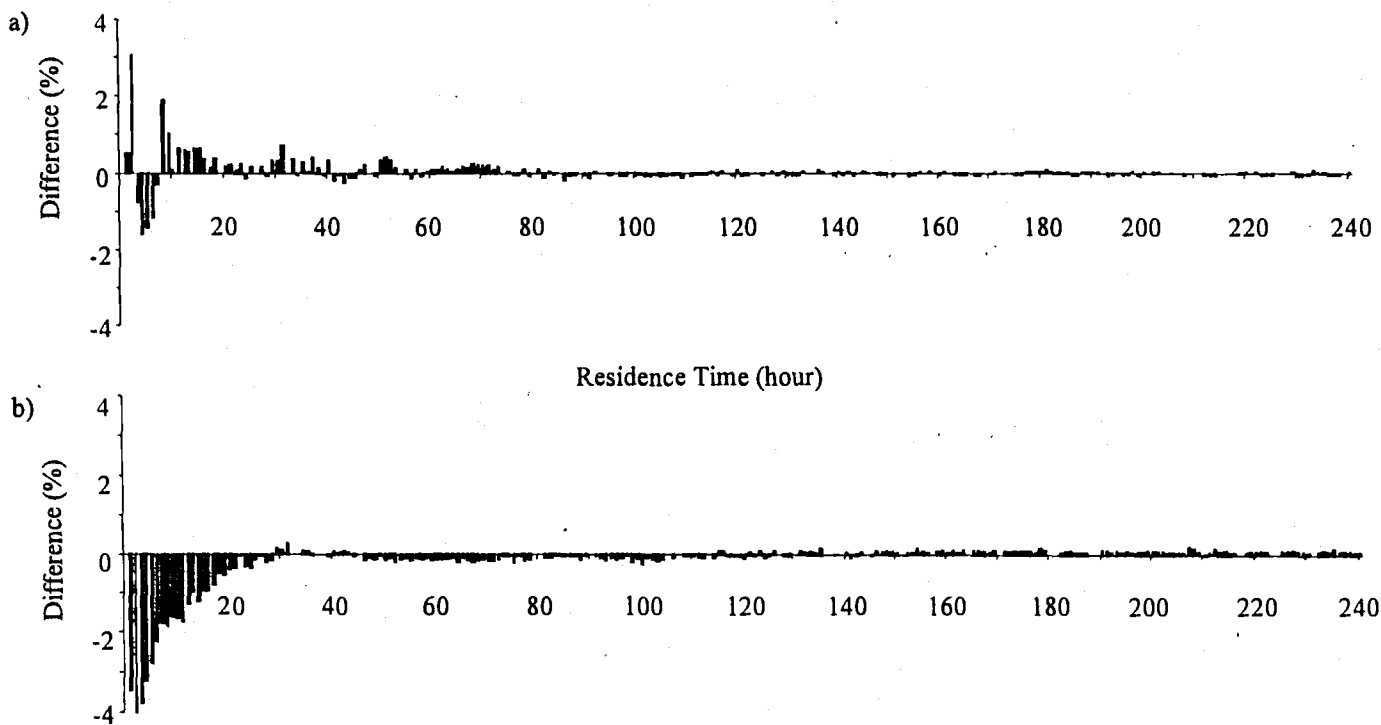
Figure 3.7 Difference in frequency distributions of estimated residence times of
hyporheic exchange flow a) between WS01 and WS03, and
b) between Middle Lookout and Lower Lookout
*Positive values indicate the high proportion of hyporheic exchange flow
at WS03 and Lower Lookout sites
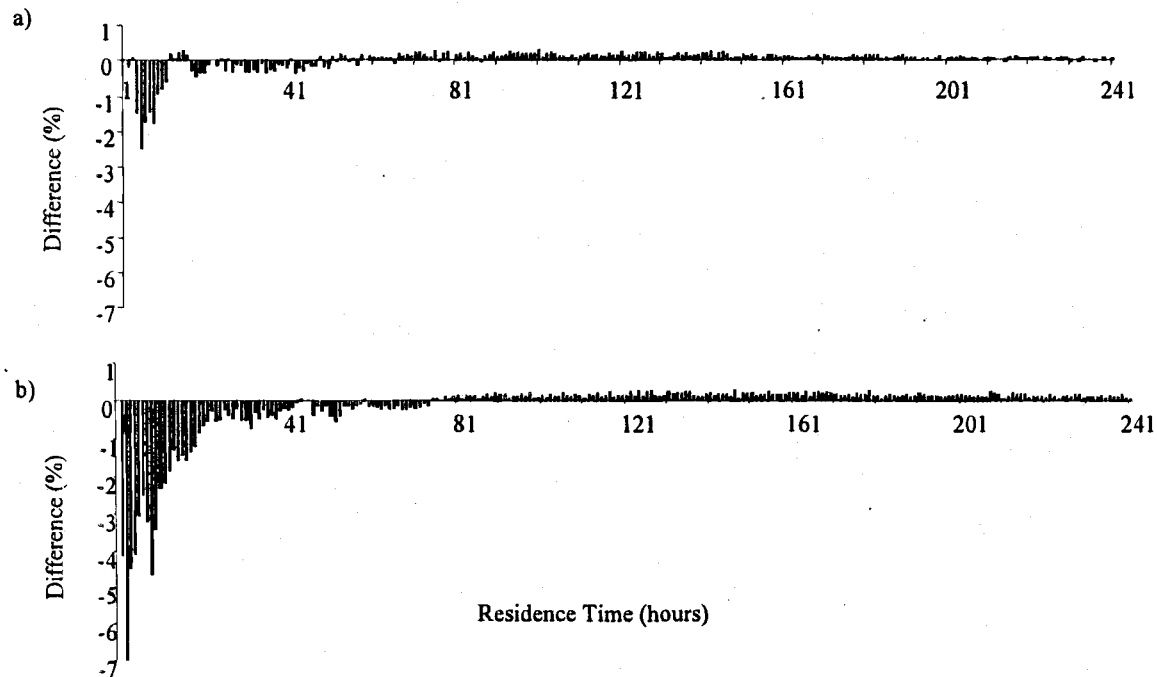
Figure 3.8 Difference in frequency distributions of estimated residence times
of hyporheic exchange flow between 5th-order and 2nd-order streams
a) unconstrained reaches, b) constrained reaches
* Negative values indicate high proportions of hyporheic exchange flow
in 5th-order streams

3.3.   Effect of Geomorphic Features on Hyporheic Exchange Flow

3.3.1   Geomorphic Features in Natural Streams

3.3.1.1   Effects of Geomorphic Features on Volume Hyporheic Exchange Flow

Reductions in hyporheic exchange following removal of a feature from the model simulations indicate the relative contribution of that particular feature to the hyporheic exchange flow budgets. Geomorphic features, such as channel splits, secondary channel, steps, riffles, and sinuosity, were individually removed from WS01 and Middle Lookout

models. The largest reduction of hyporheic exchange flow was seen when steps or riffles were removed from the models (Figure 3.9, 3.10). Removing steps or riffles reduced the volume of hyporheic exchange flow by 54 % in WS01 and by 48 % in Middle Lookout. Secondary channels and channel splits had moderate effects in the Middle Lookout site, reducing hyporheic exchange flow by about 25 %, and about 30 %, respectively. These results were surprising and conflict with the relative importance of secondary channels as judged from the distribution of head in Middle Lookout site (Figure 3.4-c). Removal of secondary channels in WS01 had little effect on the volume of hyporheic exchange flow. Sinuosity had little effect in either 2nd- order or 5th-order stream. The model without sinuosity retained 88 % of original flow in Middle Lookout and 94 % of original flow in WS01 (Figure 3.9, 3.10).
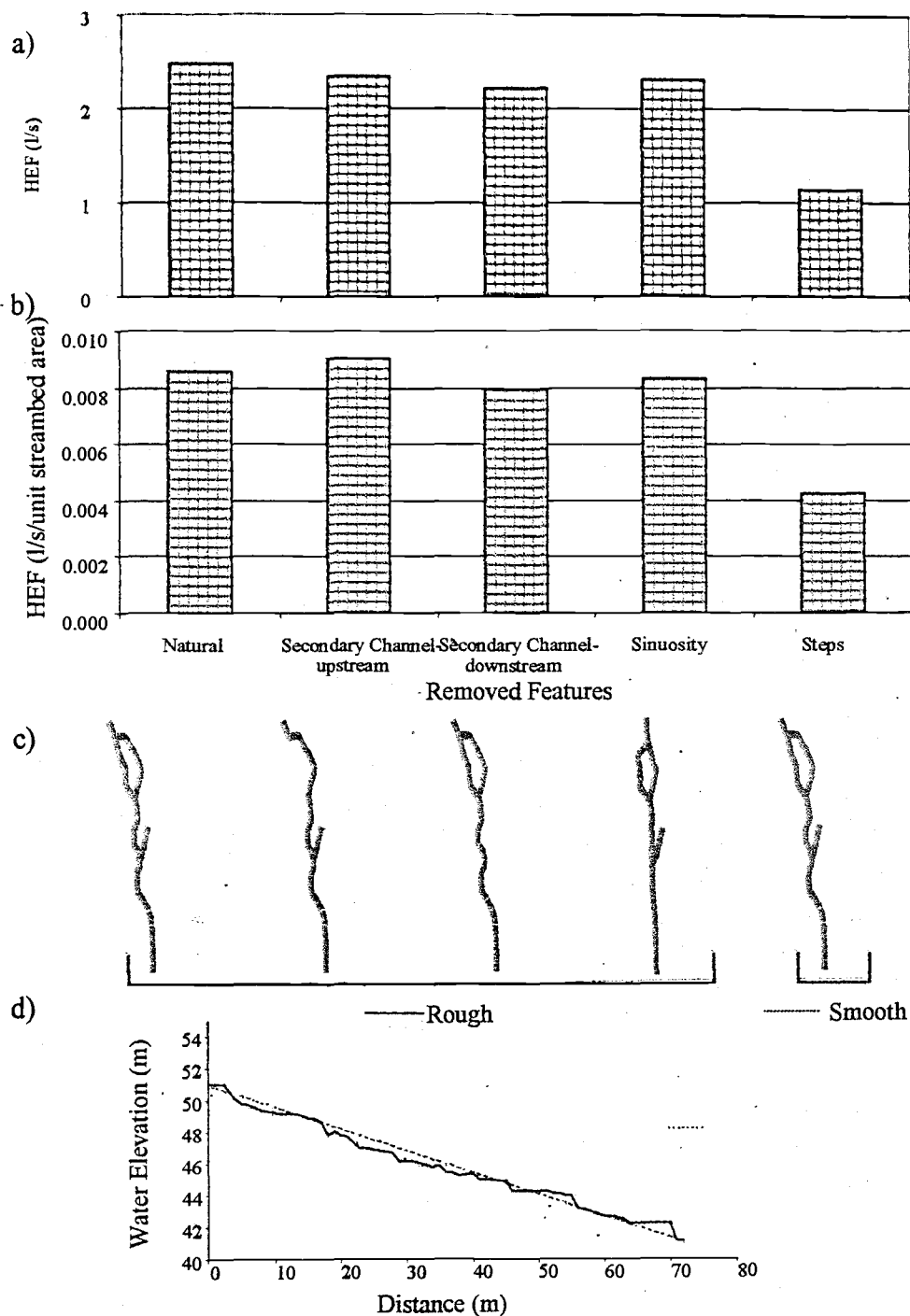
Figure 3.9 Effect of each geomorphic feature on volume of hyporheic exchange
flow (HEF) in WS01 site

    a) Volume of HEF after removal of each feature

    b) Flux of HEF after removal of each feature

    c) Horizontal view of wetted-channel in the models

    d) Longitudinal profiles of the models (main-channel only)
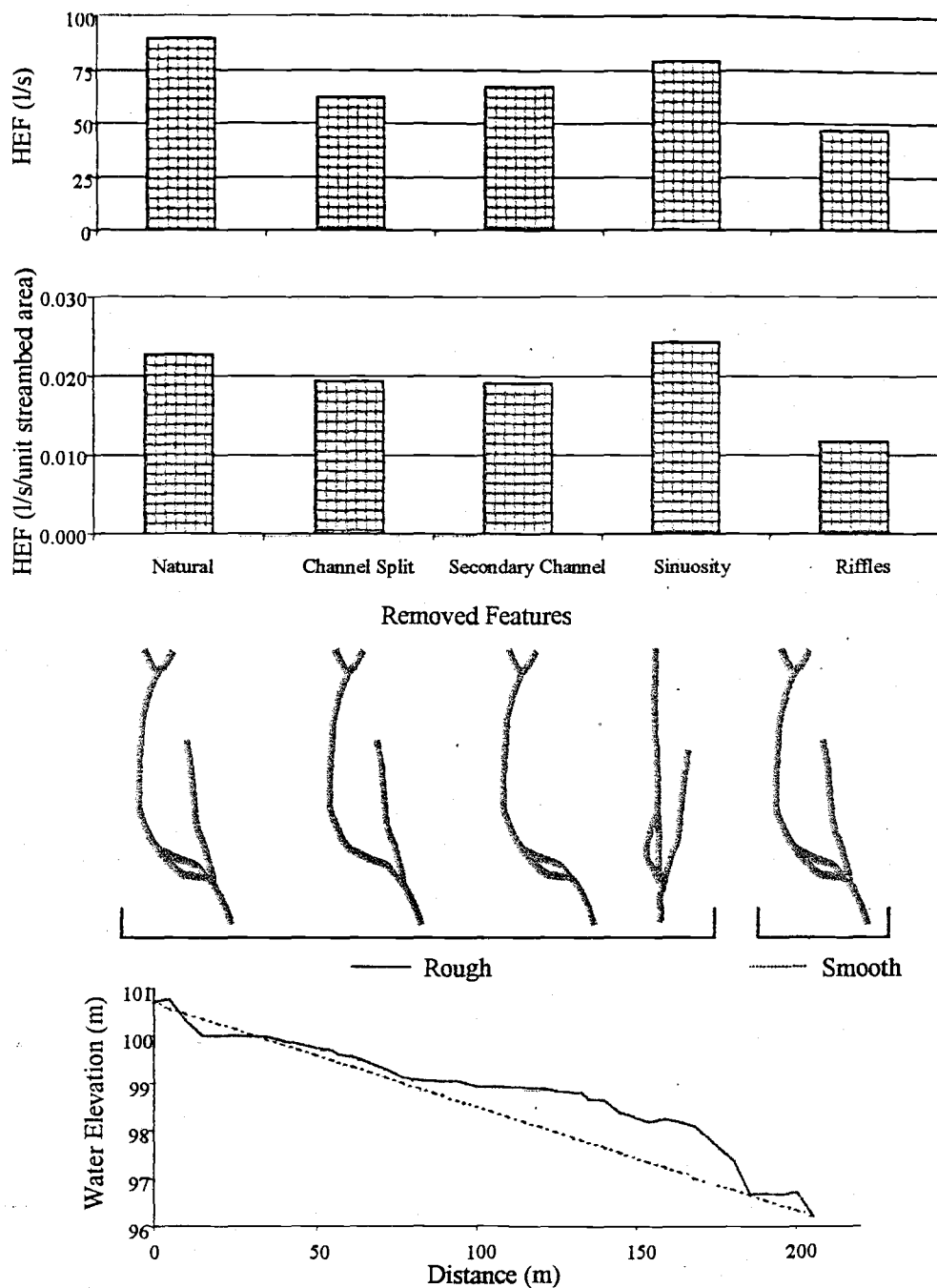
Figure 3.10 Effect of each geomorphic feature on volume of hyporheic exchange
flow (HEF) in Middle Lookout site
  a) Volume of HEF after removal of each feature
  b) Flux of HEF after removal of each feature
  c) Horizontal view of wetted-channel in the models
  d) Longitudinal profiles of the models (main-channel only)
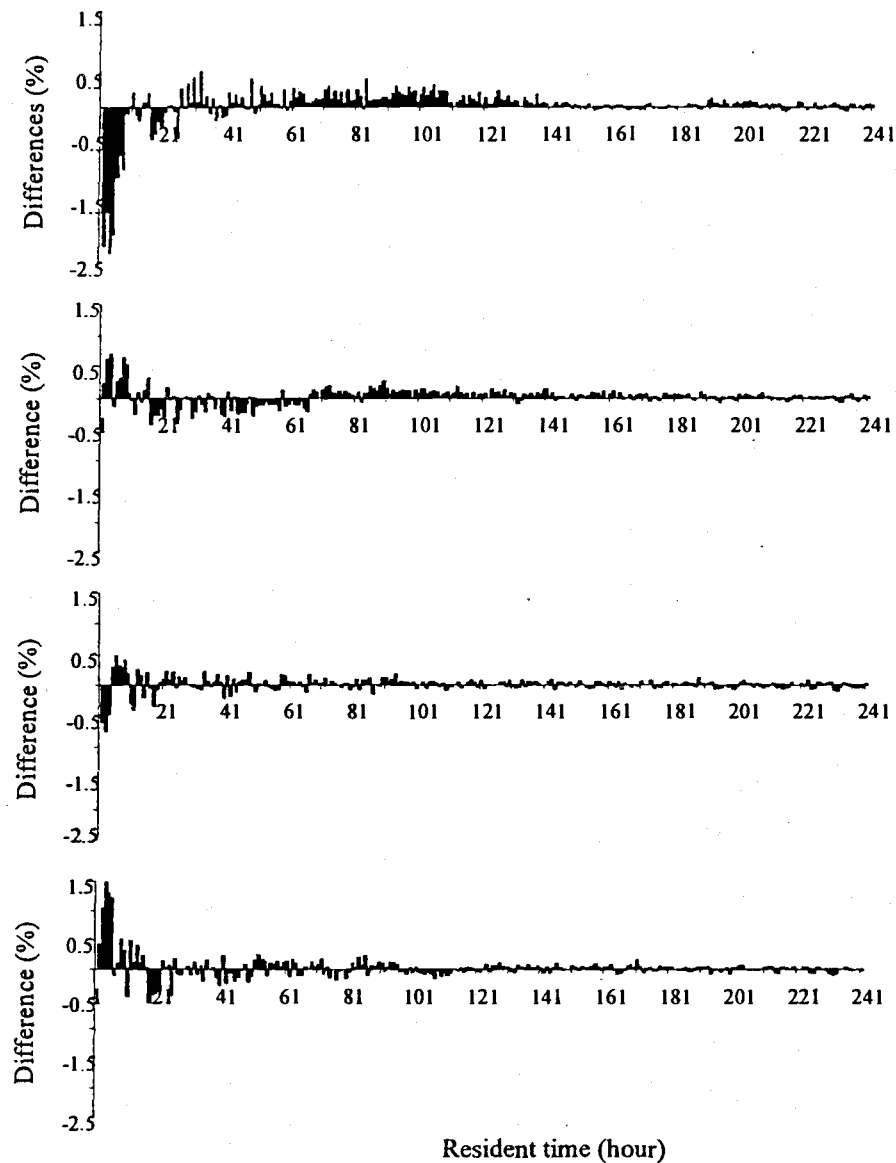
Figure 3.11 Difference in estimated residence times between original WS01 and **a)** after removal of steps, **b)** after removal of upper secondary channel, **c)** after removal of lower secondary channel, and **d)** after removal of channel sinuosity

*Positive values indicate the increase in the proportion in hyporheic exchange flow after the removal of features

3.3.1.2   Effects of geomorphic features on residence time of hyporheic exchange

3.3.1.2.1   2nd-order streams

Removal of steps from WS01 model reduced hyporheic exchange with very short residence time (less than 24 h) and increased hyporheic exchange with intermediate residence time (25 to 140 h).   Hyporheic exchange with long residence time (more than 140 h) did not change substantially (Figure 3.11-a).   Removal of the upper secondary channel reduced hyporheic exchange with short residence time, although the hyporheic exchange with residence time less than 15 h increased (Figure 3.11-b). Removal of lower secondary channel did affect residence time, but there were no apparent trends (Figure 3.11-c).   Thus, the results of removal of two secondary channels were not consistent. Further, the changes were small, mostly less than ±0.5 %.   Removal of channel sinuosity increased hyporheic exchange with very short residence times (Figure 3.11-d).

3.3.1.2.2   5th-order streams

Removal of riffles or channel splits reduced hyporheic exchange with short residence time (less than 25 h) and increased flow with intermediate to long residence times (25 to 205 h) (Figure 3.12-a, c).   In contrast, removal of secondary channels increased hyporheic exchange with short residence time and reduced hyporheic exchange with intermediate residence time (Figure 3.12-b). *Removal of channel sinuosity* reduced hyporheic exchange with residence time less than 10 h and between 55 and 100 h, and
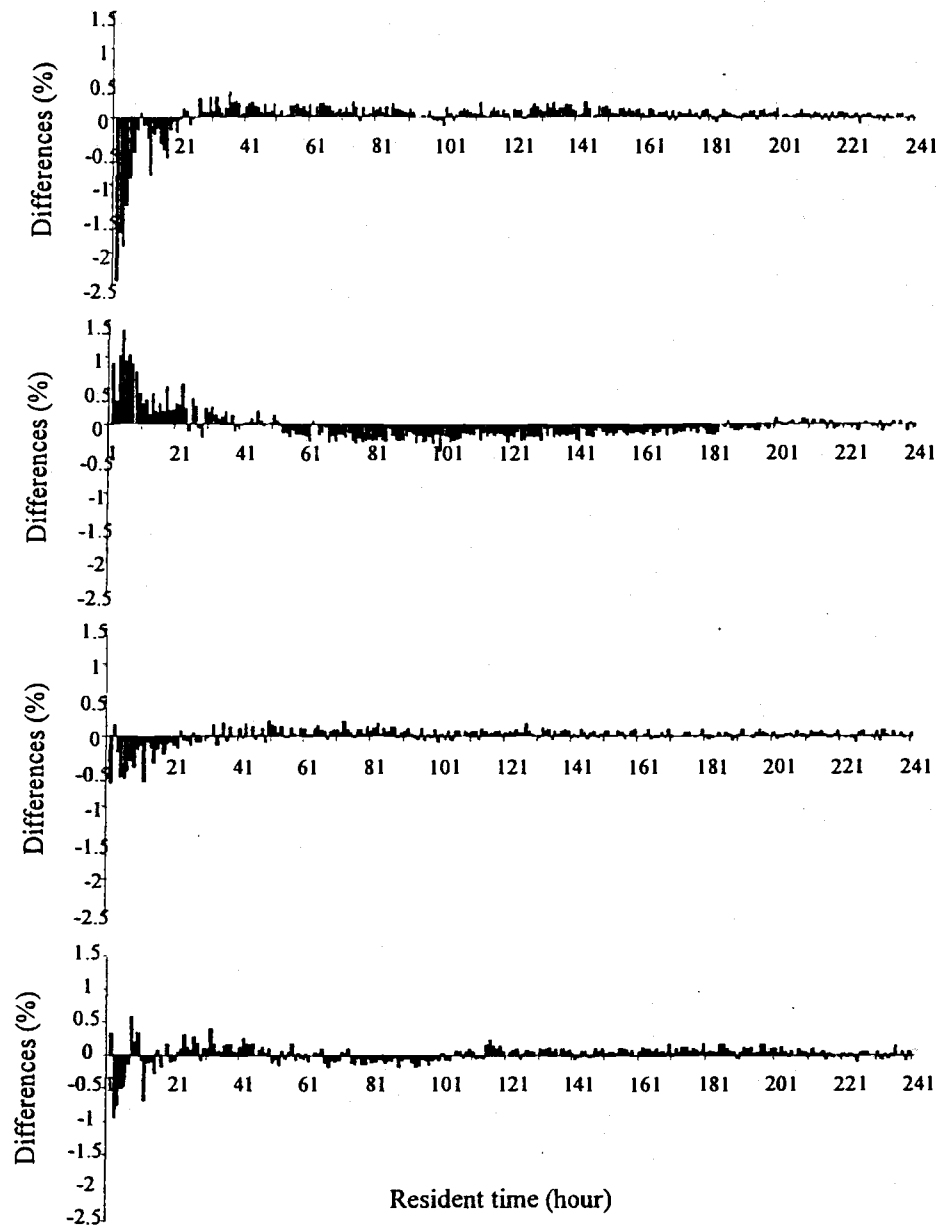
Figure 3.12 Difference in estimated residence times between original Middle Lookout and **a)** after removal of riffles, **b)** after removal of secondary channel, **c)** after removal of channel split, and **d)** after removal of channel sinuosity
*Positive values indicate the increase in the proportion in hyporheic exchange flow after the removal of features

a)

	Steps Gradient / Number (m/m) / no unit	Channel Sinuosity (m/m)	Secondary channel Length m	Gradient (m/m)
Maximum size	1.70/2	1.35	13.8	0.191
Average size	0.49/7	1.13	8.9	0.108
Minimum size	0.34/10	1.02	2.8	0.055

a)

	Riffles Gradient / Number (m/m)	Channel Sinuosity (m/m)	Secondary channel Length m	Gradient (m/m)	Channel split Length m	Gradient (m/m)
Maximum size	0.15/2	0.37	107.2	0.021	41.0	0.042
Average size	0.06/5	0.26	78.5	0.014	29.4	0.040
Minimum size	0.03/10	0.10	48.8	0.005	19.2	0.038

Table 3.4 Maximum, average and minimum sizes of features
used in simplified model simulations.

a) 2nd-order streams and **b)** 5th-order streams

* Channel sinuosity in 5th-order stream is the length/width ratio of the bar

3.3.2 Simplified Streams Model Simulations

The maximum, average and minimum sizes of geomorphic features and the
frequency of those features within a stream reach were obtained from the stream survey
of the study reaches (Table 3.4) and were used in the simplified stream model
simulations.

The stream survey showed that sinuosity in Middle Lookout reach was highly affected by active channel width (Table 3.3). The high sinuosity was observed where the active channel widened or curved. Models that reproduced the sinuosity in the simplified stream model needed to bend more sharply than was observed in the field, because the active channel width in the simplified stream models was fixed. Therefore, I used the width-length ratio of gravel bars (Figure 3.13-a) to estimate the effects of channel sinuosity on hyporheic exchange in Middle Lookout reach. There were, at least, two types of positions for gravel bars. They either overlapped down the length of the channel (Figure 3.13-b) or were spaced entirely separately (Figure 3.13-c). Because I fixed the active channel width of simplified stream models, I simulated effects of sinuosity using only overlapping gravel bars.

3.3.2.1   2nd-order streams

The range in volume of hyporheic exchange flow created by steps was large compared to other features (Figure 3.14-a). Stream survey results showed that the largest steps had gradient approximately 1.7 m/m (Table 3.4-a). Model simulations with two 1.7 m/m steps drove 0.54 l/s of hyporheic exchange flow. In contrast, ten of smallest steps (0.34 m/m) created only 0.22 l/s. Even the smallest steps created more hyporheic exchange than did other features of maximum size. Increasing sinuosity increased hyporheic exchange, as did lengthening the secondary channel or increasing cross-valley gradients (Figure 3.14-a). Hyporheic exchange flow resulting from maximum channel sinuosity was 0.14 l/s, and maximum exchange flow driven by a secondary channel was
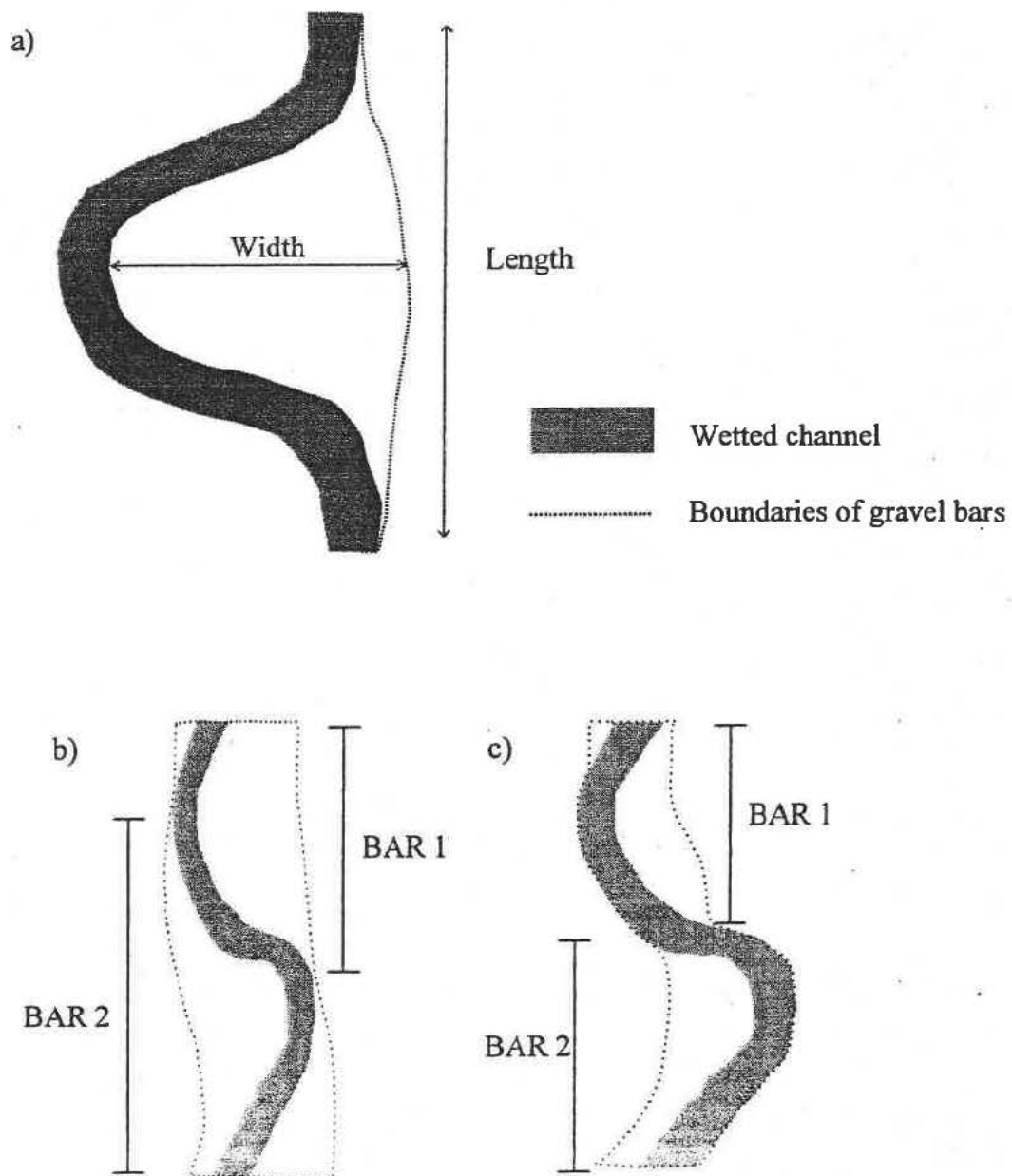
Figure 3.13 Gravel bars **a)** width and length of of gravel bars, **b)** overlapped gravel bars and **c)** separate gravel bars

a)

b)
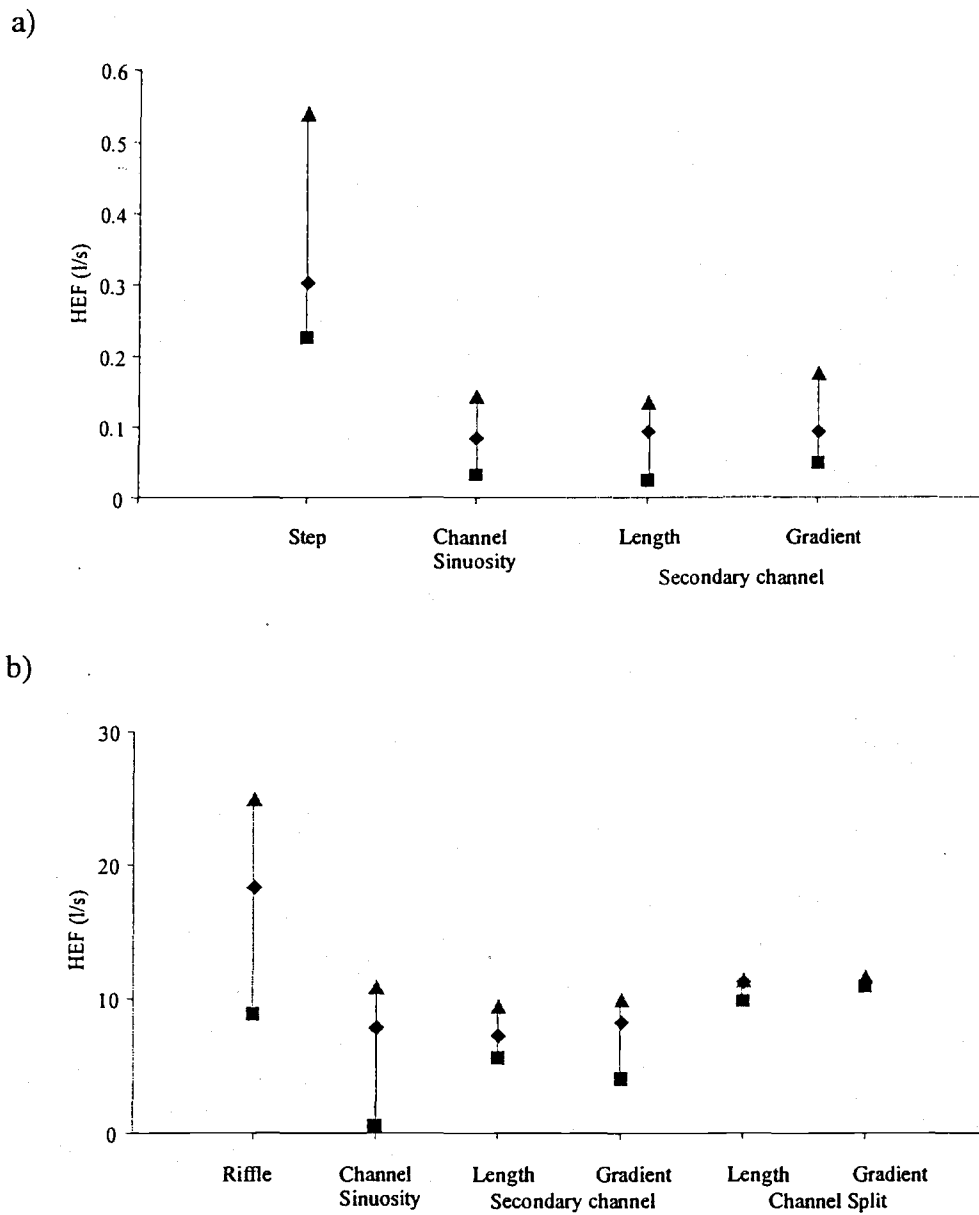
Figure 3.14 Range of effect from each geomorphic feature on HEF in
a) 2nd-order streams, and b) 5th-order streams
* ▲ -- maximum sized feature
◆ -- average sized feature
■ -- minimum sized feature
*Sizes of the features used for this analysis were shown in Table 4.4

0.17 l/s. Average sinuosity (1.13 m/m) and average sized secondary channels (8.9 m long, 0.108 m/m gradient) drove about 0.09 l/s of hyporheic exchange. Clearly, steps were the dominant geomorphic features driving hyporheic exchange flow in 2nd-order stream reaches.

Although channel gradient itself does not drive hyporheic exchange flow, the gradient does interact with other features. Channel gradients had negative correlation with steps. Increase in channel gradient decreased the volume of hyporheic exchange when sizes of steps were kept constant (Figure 3.15-a), although magnitude of change was relatively small.

Comparison between the effects of secondary channels and the effects of other features is complicated because the measurements of secondary channels were made independent of RSL. There were 10 secondary channels in the two study reaches, where there were 13 RSLs (Table 3.3). If I normalized the number of secondary channels to the number of RSL, there are about 0.8 secondary channels per RSL. Therefore, the effects of secondary channels on hyporheic exchange should be about 80 % of that described above.

3.3.2.2 5th-order stream

Riffles were the key geomorphic features driving hyporheic exchange flow in 5th-order streams, just as were steps in 2nd-order streams. However, the effect of riffles on volume of hyporheic exchange flow, relative to other features, was smaller in 5th-order streams than in 2nd-order streams. The stream survey showed that the largest riffles were approximately 0.15 m/m in 5th-order streams (Table 3.4-b). Model simulation with two

a

b
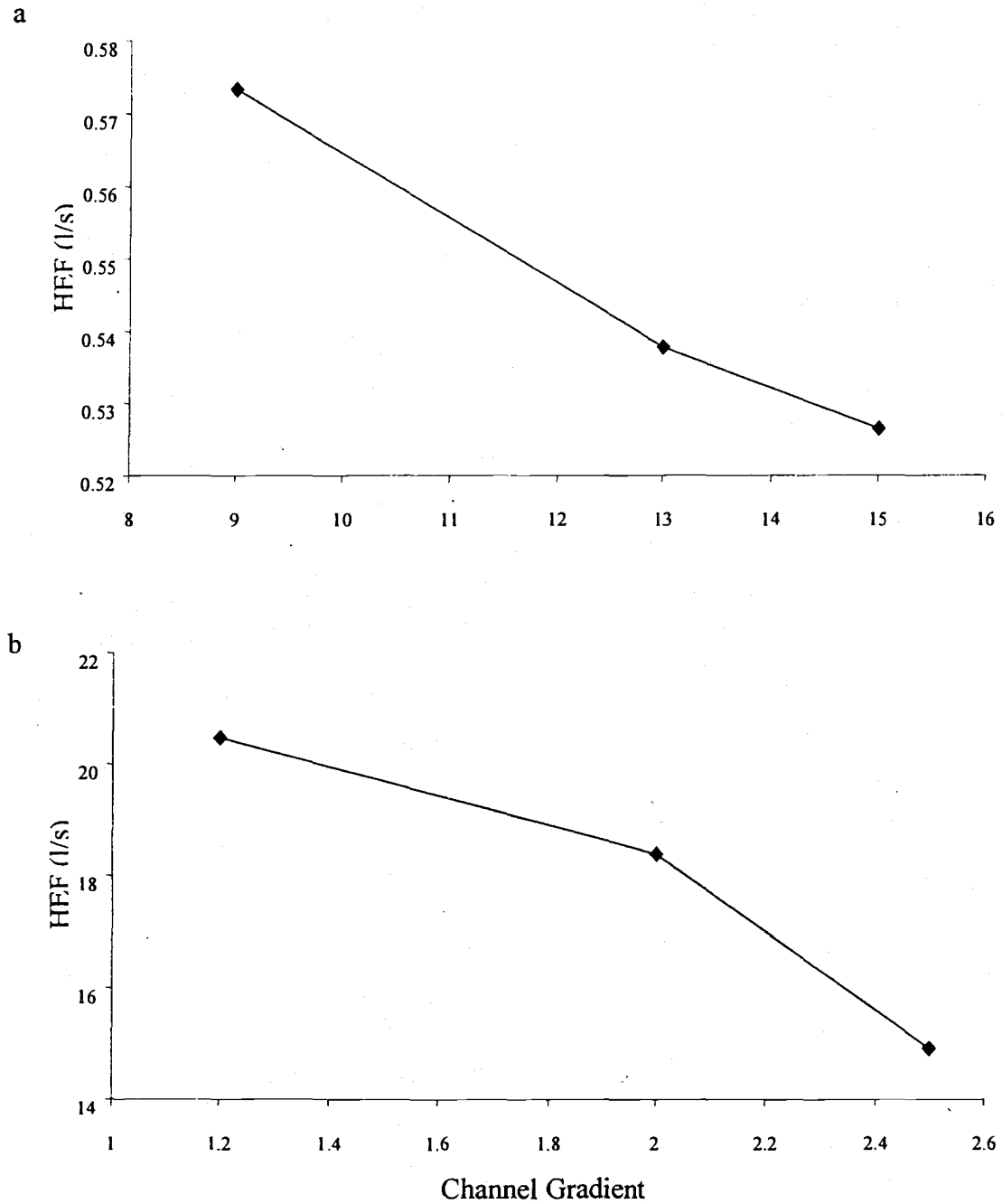
Channel Gradient

Figure 3.15 Hyporheic exchange flow in the simplified model with average size steps and riffles with changes in channel gradient; **a)** 2nd-order stream and **b)** 5th-order stream

of 0.15 m/m riffles created 24.9 l/s of hyporheic exchange flow. Ten of smallest riffles, 0.03 m/m gradients, created only 8.75 l/s. Maximum channel splits (28.0 m long or 0.04 m/m gradient), secondary channels (107.2 m long or 0.02 m/m gradient) and sinuosity (width/length ratio of the bar: 0.37 m/m) created more hyporheic exchange flow than did the minimum sized riffles (Figure 3.14-b). Ranges of effects among, secondary channel, channel split and channel sinuosity were similar.

As in 2nd-order streams, channel gradients had negative correlation with riffles (Figure 3.15-b). Increase in channel gradient decreased the volume of hyporheic exchange when sizes of riffle were constant (Figure 3.15-b). Also, channel gradient has positive correlation with channel sinuosity so that an increase in gradient increases the hyporheic exchange flow driven by channel sinuosity (Figure 3.16), although the changes were relatively small.

Again, the comparison between the effects of riffle and other features was complicated because the measurement of secondary channel, channel splits and channel sinuosity were made independently of RSLs. There were 6 secondary channels in 10 RSLs (Table 3.3). If I normalize the numbers of secondary channels and channel splits to RSL, there would be 0.6 secondary channels and 0.3 channel-splits per RSL. However, there were also three old channels, lacking surface water, in the study reach. If I assume the old channels, which do not have surface water, function similar to secondary channels and drive extensive hyporheic exchange, there would be 0.9 secondary channels per RSL. Therefore, the effects of secondary channels should be between 60 % and 90 % of that described above. Similarly, the effects of channel splits should be only 30 % of that described above.
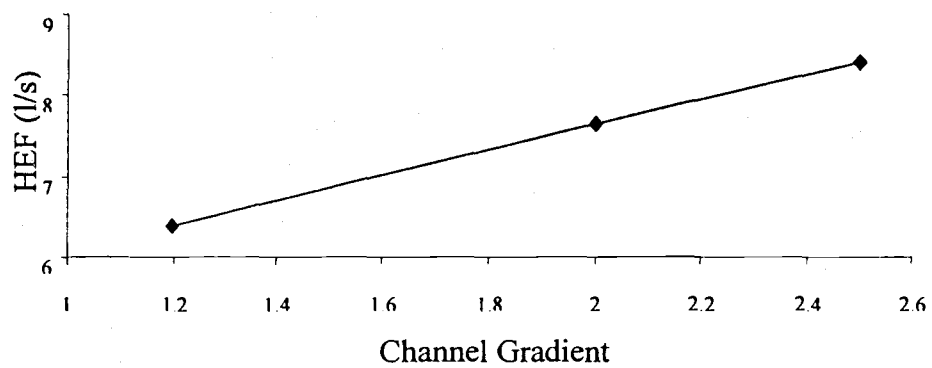
Figure 3.16 Hyporheic exchange flow with channel sinuosity with maximum, average and minimum channel

4. DISCUSSION

4.1 Geomorphic Controls on Hyporheic Exchange

Subsurface flows, including hyporheic exchange flow, are driven by hydraulic head gradients and hydraulic conductivity (Fetter 1994). Channel geomorphology has strong effects on both hydraulic head gradients and saturated hydraulic conductivities so that channel morphologic features can be a good indicator of hyporheic exchange flow. I focused on vertically extensive features, such as steps and riffles, and horizontally extensive features, such as secondary channels, channel splits and channel sinuosity, to assess the relative importance of geomorphic controls on hyporheic exchange. Different sized streams have different geomorphologic characteristics, so I hypothesized that the key features driving hyporheic exchange differ between 2nd-order and 5th-order streams. I will first discuss geomorphic characteristics and then the contribution of key geomorphic features in both sized streams.

4.1.1 2nd-order streams

4.1.1.1 Geomorphic Characteristics

WS01 and WS03 are categorized as small channels (Church 1996) and are located in the headwater of the Lookout drainage system. The two streams drain forested catchments through the v-shaped bedrock-confined valleys. The streams receive

abundant inputs of woods and boulders from adjacent hillslope. Both large woods and boulders strongly control channel morphologies in these small channels.

Logjams, boulder jams or the mixture of these commonly blocked the channels in WS01 and WS03, forming steep steps. Jams of logs and boulders are formed during floods and help stabilize the valley floor, especially in streams with steep channel gradients (Church 1996). Large wood is common in streams of the Pacific Northwest and controls accumulation of sediment. Although large woods tend to be suspended between the lower valley walls, the lodging in WS01 and debris flows in WS03 broke them down and left many large pieces of wood on the valley floor (Nakamura and Swanson 1993). Because wood from old-growth forests can be extremely large, more than 1.0 m in diameter and 20 m long, steps created by these logs had gradients close to 1.5 m/m. Jams of large boulders, which had diameter more than 0.5 m, also formed steep steps. Steps were frequent in both WS01 and WS03, and were present averaged 3 to 4 steps were present in 30 m long RSLs.

Horizontally extensive features, such as channel sinuosity and secondary channels were also present in both WS01 and WS03. Large woods and boulders obstruct wetted-channels, displacing the channels and leading to increase sinuosity. However, channel sinuosity in 2nd-order streams was relatively low, even where valley floors were wide, because steep channel gradients forced surface water to flow down-valley so that wetted-channels remained relatively straight. Secondary channels also diverge where large obstacles block channels (Davis and Gregory 1994), but these were not a common feature in WS01 and WS03. Thus, vertically extensive features, steps, dominated channel complexity, and there were little horizontally complexity so that valley constraint

had little effect on channel morphology. Consequently, vertically extensive features had strongest controls on hyporheic exchange flow.

4.1.1.2 Effects of Geomorphic Features on Hyporheic Exchange

Steps were the dominant geomorphic feature driving hyporheic exchange flow in the 2nd-order streams studied. Steps frequently drove hyporheic exchange flow (Figure 3.4-a, b), and their contribution to the total volume of hyporheic exchange flow was large in the well-network sites (Figure 3.9-a). The large volume of hyporheic exchange flow driven by steps in simplified stream models (Figure 3.13-a) suggested that the importance of steps was consistent throughout both study reaches. Although steps had negative correlation with channel gradients, even the combination of steepest observed channel-gradients and minimum sized steps resulted 0.21 l/s of hyporheic exchange in the simplified stream model, which was more than the exchange flow resulting from either average channel sinuosity or average sized secondary channels. Thus, effects of steps dominated hyporheic exchange flow in the two 2nd-order streams.

Secondary channels created shallower hydraulic gradients and were located close to the main channel. Consequently, hyporheic exchange driven by secondary channel was smaller than that driven by steps (Figure 3.9-a). Further, because secondary channels are infrequent, they make limited contribution to hyporheic exchange flow in 2nd-order streams.

4.1.2   5th-order streams

4.1.2.1   Geomorphic Characteristics

Lookout Creek is categorized as an intermediate channel (Church 1996). Although 5th-order channels had more surface discharge and were wider than 2nd-order streams, they are still small enough to have their channel morphology modified by streambed materials, such as logs and boulders. Boulders and logs can change portions or all of channel cross-sections. Fluvial processes form riffles and are mainly constructed by collection of boulders, and some are formed by microjam of logs or by single large piece of large wood (Church 1996). The gradients of riffles were relatively shallow, but the spatial extent was large compared to the steps in 2nd-order streams.

Relatively gentle channel gradients (2%) and the wide active channels width allow development of horizontally extensive features in unconstrained reaches. The wetted-channel made large bends within the active channel. There were 6 secondary channels in the sampled Middle Lookout reaches, and all of which were located on point-bars as shortcuts. Therefore, channel sinuosity and the presence of secondary channels are tightly correlated. Secondary channels were dynamic feature of the unconstrained reach of Lookout Creek (Table 3.3), because flood can dramatically change their location or remove them entirely. For example, Wondzell and Swanson (1999) showed that large floods (return interval >100 yr) could incise main channels and reduce Hyporheic Exchange Flow. Although stream incision may lead to loss of secondary channels at some bars, sediment would be deposited on other bars, creating new secondary channels. Thus, there may be little net change in the number of secondary channels at the reach

scale. Although longitudinal channel gradient in Lower Lookout reach was shallower than Middle Lookout, there were less channel sinuosity and no secondary channels because the channel was constrained between bedrock walls. Thus, the 5th-order stream contained horizontal and vertical complexity in the unconstrained reach, but the constrained reach was simple, and riffles were the only feature driving hyporheic exchange flow.

4.1.2.2   Effects of Geomorphic Features on Hyporheic Exchange

The secondary channel drove the most spatially extensive hyporheic exchange flow at the well-network site in the Middle Lookout reach (Figure 3.4-c). Although the data were limited in the well-network sites, the reach maps showed that secondary channels and main channels often located at the opposite edge of the active channels (Figure 3.4-c), and secondary channels had lower water elevation than main channels. Therefore, I expected that secondary channels drove extensive hyporheic exchange throughout the unconstrained study reach. Although riffle showed small effects on the extent of hyporheic exchange (Figure 3.4-c, d), they drove the largest volumes of hyporheic exchange was within the study reach (Figure 3.10, 14-b).

Detailed investigations showed that relatively high cross-valley hydraulic head gradients between secondary and main channels and between split channels were maintained by riffles present in either channel. Cross-valley gradients increased downstream of riffles, and then gradually reduced until the next riffle. For example, the channel split located in well-network site of Middle Lookout had gradients exceeding

0.05 m/m in parts, even though the average gradient was only 0.03 m/m (Figure 4.1).
The presence of locally steep gradients may dramatically increase the hyporheic
exchange around secondary channels and channel splits. There were five riffles in the
well-network site of Middle Lookout, and three were located in the area of the secondary
channel and channel split. Thus, steps and secondary channel or channel-splits appear to
interact and drive high volume of hyporheic exchange over extensive areas. The removal
of steps reduces the effects of secondary channels and channel splits on hyporheic
exchange as well as eliminates the direct effects of step. Therefore, the effects of
secondary channels and channel splits on volume of hyporheic exchange flow should be
substantial, although the reduction of the volume of hyporheic exchange flow was much
larger after the removal of steps than after the removal of secondary channel or channel
splits.

All of the channel splits in the study reach created steep cross-valley gradients
and drove high volumes of hyporheic exchange (Figure 3.4-c). However, only three
channel splits were present in the 1500 m reach so that the effects of channel splits were
small at the reach scale. In contrast, secondary channels drove spatially more extensive
and were more common features in the unconstrained reach. Therefore, channel splits
drove locally large hyporheic exchange flows, and secondary channel drove large
hyporheic exchange throughout the study reach.

Channel gradient also had interactions with channel sinuosity and riffles.
Although channel gradient does not drive hyporheic exchange by itself, increases in
channel gradient decreases the hyporheic exchange driven by riffles, because the
difference in gradient of riffle relative to the channel gradient declines (Figure 3.15). In

contrast, increases in channel gradient increase the volume of hyporheic exchange driven by channel sinuosity (Figure 3.16). Because sinuosity has interactions with secondary channels, channel gradient also has indirect effects on hyporheic exchange driven by secondary channels. Thus, multiple features, which are horizontally and vertically extensive, interact to enhance the extent and volume of hyporheic exchange in 5th-order streams. Further, channel constraint is an important controlling feature because horizontally extensive features can only develop in unconstrained reaches.
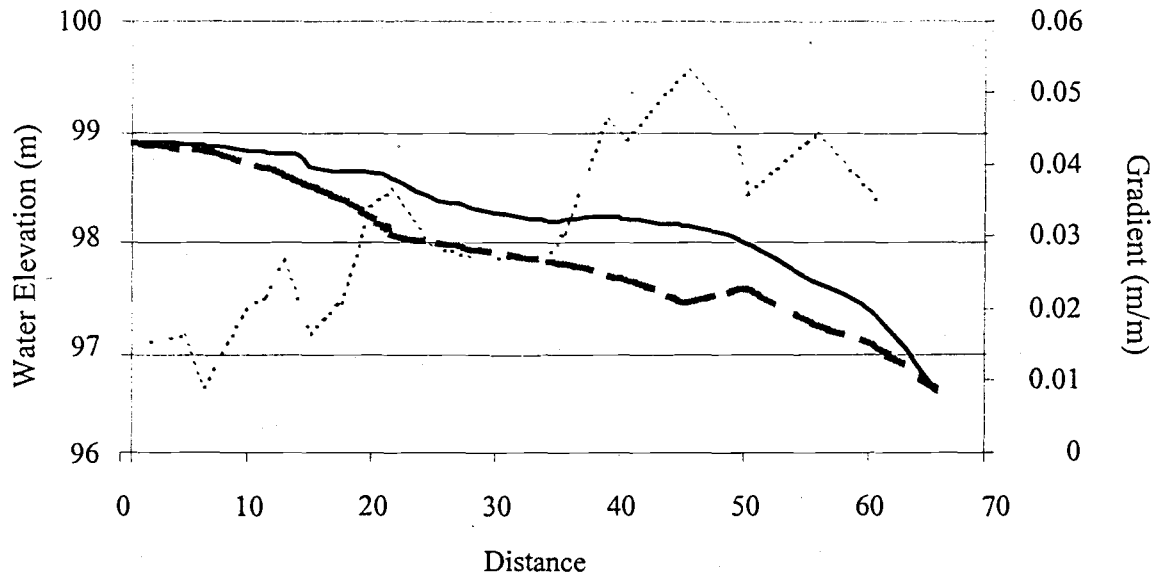
Figure 4.1 Water elevation of split channels and hydraulic gradient
between the two channels
———— Water elevation of main channel
— — Water elevation of secondary channel
••••••• Hydraulic gradient between secondary and main channels

Overall, vertical complexity, such as steps and riffles, was important in driving hyporheic exchange. Steps were especially dominant in 2nd-order streams. In addition to

the independent contribution of vertical complexity, interactions between horizontal and vertical complexities enhanced the forces of driving hyporheic exchange in unconstrained 5th-order streams.

4.2 Three Factors of Hyporheic Exchange Flow; Spatial Extent, Relative Volume, and Residence Time

The effects of hyporheic exchange on stream ecosystems are dependent on three factors; 1) spatial extent, 2) relative volume, and 3) residence time of hyporheic exchange flow. These three factors are not independent, but I discuss these three separately. The extent of the hyporheic zone expresses the spatial distributions of hyporheic characteristics. The volume of hyporheic exchange is crucial to quantify the effects of hyporheic exchange on stream ecosystem, whereas the residence time determines the physical and biogeochemical characteristics of hyporheic exchange water. Thus, the integration of these three hydrological factors and the biogeochemical environments determine effects of hyporheic exchange flow. This study investigated only the hydrological factors and did not examine biogeochemical environments. A detailed discussion of the biological and biogeochemical effects of hyporheic exchange flow on stream ecology would require further investigation.

4.2.1 Spatial Extent of Hyporheic Exchange Flow

The spatial extent of the hyporheic zone is important because it provides habit for aquatic invertebrates and creates a diversity of biogeochemical environments. Hyporheic

exchange flows can extend from centimeters to tens of meters from stream channels, depending on the morphologic and hydrologic conditions of the channels (White 1993). Extensive hyporheic zones may enlarge habitats and provide refugia for aquatic invertebrates. For example, aquatic invertebrates typical of stream environments can be found tens of meters away from the wetted channel where hyporheic zones are extensive (Stanford and Ward 1988). Clearly, aquatic invertebrates can use extensive subsurface areas where hyporheic exchange flow creates environmental conditions that meet their needs. Extensive refugia in the hyporheic zone (Stanford and Ward 1993) may decrease the probability that a disturbance will drive populations locally extinct, and thus may contribute to the quick recovery of the benthic communities after disturbances.

Extensive hyporheic zones contain diverse biogeochemical environments, because riparian areas are ecotones between terrestrial and aquatic ecosystems and have steep gradients of environs (Gregory et al. 1991). Biogeochemical characteristics, such as concentration of dissolved oxygen, dissolved organic carbon and total carbon (Groffman et al 1996) and water temperature (personal communication with Johnson, S.L. Figure 4.2) vary considerably at stream-sediment interfaces. These steep gradients of environs lead to a diversity of biogeochemical processes occurring in hyporheic zone. As the hyporheic zone extends away from the wetted-channel, the zone may be increasingly affected by biogeochemical processes, which could further diverse the biogeochemical environments. For example, dissolved oxygen concentrations decrease with distance from the wetted-channel (Groffman et al. 1996) so that the dominant biogeochemical processes change from aerobic to anaerobic ones. Hyporheic exchange flows return to the wetted-channel over relatively short period of time, so that the biological

environments to which hyporheic exchange flows are exposed can affect surface water chemistry.
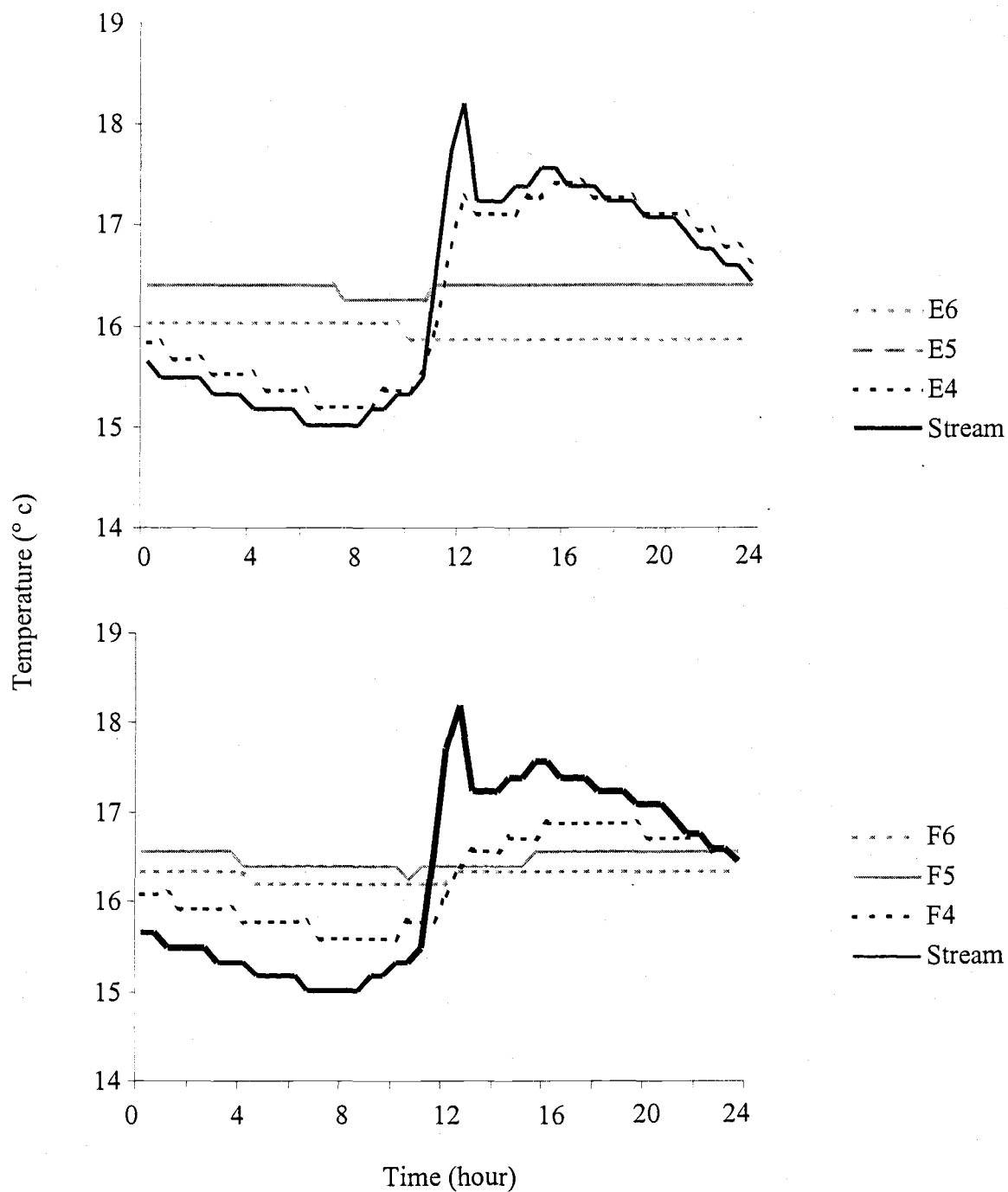

Figure 4.2 Daily water temperature fluctuation in
wells and streams of well transects E and F
in WS03 on August 21st

The unconstrained reach of the 5th-order stream had the most extensive hyporheic zone among the four well-network sites (Figure 3.4-c). This hyporheic zone, which is created by secondary channels, extended laterally about 30 m from the wetted-channel in Middle Lookout well-network site, whereas the largest extent of the hyporheic zone was just about 5 m from the wetted-channels in the 2nd-order streams and Lower Lookout sites. Because secondary channels were common, extensive hyporheic zones should be found throughout unconstrained reaches of 5th-order streams. Thus, 5th-order streams have larger potentials to have extensive hyporheic zone compared to 2nd-order channels, although channel constraints controls extent.

The extensive hyporheic zone in Middle Lookout study reach may provide larger refugia for aquatic invertebrates than in either 2nd-order stream sites or the constrained 5th-order site. However, because hyporheic exchange flow created by secondary channels in the 5th-order stream had relatively long residence time (Figure 3.12), extent of available hyporheic habitat should be dependent on the geochemical environments of the hyporheic zone. Also, the scale of disturbances is much larger in 5th-order streams, and relative capacity of hyporheic refugia to scale of disturbance, which may have strong controls on the rate of recovery, is uncertain.

The most extensive hyporheic zone was located between main and secondary channels, where terrestrial vegetation is not well developed. Therefore, hyporheic exchange flow might be affected little by the terrestrially oriented processes, even though it extended tens of meter from wetted-channels. However, the changes from aerobic to anaerobic conditions over long flow paths should lead to a diversity of biogeochemical processes. The gradients of environs in riparian areas of 2nd-order stream may be steeper

than in 5th-order streams because hillslopes are much closer to the channel and because riparian vegetation is well developed. Consequently, the hyporheic zone in 2nd-order stream sites may have more diverse biogeochemical environments than 5th-order streams, even though the spatial extent of the hyporheic zone was small. Thus, the hyporheic zone in 5th-order streams was larger than the hyporheic zone in 2nd-order streams. However, the size of hyporheic function is highly dependent on biological and geochemical environment, and the comparison of effective hyporheic zone between sites is not possible from results of this study.

Hydraulic heads gradients determine the extent of hyporheic zone. As I mentioned above, the secondary channels in 5th-order streams were common features and contributed to the laterally extensive hyporheic zone. Steep steps were the key features in 2nd-order stream to drive spatially extensive hyporheic zone. Steps showed distinctive hyporheic flow paths within the area where secondary channel had effects. It implies that effects of steps were much stronger than the effects of secondary channels. Although effects of steps were localized, the appearance of steps was frequent so that effective range of steps was spatially extensive (Figure 3.4-a, b).

4.2.2 *Quantity of Hyporheic Exchange Flow*

The volume of hyporheic exchange flow is critical in determinating its effects on stream ecosystems, but scaling to the size of stream is needed to accurately express the effects and to compare the relative effects of hyporheic exchange flow among study reaches. Scaling can be done relative to stream discharge and relative to streambed area.

Both values are important when trying to quantify the biological or the biogeochemical effects of hyporheic exchange on stream ecosystems.

4.2.2.1 Volume of Hyporheic Exchange Relative to Stream Discharge

The volume of hyporheic exchange relative to stream discharge may be useful for estimating the effects of biogeochemical processes in hyporheic zone on stream nutrient budgets (Triska et al. 1993, Valett et al. 1996). Similarly, the volume of hyporheic exchange relative to stream discharge may contribute more to stabilizing of stream water temperature. Previous studies have used ratios of cross-sectional area of transient storage zone to wetted-channel (As/A) estimated from stream tracer experiments (D'Angelo et al. 1993, Valett et al. 1996). However, substantial problems exist in the use of parameters estimated from a one-dimensional transport and storage model to compare different sized streams (Harvey et al. 1996, Wondzell submitted). In contrast, estimates of volume of hyporheic exchange flow from MODFLOW simulations are not influenced by stream discharge, and thus should give more realistic estimates of the relative volume of hyporheic zone.

The volume of hyporheic exchange relative to stream discharge was much larger in 2nd-order stream sites than in 5th-order stream sites (Figure 3.5), which suggests that biogeochemical transformations occurring in the hyporheic zone would have larger effects in 2nd-order streams than 5th-order streams. MODFLOW simulations of hyporheic exchange flow depend on the boundary conditions. Although stream discharge and water elevation are positively correlated, the increase in discharge is larger than the increase in

water elevation (Gregory and Walling 1973). Therefore, volumes of hyporheic exchange flow relative to stream discharge decrease with increasing stream discharge. Consequently, I expect that the effects of hyporheic exchange on stream nutrient budgets and water temperature would decrease with increase in stream size from either increase in stream order or from seasonal changes in stream discharge.

Gradients of hydraulic heads and hydraulic conductivity control the volume of hyporheic exchange. Steps created steep hydraulic gradients and drove large volumes of hyporheic exchange in 2nd-order stream (Figure 3.9, 14-a). Riffles individually drove most hyporheic exchange in 5th-order sites (Figure 3.10, 14-b), although interactions between riffles and horizontal features increased exchange flows as I described above. Thus, steps in 2nd-order stream and riffles in 5th-order stream were the most contributing feature to increase the relative volume of hyoprheic exchange to stream discharge. Besides the visible geomorphic features, which I focused on, saturated hydraulic conductivity has strong controls on the volume of hyporheic exchange (Morrice et al. 1997). Streambed sediment with higher conductivity will have larger hyporheic exchange. The geometric means of saturated hydraulic conductivity was the same between WS01 and WS03 sites, but WS03 had wider range in the values (Figure 3.3). Locally high hydraulic conductivities might contribute to the larger volume of hyporheic exchange flow in WS03 than WS01. The geometric means of saturated hydraulic conductivity in Middle Lookout site was twice as high as in Lower Lookout site (Figure 3.3). Previous study showed that stream sediment with about three times higher saturated hydraulic conductivity had about 76 times larger cross-sectional area of transient storage zone (Morrice et al. 1997). Therefore, beside the difference in geomorphic features, the

higher conductivity in Middle Lookout might increase the differences in volume of

hyporheic zone between Middle Lookout and Lower Lookout sites.

4.2.2.2 Volume of Hyporheic Exchange Flow Relative to Streambed Area

Hyporheic exchange flow per unit streambed area expresses the average rate of

hyporheic exchange through the streambed. Groundwater and hyporheic exchange flow

are upwelling at some locations in the streambed, and stream water is entering to

sediment (downwelling) at some locations in the streambed. Also, water may neither

upwell nor downwell at other locations. Therefore, hyporheic exchange per unit

streambed area is equivalent to the normalized flux of exchange flow in study sites.

Although actual flux of downwelling and upwelling should be locally larger than average

values, I assume that hyporheic exchange flow per unit area is an indicator to compare

the exchange rate among study sites. I call the hyporheic exchange flow per unit area as

flux.

Flux determines physical characteristics of hyporheic exchange flow, such as

supply of dissolved oxygen, water temperature and supply rate of stream-originated

materials to the hyporheic zone at downwelling spots. These physical characteristics

control biological and biogeochemical processes. Aquatic invertebrates require oxygen,

and increased in oxygen supply enhances the quality of hyporheic zone as their habitats.

High supply of dissolved oxygen enhances aerobic transformations, such as nitrification

and the oxidation of hazardous metals (Triska et al. 1993a, Harvey and Fuller 1998,

Fuller and Harvey 2000). Changes in the flux of stream-originated materials should also

affect biogeochemical transformations in hyporheic zone. For example, supply of

dissolved organic carbon (DOC) can limit biogeochemical processes (Hedine et al. 1996). Further, the lability of DOC may differ between stream and groundwater sources. Therefore, the rate and type of biogeochemical transformations in downwelling locations can be altered when the compositions of DOC changes.

Flux of hyporheic water in upwelling locations affects the quality of spawning gravel for salmonid species. Also, the flux at upwelling spot controls supply rate of transformed materials from hyporheic zone back to the surface stream ecosystem. In nitrogen limited mountain streams, the hyporheic zone can be an important source of nitrogen (Wondzell and Swanson 1996b). Biomasses of net primary productions in mountain streams are benthic algae. Because of nitrogen limitation, streambed algae would be expected to immediately uptake the available nitrogen released from hyporheic zone before the nutrients enter the water column. This conceptual model suggests that transformed nutrients from the hyporheic zone directly affect benthic communities in limited area around the upwelling locations.

There has been strong research focus on estimation of the volume of hyporheic exchange relative to stream discharge to weigh the effects of hyporheic exchange on stream ecosystems (D'Angelo et al. 1993, Valett et al. 1996, Morrice et al. 1997). However, the rate of nutrient supply from hyporheic zone to the streambed, as measured by water flux at upwelling spots, may be the better criterion in nutrient limited mountain streams. Further, Wondzell and Swanson (1996a) showed that the volume of hyporheic exchange flow is independent of stream discharge, consequently the relative importance of hyporheic exchange to stream ecosystem may not be predicted from the relative volume of hyporheic exchange to stream discharge. Therefore, the flux of water is likely

to be the better measure to assess the importance of hyporheic exchange in stream ecosystems in nutrient limited mountain streams. This situation may shift in lowland streams characterized by eutrophication.

If the flux is a better criterion to measure the effects of hyporheic exchange flow, the Middle Lookout site had largest effect among four sites and Lower Lookout has least effect. This suggests that intermediate-sized streams have potential to have more effective hyporheic exchange flow than small streams. This result conflicts with the previous studies, which used the relative volume of hyporheic exchange to stream discharge as the criterion (D'Angelo et al. 1993) and concluded that hyporheic zone has larger effects in smaller streams.

The importance of hyporheic exchange flow should be measured relative to the stream ecosystem process of interest. Muss-budget measurements, including stream-nutrient budgets or stream temperatures, will be most affected by the volume of exchange flow relative to stream discharge. Net primary production in nutrient limited streams will be more sensitive to the flux of hyporheic exchange flow where the hyporheic zone is an important source of limiting nutrients.

Flux is controlled by hydraulic head gradients and saturated hydraulic conductivities. The dense contour lines between split channels in Middle Lookout well-network site and reduction in hyporheic exchange with short residence time after the removal of channel split indicated that channel splits contributed intensive (high-rate) hyporheic exchange (Figure 3.4-c, Figure 3.12-c). The reduction of flux after the removal of riffles (Figure 3.10-b) as well as close spacing between equipotential lines and the reductions in hyporheic exchange with short residence time, confirmed that riffles

also created high-rate of hyporheic exchange in 5th-order streams (Figure 3.4-c, d, 3.12-a). Although the effects of channel split on flux were strong, it was not a common feature in the study reaches in 5th-order (Table 3.3). Therefore, channel split has locally strong effects, but not in the reach scale. Because of the frequent appearance, riffle may be the key feature increasing flux at the reach scale. In 2nd-order stream, steps drove intensive hyporheic exchange (Figure 3.9 b) because of their steep gradient and frequent appearance.

4.2.3 Residence Time

Residence time is a function of both flux and length of flow hyporheic exchange flow paths:

Residence time = f (length of flow path) / f (Flux)

Increase in flux reduces residence time, and expansion in length of flow paths increase residence time. Because flux and length of flow path have opposite correlations with residence time, the hyporheic exchange with high flux and large aerial extent and the hyporheic exchange with low flux and small extent may have similar residence times. However, the two types of flow may be exposed to dramatically different biogeochemical environments and have distinctly different influences on stream ecosystems. Despite this complication, residence time is an important measure for categorizing hyporheic exchange flow because residence time is a measure of the contact time with sediment. For example, concentration of dissolved oxygen decreases (Findlay 1995) and water temperature becomes close to sediment temperature, as residence time increases. These

physical characteristics often determine the type and rate of biogeochemical processes occurring in the hyporheic zone. Therefore, residence time is an important aspect of hyporheic exchange flow. The mixture of characteristics between surface water and subsurface environments determines hyporheic functions, and the hyporheic water may loose its distinctive biogeochemical characteristics after some limiting length of residence time in subsurface. One previous study arbitrarily defined the hyporheic zone as the area where residence time was less than 10 days (Wroblicky et al. 1994), but the effects on resident time of biogeochemical processes has not been examined.

Hyporheic exchange in 2nd-order streams had a higher proportion of short residence time (less than 48 h) hyporheic exchange flow than did 5th-order streams (Figure 3.8, Table 4.1-a). The extent of hyporheic zone was about 6 times larger in Middle Lookout than in either 2nd-order stream, whereas the flux of hyporheic exchange flow was only twice as large. Thus, the difference in length of flow path, rather than the flux, probably account for the shorter residence time in 2nd-order streams. The short residence time indicates that hyporheic exchange in 2nd-order streams would contain more characteristics of surface water than would hyporheic exchange in 5th-order streams. WS01 and WS03 did not have distinct differences in their distribution of residence time (Figure 3.7-a, Table 4.1-a), but the volume of hyporheic exchange flow, which has residence time less than 120 h was constantly twice as large in WS03 as in WS01 site (Table 4.1-b). Therefore, WS03 may have more hyporheic exchange flows with stream characteristics. Residence times in Lower Lookout site were relatively long (Figure 3.7-b, Table 4.1-a), but the volume of hyporheic exchange is very small

a)

	<1	1~6	6~12	12~24	24~48	48~120	120~240	240~
				Residence time (hour)				
WS01	3.6	23.3	15.7	15.5	14.5	13.1	5.3	9.0
WS03	4.1	21.4	19.5	18.5	16.6	13.1	2.6	4.2
Middle Lookout	3.4	16.3	11.9	14.3	10.4	21.7	15.4	6.5
Lower Lookout	0.0	0.4	2.0	6.9	10.0	14.1	19.9	46.7

* unit is in %

b)

	<1	1~6	6~12	12~24	24~48	48~120	120~240	240~
				Residence time (hour)				
WS01	12.67	81.81	55.05	54.31	50.82	46.06	18.76	31.53
WS03	27.28	142.56	130.30	123.14	110.68	87.52	17.27	28.26
Middle Lookout	173.27	822.25	601.37	720.74	525.06	1091.43	774.99	325.89
Lower Lookout	0.00	0.84	4.55	15.29	22.22	31.55	44.43	104.12

* unit is in l/s/100m

Table 4.1   Distribution of residence time of hyporheic exchange flow (HEF) at each study site
a) percentage of total HEF, which has residence time between the range
b) estimated volum of HEF in 100 m reach, which has residence time
   between the range

compared to Middle Lookout. Even the contribution to the volume of hyporheic exchange with long residence time was smaller in Lower Lookout (Table 4-1-b).

Riffles and channel splits contributed to hyporheic exchange with short residence time (less than 24 h), and secondary channel contributed to create long residence time (longer than 50 h) in 5th-order streams (Figure 3.12). Therefore, the hyporheic exchange driven by secondary channels may have different hyporheic functions compared to the hyporheic exchange driven by riffles and channel splits. Because unconstrained 5th-order streams have multiple controlling features, there may be two or more types of hyporheic exchange flow. In contrast, steps were the dominant features driving hyporheic exchange so that 2nd-order streams may have relatively homogeneous hyporheic exchange compared to 5th-order streams.

4.3 Uncertainty

The results presented here are subject to unknown, but potentially substantial, simulation and other uncertainties. The primary sources of uncertainty result from estimating the saturated hydraulic conductivity and the thickness of aquifer sediment. Saturated hydraulic conductivity was estimated from both slug tests and well tracer injection tests. Slug test are subject to order of magnitude of errors (Hyder and Butler 1995), and the error is directly proportional to the volume of hyporheic exchange flow estimated from MODFLOW. I conducted three slug tests in each well to decrease this uncertainty. However, there were large differences among the results of three tests for some wells. Also, the results of slug test are applicable only to a small area around the
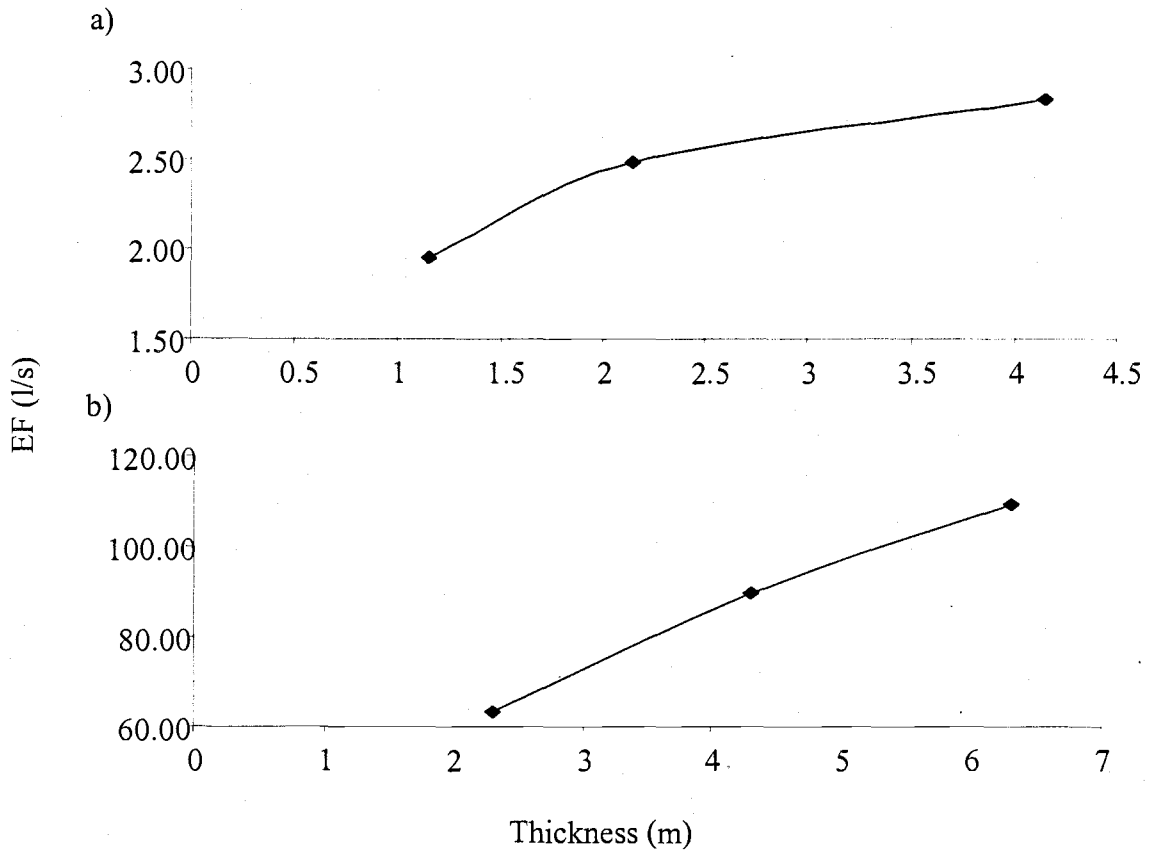
a)

b)

Thickness (m)

Figure 4.3 Hyporheic exchange flow (HEF) with three
different saturate aquifer thickness in **a)** WS01 model
and **b)** Middle Lookout model

test wells, which introduces additional uncertainty. Continuous tracer injection tests in

wells estimate the spatially averaged estimates of saturated hydraulic conductivity and

may contain less error than do slug tests. However, well injections do not provide

information on spatial heterogeneity of hydraulic conductivity. Therefore, the

combination of saturated hydraulic conductivity estimated from slug tests and continuous

tracer injection tests is the best way to estimate the hydraulic saturated conductivity.

Because I did not have sufficient data from continuous tracer injections, I could not

combine the saturated hydraulic conductivity obtained by the two methods and used slug test data only. However, the final models matched observed heads well, so I assumed that the estimation of hydraulic conductivity was reasonable. I did not conduct any validation of the model. Validation of models using, for example, using different boundary conditions, will create more accurate models.

The saturate thickness of the streamside aquifers was an unknown. Thickness controls the bottom boundary of the model so that all simulation results will be affected by the change in thickness, such that the increase in thickness increased the hyporheic exchange (Figure 4.3). I assumed the values, 2.15 m for 2nd-order streams and 4.3 m for 5th-order streams. These values seems reasonable from the field observation, such as exposures of bedrock in wetted channels. However, better data on aquifer thickness will be needed to estimate hyporheic exchange flow more accurately.

The main objective of this study was to compare the effects of geomorphic features on hyporheic exchange flow. While uncertainties in estimates of absolute volume of hyporheic exchange flow may be large, these uncertainties are also likely to be consistent among simulations. Therefore, the comparative analyses of the effects of geomorphic features on hyporheic exchange are valid as long as values for saturated hydraulic conductivity and saturated thickness did not change.

5.   **CONCLUSION**

Visible morphologic features of stream channels create head gradients between stream water and underlying aquifers that drive hyporheic exchange flow. One geomorphic feature, steps, was dominated hyporheic exchange flow in 2nd-order streams. Steps contributed to both extent and volume of hyporheic exchange flow, and the exchange flow driven by steps had relatively short residence time. In contrast, multiple geomorphic features were key in 5th-order streams. Horizontally extensive features, such as secondary channels and channel splits, drove extensive hyporheic exchange flow. Vertically extensive feature, such as riffles, was also important in 5th-order stream, and the interactions between the vertically and horizontally extensive features were important. Because horizontally extensive features were important, channel constraint strongly affected the hyporheic exchange flow in 5th-order streams. The Middle Lookout site, which had wide active channels, had larger volume of hyporheic exchange than sites in both unconstrained and constrained reaches of 2nd-order stream. The Lower Lookout site, which had a narrow active channel, had the smallest hyporheic exchange flow among four study sites. The hyporheic exchange flow in 5th-order streams was more heterogeneous than the one in 2nd-order streams. Riffles and channel splits drove hyporheic exchange with short residence time, where secondary channel drove one with long residence time.

LITERATURE CITED

Anderson, M.P. and W.W. Woessner. 1992. Applied groundwater modeling, simulation of flow and advective transport. Academic press, San Diego.

Bower, H. and R.C. Rice. 1976. A slug test for determinating hydraulic conductivity of unconfined aquifers with completely or partially penetrating wells. Water Resources Research 12 (3): 423-428

Castro, N.M., and G.M. Hornberger. 1991. Surface-subsurface interactions in an alleviated mountain stream channel. Water Resource Research 27 (7): 1613-1621.

Church, M. 1996. Channel morphology and typology, p. 185-202. In G. Petts and P. Calow (ed.) River flows and channel forms. Blackwell science Ltd.

Criss, R.E. and M.L. Davisson. 1996. Isotopic imaging of surface water/groundwater interactions, Sacramento Valley, California. Journal of Hydrology 178:205-222

D'Angelo, D.J., J.R. Webster, S.V. Gregory, AND J.L.Meyer. 1993. Transient storage in Appalachian and Cascade mountain streams as related to hydraulic characteristics. Journal of North American Benthological Society 12 (3): 223-235.

Davis, R.J. and K.J. Gregory. 1994. A new mechanism of river bank erosion in a forested catchment. Journal of Hydrology 157:1-11

Fetter, C.W. 1994. Applied hydrogeology.

Findley, S. 1995. Importance of surface-subsurface exchange in stream ecosystems: The hyporheic zone. Limnology and Oceanography 40 (1): 159-164

Fuller, C.C. and J.W. Harvey. 2000. Reactive uptake of trace materials in the hyporheic zone of a mining-contaminated stream, Pinal Creek, Arizona. Environment Science and Technology 34(7): 1150-1155)

Geist, D.R., and D.N. Dauble. 1998. Redd site selection and spawning habitat use by Fall Chinook Salmon: The importance of geomorphic features in large river. Environmental Management 22 (5):655-669

Grant, G.E. and F.J. Swanson 1995. Morphology and processes of valley floors in mountain streams, Western Cascade, Oregon.

Gregory, S.V., F.J. Swanson and K.W. Cummins. 1991. An ecosystem perspective of riparian zone, focus on link between land and water. Bioscience 41(8):540

Gregory, K.G. and D.E. Walling. 1973. Drainage basin form and process. John Wiley & Sons Ltd, New York

Groffman, P.M., G. Howard, A.J.Gold AND W.M. Nelson. 1996. Microbial nitrate processing in shallow groundwater in riparian forest. Journal of Environmental Quality 25:1309-1316

Harvey, J.W., B.J. Wagner and K.E. Bencala. 1996. Evaluating the reliability of the stream tracer approach to characterize stream-subsurface water exchange. Water Resources Research 32 (8): 2441-2451

Harvey, J.W., and K.E. Bencala. 1993. The effect of streambed topography on surface-subsurface water exchange in mountain catchments. Water Resources Research 29 (1): 89-98

Harvey, J.W. and C.C. Fuller. 1998. Effects of enhanced manganese oxidation in the hyporheic zone on basin-scale geochemical mass balance. Water Resources Research 34 (4): 623-636

Hedin, L.O, J.C. Von Fischer, N.E. Ostrom, B.P. Kennedy, M.G. Brown, and G.P. Robertson. 1998. Thermodynamic constraints on nitrogen transportations and other biogeochemical processes at soil-stream interfaces. Ecology 79 (2): 684-703

Hill, M.C. 1993. Preconditioned conjugate-gradient 2 (PCG2), A computer program for solving groundwater flow equations. U.S. Geological Survey Open-file Report 92-477

Hill, A.R. and D.J. Lymburner. 1998. Hyporheic zone chemistry and stream-subsurface exchange in two groundwater-fed streams. Canadian Journal of Fisheries and Aquatic Science 55: 495-506

Holmes, R.T., S.G. Fisher and N.B. Grimm. 1994. Parafluvial nitrogen dynamics in a desert stream ecosystem. Journal of North American Benthological Society 13: 468-478

Holmes, R.T., J.B. Jones, Jr., S.G. Fisher and N.B. Grimm. 1996. Denitrification in a nitrogen-limited stream ecosystem. Biogeochemistry 33: 125-146

Jones, J.B., and R.M. Holmes. 1996. Surface-subsurface interactions in stream ecosystems. TREE 11(6): 239-242

Jones, J.B., S.G. Fisher and N.B. Grimm. 1995. Nitrification in the hyporheic zone of a desert stream ecosystem. Journal of North American Benthological Society 14 (2): 249-258

Maddock, I.P., G.E. Petts, E.C. Evans, and M.T. Greenwood. 1995. Assessing river-aquifer interactions within the hyporheic zone, p.53-74. *In* A.G. Brown (ed.) Geomorphology and groundwater, John Wiley and Sons Ltd., Chichester.

McDonald, M.G. and A.W. Harbaugh. 1988. A Modular three-dimensional finite difference groundwater flow model. U.S. Geological Survey Open-file Report 83-875

Morrice, J.A., H.M. Valett, C.N. Dahm, and M.E. Champana. 1997. Alluvial characteristics, groundwater-surface water exchange and hydrological retention in headwater streams. Hydrological Processes 11:253-267.

Nakamura, F. and F.J. Swanson. 1994. Distribution of course woody debris in a mountain stream, western Cascade Range, Oregon. Canadian Journal of Forestry Resources 24:2395-2403

Nelson, W.M., A.J. Gold and P.M. Groffman. 1995. Spatial and temporal variation in groundwater nitrate removal in riparian forest. Journal of Environmental Quality 24:691-699.

Olea, R.A. 1999. Geostatistics for engineers and earth scientists, Kluwer Academic publishers, Boston.

Pinay, G.., N.E. Haycock, C. Ruffinoni and R. M. Holmes. 1994. The rule of denitrification in nitrogen removal in river corridors. P. 107-111 *In* Misch, W.J. (ed.) Global wetlands: Old world and new.

Pollock, D.W. 1994. User's guide for MODPATH/MODPATH-PLOT, version 3: A particle tracking post-processing package for MODFLOW, the U.S. Geological Survey finite-difference ground-water flow model

Rinkel, R.L. and R.E. Broshears. 1991. One dimensional transport with inflow and storage (OTIS): a solute transport model for small streams. CADSWES Technical report 91-10. Boulder, p.85

Stanford, J.A. and J.V. Ward. 1988. The hyporheic habitat of river ecosystems. Nature 335:64-66

Stanford, J.A. and J.V. Ward. 1993. An ecosystem perspective of alluvial rivers: connectivity and hyporheic corridor. Journal of North American Benthological Society 12 (1): 48-60

Stanley, E.H. and A.J. Boulton. 1993. Hydrology and the distribution of hyporheos: perspectives from a mesic river and desert stream. Journal of North American Benthological Society 12 (1): 79-83

Swanson, F.J. and M.E. James. 1975. Geology and geomorphology of the H.J. Andrews experimental forest, western Cascades, Oregon. USDA Forest Service Research Paper PNW-188.

Townsend, C.R. 1996. Concepts in river ecology: pattern and process in the catchment hierarchy. Archive fur Hydrobiologie, Supplement-band 113:3-21

Triska, F.J., V.C. Kennedy, and R.J. Avanzino. 1989. Retention and transport of nutrients in a third-order stream in northwestern California: hyporheic process. Ecology 70: 1893-1905

Triska, F.J., J.H. Duff, and R.J. Avanzino. 1993-a. Patterns of hydrological exchange and nutrient transformation in hyporheic zone of a gravel-bottom stream: examining terrestrial-aquatic linkages. Freshwater Biology 29: 259-274

Triska, F.J., J.H. Duff, and R.J. Avanzino. 1993-b. The role of water exchange between a stream channel and its hyporheic zone in nitrogen cycling at terrestrial-aquatic interface. Hydrobiologia 251: 167-184

Valett, H.M., J.A. Morrice, C.N. Dahm, AND M.E. Campana. 1996. Parent lithology, surface-groundwater exchange, and nitrate retention in headwater streams. Limnology and Oceanography 41(2): 333-345

Valett, H.M., C.N. Dahm, M.E. Campana, J.A. Morrice, M.A. Baker, and C.S. Fellows. 1997. Hydrologic influences on groundwater-surface water ecotones: heterogeneity in nutrient conposition and retention. Journal of North American Benthological Society 16 (1): 239-247

Ward, J.V. 1989. The four dimensional nature of lotic ecosystems. Journal of North American Benthological Society 8(1): 2-8

White, D.S. 1993. Perspectives on defining and delineating hyporheic zones. Journal of North American Benthological Society 12 (1): 61-69

White, D.S., C.H. Elizang, and S.P. Hendricks. 1987. Temperature patterns within the hyporheic zone of a northern Michigan river. Journal of North American Benthological Society 6(2): 85-91

Williams, D.D. 1993. Nutrient and flow vector dynamics at the hyporheic/groundwater interface and their effects on the interstitial fauna. Hydrobiologia 251: 185-198

Wondzell, S.M. and F.J. Swanson. 1996a. Seasonal and storm dynamics of the hyporheic zone of a 4th-order mountain stream. I: Hydrologic processes. Journal of North American Benthological Society 15 (1): 3-19

Wondzell, S.M. and F.J. Swanson. 1996b. Seasonal and storm dynamics of the hyporheic zone of a 4th-order mountain stream. II: Nitrogen cycling. Journal of North American Benthological Society 15 (1): 20-34

Wondzell, S.M. and F.J. Swanson. 1999. Floods, channel change, and the hyporheic zone. Water Resources Research 35(2): 555

Wroblicky, G.J., M.E. Campana, C.N. Dahm, H.M. Valett, J.A. Morrice, K.S. Henry, and M.A. Baker. 1994. Simulation of stream-groundwater exchange and near-stream flow paths of two first-order streams using MODFLOW, p.187-196. *In* J.A. Stanford and H.M. Valett (ed.) Second international conference on groundwater ecology,